THE REGULATION OF RAB5 BY PHOSPHATIDYLINOSITOL 3′-KINASE

A Thesis Submitted to the College of Graduate Studies and Research

in Partial Fulfillment of the Requirements of the Degree of

Master of Science

in the Department of Biochemistry

University of Saskatchewan

Saskatoon

by

Dielle Detillieux

PERMISSION TO USE

In presenting this thesis in partial fulfillment of the requirements for a Postgraduate degree from the University of Saskatchewan, I agree that the Libraries of this University may make it freely available for inspection. I further agree that permission for copying of this thesis in any manner, in whole or in part, for scholarly purposes may be granted by the professor or professors who supervised my thesis work or, in their absence, by the Head of the Department or the Dean of the College under which this thesis work was done. It is understood that any copying or publication or use of this thesis or parts thereof for financial gain shall not be allowed without my written permission. It is also understood that due recognition shall be given to me and to the University of Saskatchewan in any scholarly use which may be made of any material in my thesis.

Request for permission to copy or to make other use of materials in this thesis in whole or in part should be addressed to:

Dr. Deborah H. Anderson
Saskatchewan Cancer Agency Cancer Research Unit
20 Campus Drive
University of Saskatchewan
Saskatoon, SK
S7N 4H4

ABSTRACT

Rab5 (Ras-related in brain) and Rab4 are small monomeric GTPases that mediate the intracellular trafficking of endocytosed growth factor receptors. Active Rab5-GTP has low intrinsic GTP hydrolysis activity that is stimulated by GTPase activating proteins (GAPs) to make inactive Rab5-GDP. GAPs provide both a catalytic arginine and switch region stabilization functions. The p85 regulatory subunit of phosphatidylinositol 3′-kinase (PI3K) has GAP activity towards Rab5 and Rab4, which is not seen in other PI3Ks. The arginine "finger" residue within p85 is R274. It is unlikely that p85 stabilizes the switch regions of Rab5, which undergo large conformational changes between activation states, because it interacts with both Rab5-GTP and Rab5-GDP. In contrast, the PI3K catalytic subunit p110β binds only Rab5-GTP, suggesting it interacts with the switch regions. Thus, the GAP functions may be provided to Rab5 by the subunits of PI3K acting together, where p85 provides the arginine finger and p110β stabilizes the switch regions. The binding interface of Rab5:p85 was sought using mutations of Rab5 residues not present in the switch regions which were conserved in p85-binding Rab proteins (S84, E106, N113, F145, E172, M175, K179, K180) in GST pull-down experiments with FLAG-p85. The p85 binding site was not resolved with these experiments, suggesting that p85 interaction may involve the contribution of multiple residues of the Rab5 protein. The p110β interaction site on Rab5 was investigated using Rab5 switch region mutants. Pull-down experiments using a stabilized p110 protein construct, where the p85-iSH2 domain was fused to p110 (alpha or beta), were performed. Rab5 mutants I53A, F57A, W74A, Q79L, E80R, Y82A, H83E, L85A, M88A, Y89A and R91E showed reduced p110β binding. All of these residues except E80 and H83 are involved in binding other Rab5 effectors. The Rab5 binding site on p110β was also resolved through mutation of p110β in its Ras binding domain, and includes residues I234, E238 and Y244. This generation of non-binding mutants of both Rab5 and p110β will be invaluable in the characterization of the importance of the p110β:Rab5-GTP interaction for receptor trafficking to endosomes in mammalian cells.

ACKNOWLEDGEMENTS

I would like to thank my supervisor, Dr. Deborah Anderson, for her guidance in this project. I would also like to acknowledge my committee members, past and present, including Dr. Ronald Geyer, Dr. Scot Leary, and Dr. Jeremy Lee. They have helped me to see beyond the bench-top and to analyze objectively what my data was saying. My thanks are also extended to Dr. Stanley Moore, who helped me with molecular modeling and helped select residues for mutation. In addition, the members of the Anderson lab have been helpful in every aspect of my project from experimental design to practical problem solving and the interpretation of results. So I thank them from the bottom of my heart.

This work is dedicated to all those who supported me in my pursuit of knowledge.

Thank you for believing in me.

TABLE OF CONTENTS

LIST OF TABLES

LIST OF FIGURES

LIST OF ABBREVIATIONS

AA	amino acid
ABD	adaptor binding domain
AEBSF	4-(2-Aminoethyl) benzenesulfonyl fluoride
AP-2	adaptor protein 2
BAD	Bcl-2 associated with death
BH	breakpoint cluster region homology domain
BSA	bovine serum albumin
COS-1	*Cercopithecus aethiops* (green monkey) SV40 transformed kidney cells
CREB	cAMP response element binding protein
cSH2	carboxy-terminal SH2 region of p85
DMEM	Dulbecco's modified eagle medium
DTT	dithiothritol
E. coli	*Escherichia coli*
EEA1	early endosomal antigen-1
EDTA	ethylenediaminetetraacetic acid
EGF	epidermal growth factor
EGFR	epidermal growth factor receptor
EPS15	epidermal growth factor receptor pathway substrate 15
ERK	extracellular signal related kinase
FBS	fetal bovine serum
FCHO	FER/ CIP4 homology domain only
FYVE	Fab1/ YOTB/ Vac1/ EEA1
GAP	GTPase activating protein
GDF	GDI displacement factor
GDI	GDP dissociation inhibitor
GDP	guanosine diphosphate
GEF	guanine nucleotide exchange factor
GGT	geranylgeranyl transferase
GNP	guanosine 5′ [β, γ]- imidotriphosphate

GPCR	G-protein coupled receptor
GppCp	guanosine 5′ [β, γ methyleno]-triphosphate
GSK3β	glycogen synthase kinase-3β
GST	glutathione S-transferase
GTP	guanosine triphosphate
GTPγS	guanosine 5′ [gamma-thio]-triphosphate
IGF-1	insulin-like growth factor-1
IGFR	insulin-like growth factor receptor
IgG	immunoglobulin G
IR	infrared
iSH2	inter-SH2 domain of p85
LB	Luria Bertani broth
mAb	monoclonal antibody
MAPK	mitogen activated protein kinase
MEK	MAPK/ERK kinase
MNK	MAPK interacting kinase
mTORC	mammalian target of rapamycin complex
NEB	New England Biolabs
nSH2	amino terminal SH2 domain of p85
OD	optical density
p90RSK	protein 90 kDa, ribosomal S6 kinase
PDGF	platelet-derived growth factor
PDGFR	platelet-derived growth factor receptor
PDK-1	phosphoinositide-dependent kinase-1
PH	pleckstrin homology domain
PHLPP	PH-containing leucine-rich repeat protein phosphatase
PI3K	phosphatidylinositol 3′-kinase
PLB	Prescission lysis buffer
PP2A	protein phosphatase 2A
PTB	phosphotyrosine binding domain

PTEN	phosphatase and tensin homologue (deleted on chromosome 10)
PtdIns	phosphatidylinositol
pY	phosphorylated tyrosine residue
Rab	Ras-related in brain
RBD	Ras binding domain on p110
REP	Rab escort protein
RGS	regulator of G-protein coupled receptor signaling
Rin1	Ras and Rab interactor 1
RTK	receptor tyrosine kinase
SAP	shrimp alkaline phosphatase
SDH^-	yeast media containing dextrose as a sugar source and lacking histidine
SDW^-	yeast media containing dextrose as a sugar source and lacking tryptophan
SDS	sodium dodecyl sulfate
SDS-PAGE	sodium dodecyl sulfate-polyacrylamide gel electrophoresis
$SG(HWLA)^-$	yeast media containing galactose as a sugar source, lacking histidine, tryptophan, leucine and adenine
SH2	src homology 2 domain
SH3	src homology 3 domain
SNARE	soluble N-ethylmaleimide-sensitive attachment protein receptor
SOS	son of sevenless
STAT	signal transducer and activator of transcription
SV40	simian vacuolating virus 40
TBC	Tre-2/Bub-2/Cdc16 homology domain
TGFβR	transforming growth factor β receptor
TIRFM	total internal reflection fluorescence microscopy
Tm	melting temperature
TSC	tuberous sclerosis complex
wt	wild-type
Xgal	5-bromo-4-chloro-indolyl-β-D-galactopyranoside

1.0 INTRODUCTION

1.1 Overview of signal transduction pathways

Cell growth and proliferation within an organism is regulated in part by extracellular cues. Growth factor receptors interact with extracellular ligands to transmit signals that cascade through protein effectors resulting in cell growth and differentiation (Lemmon and Schlessinger, 2010; Heldin and Westermark, 1999). These signals must be turned off in a timely manner which is achieved by deactivating the receptor. Some transformed cells exhibit increased cell proliferation and survival through the actions of enhanced or sustained growth factor signaling pathways (Fleming *et al.,* 1992; Liu and Tsao, 1993; Takeuchi and Ito, 2011). These signaling pathways include the Ras/Mitogen Activated Protein Kinase (MAPK) and Phosphatidylinositol 3′-kinase (PI3K)/Akt cascades which are activated by receptor tyrosine kinases (RTKs) such as the epidermal growth factor receptor (EGFR) and the platelet-derived growth factor receptor (PDGFR) (Bartholomeusz and Ganzalez-Angulo, 2012; Jechlinger *et al.,* 2006) (see Figure 1.1). Amplification of the growth factor receptor *HER2* (also known as *EGFR2*) gene, for example, is found in 20%-30% of early stage breast cancers, and leads to increased activation of the PI3K/Akt and Ras/MAPK pathways (Hurvitz *et al.,* 2012). The regulation of growth factor receptor tyrosine kinase signaling attenuation and degradation is a major area of cancer research.

1.2 Receptor tyrosine kinase signaling

Growth factor signaling begins at the receptor level. As mentioned, an extracellular ligand such as epidermal growth factor (EGF) interacts with its RTK, *e.g.* EGFR, which causes the receptor to change its conformation, dimerize and phosphorylate tyrosine residues of the cytoplasmic domain *in trans* via its tyrosine kinase domain (Lemmon and Schlessinger, 2010; Figure 1.1). These phosphorylated tyrosine residues (pY) recruit proteins with either a Src homology 2 (SH2) or a phosphotyrosine binding (PTB) domain, both of which have a high affinity for pY in specific amino acid motifs (*e.g*. the SH2 domain of p85 recognizes pY-x-x-M; where x indicates any amino acid) (Felder *et al.,* 1993; Mellor *et al.,* 2012). Truncation of the cytoplasmic domain of EGFR, and thus removal of the pY residues, inhibits downstream signaling by lack of recruitment and disrupts receptor endocytosis (Barbieri *et al.,* 2000).

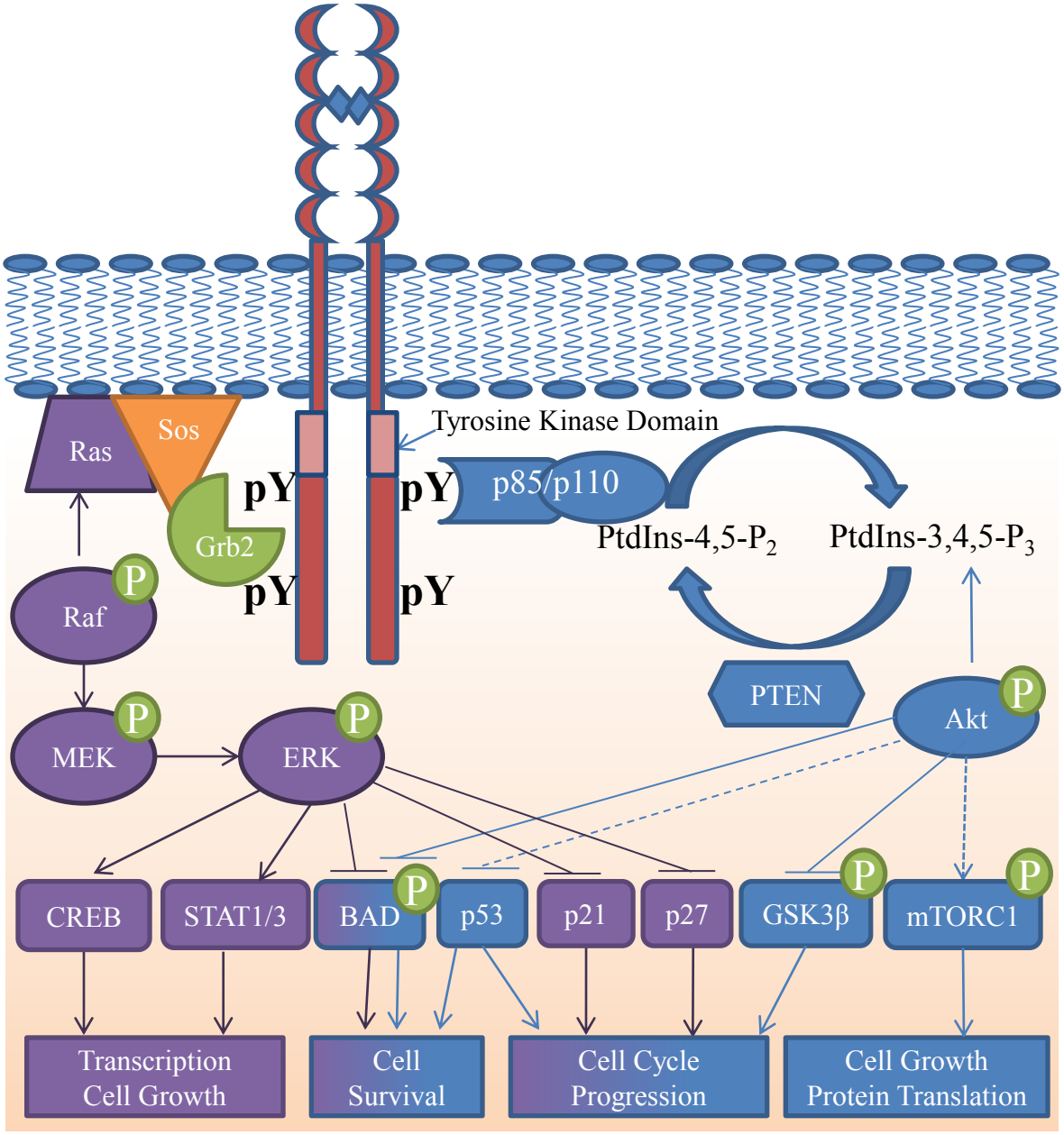

Figure 1.1 Receptor tyrosine kinase signaling pathways. Receptor tyrosine kinases (*red*) such as EGFR and PDGFR interact with an extracellular peptide ligand (*blue diamonds*) EGF or PDGF, respectively, which induces receptor dimerization and phosphorylation of tyrosine residues in its cytoplasmic domain. These phosphorylated tyrosines (pY) recruit SH2-containing proteins to the plasma membrane such as p85 (*blue*) and Grb2 (*green*). p85 binding to pY alleviates its inhibition on p110 which then phosphorylates PtdIns-4,5-bisphosphate to PtdIns-3,4,5-trisphosphate, activating the PI3K/Akt signalling axis (*blue*) which results in cell survival by inactivation of pro-apoptotic proteins BAD and p53, cell cycle progression, cell growth and protein translation. Grb2 recruits SOS (*orange*) which is a GEF to Ras. Active Ras induces the Ras/MAPK signaling pathway (*purple*) which results in transcription, cell growth, cell survival and cell cycle progression through the actions of proteins and transcription factors pictured, which are discussed in detail in the text. Dashed lines indicate indirect regulation between proteins.

Normally, the pY-binding SH2-containing proteins transmit signals within the cell by activating or recruiting other protein "effectors", or proteins that act to alter cellular functions such as metabolism and transcription, in response to growth factor binding. Two major pathways activated by RTKs will be discussed in greater detail below: the Ras/MAPK pathway and the PI3K/Akt pathway.

1.2.1 Ras/MAPK signaling

Arguably the most well studied RTK signaling cascade is the Ras/MAPK pathway. The incidence of somatic mutation of *ras* genes, especially K-*ras,* in all human tumors is as high as 30% (Fernández-Medarde and Santos, 2011). Activation of this pathway, by RTK signaling or by gain of function mutation of downstream proteins, results in cell cycle progression, cell survival and increased gene expression by transcription factors. One example of a common gain of function mutation in human cancers is in the *B-RAF* gene, which increases cell growth and survival through MAPK1/2, (which is also called extracellular signal related kinase [ERK] 1/2). Such mutations also decrease the efficacy of therapeutic inhibitors targeting upstream EGFR used to circumvent inappropriate signaling in cancer (Raponi *et al.*, 2008).

1.2.1.1 The G protein Ras

Ras is a small GTPase which functions like a molecular switch to initiate the Ras/MAPK signaling cascade through its cycling between two conformational states: the GTP-bound active state and the GDP-bound inactive state (Figure 1.2). Crystal structures of Ras proteins reveal a typical GTPase fold of 6 beta sheets surrounded by 5 alpha helices. Two loops near the nucleotide binding site are called "switch regions" because they undergo conformational changes when Ras switches activation states (Figure 1.2) (Shima *et al.,* 2010; Milburn *et al.,* 1990). The switch regions are important in effector recognition of Ras (Pacold *et al.,* 2000; Nassar *et al.*, 1995). When Ras is bound to GTP, main chain amine groups of both a threonine (Thr-35) from switch I (AA 30-38) and a glutamine (Gln-60) from switch II (AA 60-75) make hydrogen bonds with the γ-phosphate group of GTP, while a conserved serine (Ser-17) hydroxyl group displays charge-charge interaction with an essential Mg^{2+} ion (Shima *et al.*, 2010). The γ-phosphate interactions hold the switch loops in an ordered shape. In the GDP-bound state, the missing hydrogen bonds with the γ-phosphate oxygens destabilize both flexible switch regions often resulting in disorder within the two loops (Vetter and Wittinghofer, 2001).

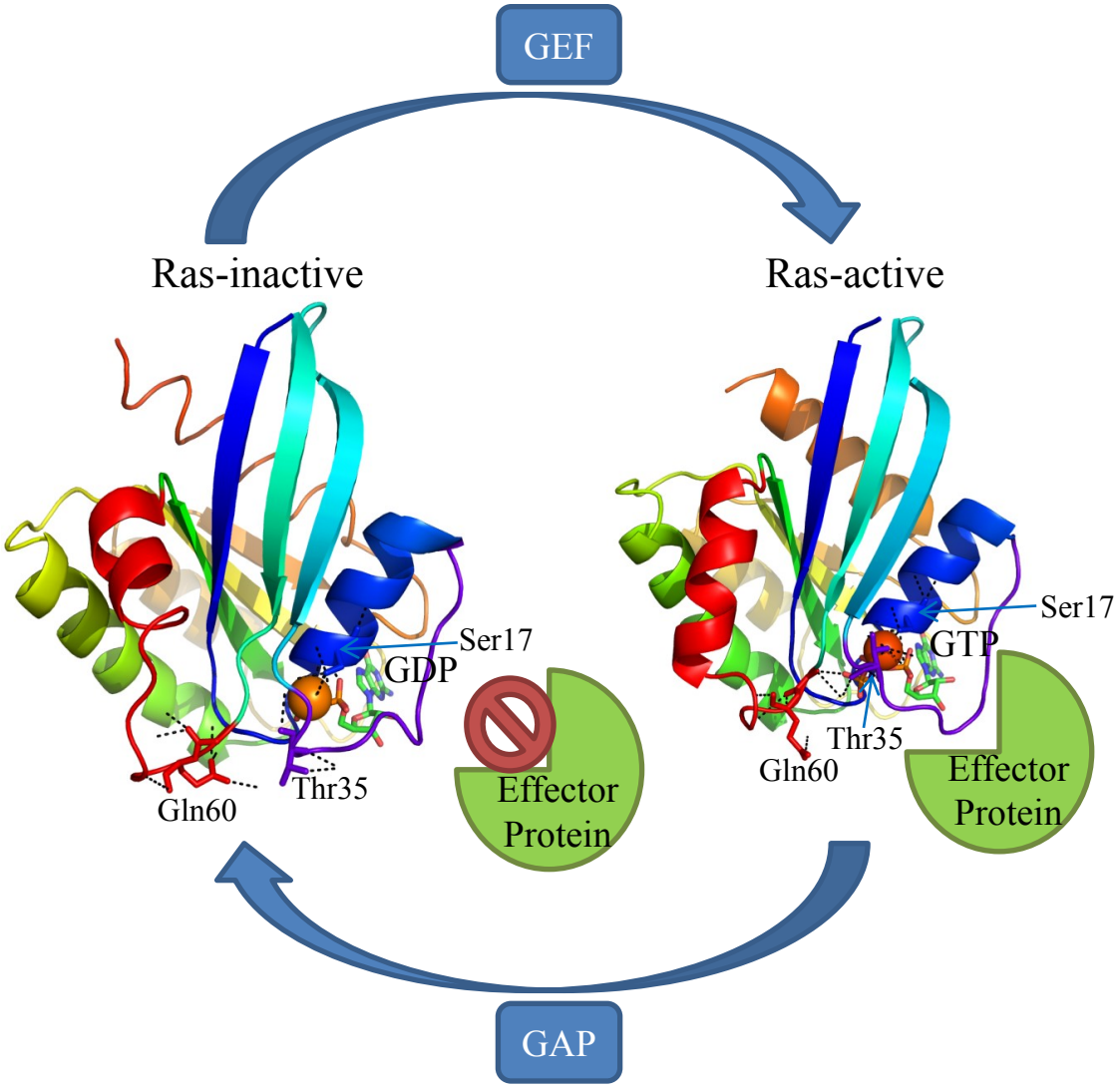

Figure 1.2 Ras structure and activation. When bound to GDP (*left*) Ras cannot interact with its effector proteins and is in its inactive conformation. Guanine nucleotide exchange factors or GEFs facilitate the exchange of GDP for GTP, bringing Ras into its active conformation (*right*). Amino acids Thr35 and Gln60 make hydrogen bonds with the γ-phosphate of GTP, stabilizing the position of both switch I *(purple*) and switch II *(red*) loops. The Ser17 hydroxyl interacts with the charged Mg^{2+} ion. Effector proteins recognize the active conformation and are able to bind to Ras. GTPase activating proteins or GAPs enhance the GTPase activity of Ras, converting GTP to GDP and completing the Ras activation cycle. Crystal structures from PDB, ID SP21 (*left*), 4Q21 (*right*). Dashed black lines indicate hydrogen bonding.

Interaction with Ras and other small GTPases depends on the conformation of the switch regions, and thus by alternating between GDP- and GTP-bound states they become the on/off switch of downstream events.

Regulation of small GTPases, or G proteins, involves both guanine nucleotide exchange factors (GEFs) and GTPase activating proteins (GAPs) to efficiently bind and hydrolyze GTP, respectively. Ras requires a GEF to exchange its bound GDP for GTP in order to be activated. The GEF facilitates the release of GDP by destabilization of the nucleotide binding site in a push-and-pull mechanism whereby the switch I region is pushed out of position and the switch II region is pulled toward the nucleotide binding site (Vetter and Wittinghofer, 2001). Upon GTP binding, Ras interacts with its effectors, such as Raf, via switch regions epitopes, which are only presented in the active conformation. Deactivation of Ras requires the hydrolysis of GTP, which can be achieved through its intrinsic GTPase ability, though the rate of reaction is slow. Stimulation of GTP hydrolysis by GAPs, which provide a catalytic "arginine finger" residue as well as stabilization of the switch regions, ensures proper temporal regulation of Ras (Fidyk and Cerione, 2002).

1.2.1.2 Signaling cascade downstream of Ras

Activation of Ras is tied to RTK signaling by its GEF Son of Sevenless (SOS). The Ras/MAPK (ERK) pathway becomes active after RTK phosphorylation, which recruits the SH2 domain of adaptor protein Grb2 either directly (Figure 1.1) or indirectly through interaction with Shc (which also binds to pY on RTKs) (Reeby *et al.*, 2012). Once Grb2 is recruited to the plasma membrane, the Grb2 Src homology 3 (SH3) domain interactions with the proline rich region on SOS, thus bringing the GEF proximal to its substrate Ras-GDP (Egan *et al.*, 1993). SOS facilitates the exchange of Ras-bound GDP for the more abundant GTP. Activated Ras-GTP recruits Raf, a serine/threonine kinase, from the cytoplasm to the plasma membrane where it is activated itself by phosphorylation (Roskoski, 2010). A cascade of protein activation by phosphorylation continues with Raf phosphorylation of MAPK/ERK kinase (MEK), to MEK phosphorylation of MAPK/ERK which then phosphorylates many proteins and transcription factor targets (Sebolt-Leopold and Herrera, 2004).

MAPK/ERK signaling affects cell cycle regulation through the inhibition of cyclin dependent kinase inhibitors $p21^{WAF1/CIP1}$ and $p27^{KIP1}$. Growth advantages in tumors with abnormal activation of the Ras/MAPK pathway are due to the downregulation of the pro-apoptotic function of Bcl-2 associated with death (BAD) as well as transcription of pro-survival genes through the cAMP response element binding protein (CREB) transcription factor. Additional gene expression through the activation of transcription factors including c-Fos, signal transducer and activator of transcription (STAT)1 and STAT3 (Sebolt-Leopold and Herrera, 2004; Figure 1.1) by MAPK/ERK may also play a role in tumorigenesis. Some of the protein targets of this pathway are activated by phosphorylation, *i.e.* ribosomal S6 kinase (p90RSK) and MAPK-interacting kinase (MNK), while others are inactivated, *i.e.* tuberous sclerosis complex (TSC) (De Luca *et al.,* 2012; Figure 1.1). The pathway is subject to negative feedback regulation, reducing the magnitude or duration of its activation. It has been shown in different cell lines that transient MAPK/ERK activation has different biological outcomes than those associated with sustained MAPK/ERK activation (Andreadi *et al.,* 2012).

1.2.2 Phosphatidylinositol 3′-kinase/Akt signaling

Other SH2-containing proteins act as adaptors, binding the pY residues of activated RTKs and effector proteins with separate domains, linking their activity to growth factor binding. PI3K is recruited by activated receptor pY residues and phosphorylates its lipid substrate phosphatidylinositol-4,5-bisphosphate (PtdIns-4,5-P_2) at the 3′ OH of the inositol ring, creating PtdIns-3,4,5-P_3 at the plasma membrane (Figure 1.1). PtdIns-3,4,5-P_3 is an important second messenger in the PI3K/Akt pathway, as it recruits proteins with a pleckstrin homology (PH) domain, such as Akt, to membranes enriched in this phospholipid. Activation of Akt serine/threonine kinase activity by phosphorylation results in the phosphorylation of its target proteins (as many as 50 proteins have been characterized) which can induce an anti-apoptotic response, cell cycle progression and/or cell growth (Manning and Cantley, 2007; Vasudevan and Garraway, 2010). Phosphatase and tensin homologue deleted on chromosome 10 (PTEN) acts to downregulate this pathway by dephosphorylating PtdIns-3,4,5-P_3 at the 3′ position, inhibiting the recruitment of Akt and reducing the signal generated by the activated receptor.

1.2.2.1 Phosphatidylinositol 3′-kinase

PI3K is an obligate heterodimer consisting of a regulatory subunit and a catalytic subunit (Hirsch *et al.,* 2007). PI3Ks are subdivided into three classes based on differences in structure and substrate specificity (Vanhaesebroeck and Waterfield 1999). The class I PI3K catalytic subunits are p110 proteins, and are expressed as different isoforms p110α, p110β, p110δ, and p110γ. All p110 proteins are responsible for the kinase activity of PI3K on their substrate PtdIns-4,5-P_2. Regulatory subunits of class IA PI3Ks may be one of p85α, p55α, p50α, p85β, or p55γ. Only p110γ pairs with the regulatory subunit p101 and is therefore classified as Class IB.

Class IA PI3Ks (from now on designated only as "PI3K") are the most studied because of frequent mutations found in both the gene of the p110α catalytic subunit *PIK3CA* and the p85α regulatory subunit gene *PIK3R1* (Vogt *et al.,* 2010; Yuan and Cantley, 2008). Oncogenic mutation of either gene can result in the increased activation of the catalytic subunit of PI3K, p110α, which leads to increased activation of Akt and downstream signaling (Samuels and Waldman, 2010; Cheung *et al.,* 2011; Sun *et al.,* 2010). The loss of PTEN, a tumor suppressor gene, (by loss of function mutation or loss of heterozygosity) also leads to increased Akt signaling by lack of dephosphorylation of PtdIns-3,4,5-P_3 (Nardella *et al.,* 2011). Because of its importance in signal transduction and its frequent mutation in cancer, PI3K has been studied extensively.

1.2.2.1.1 Regulatory subunit: p85

The regulatory subunit of PI3K is encoded by three genes: *PIK3R1* (p85α; can also be expressed as splice variants p50α and p55α), *PIK3R2* (p85β), and *PIK3R3* (p55γ). The smaller isoforms p50α, p55α and p55γ are composed an inter-SH2 (iSH2) domain which is flanked by two SH2 domains (Figure 1.3). Interaction between the iSH2 domain and the catalytic subunit, p110, confers stability to both proteins by protecting p110 from degradation (Klippel *et al.,* 1993). The iSH2 domain is a hotspot for mutation in cancers, specifically glioblastomas and endometrial cancers (Sun *et al.,* 2010; Jaiswal *et al.,* 2009; Cheung *et al.,* 2011). Mutations in this region are tumorigenic when they disrupt p110 inhibition (discussed in section 1.2.2.1.3) without affecting the stabilizing contacts between the proteins (Gabelli *et al.,* 2010). The larger isoforms p85α and p85β contain an N-terminal SH3 domain, two proline rich domains, and a

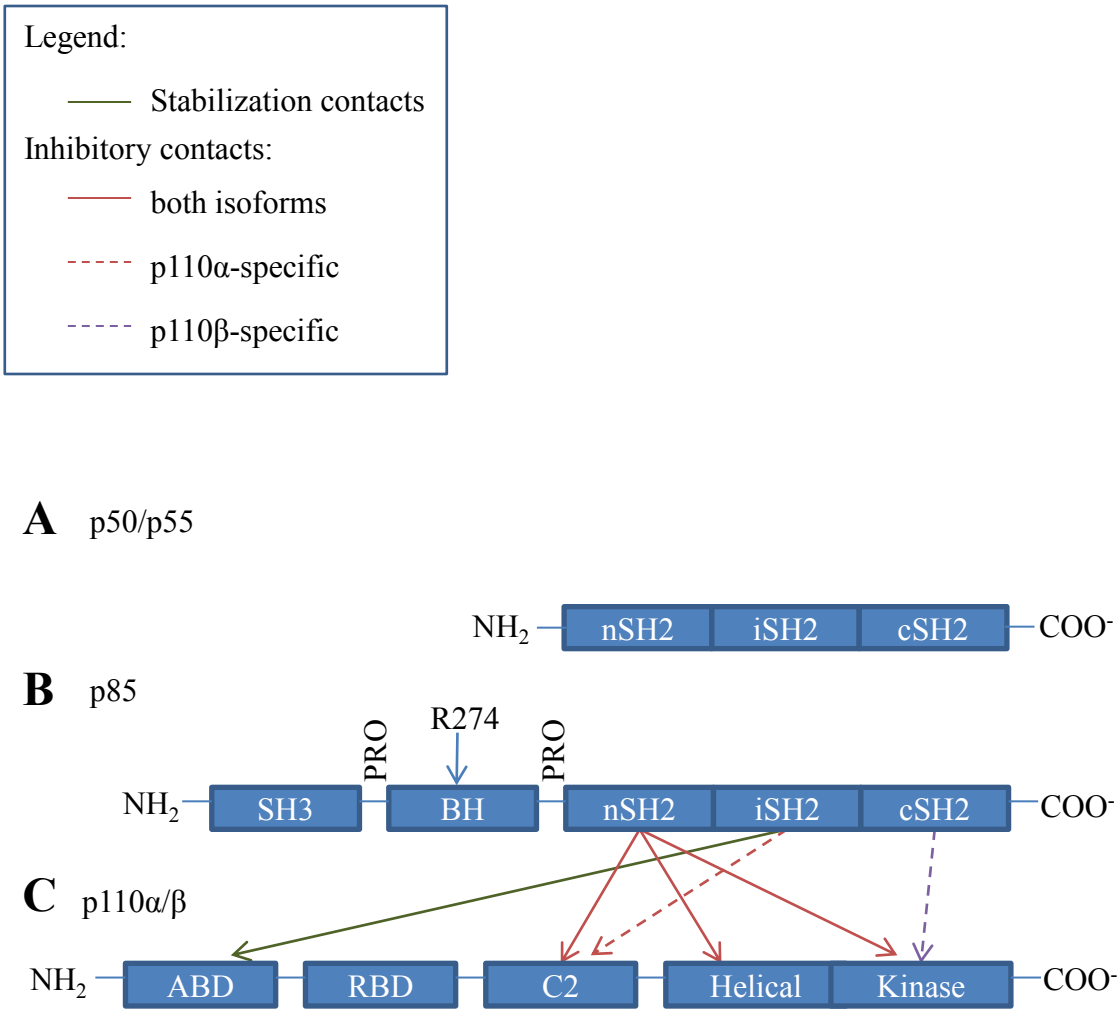

Figure 1.3 Domain structure of PI3K subunits. A. Domains of the regulatory subunit of phosphatidylinositol-3`-kinase smaller isoforms, p50 and p55, and **B.** larger isoforms, p85. SH3, Src homology 3 (interacts with proline rich domains); SH2, Src homology 2 (interacts with phosphorylated tyrosine motifs); PRO, proline rich domain; BH, Breakpoint cluster region homology (GAP domain); R274, arginine finger; iSH2, inter-SH2 domain (interacts with p110). **C.** Domain structure of catalytic subunit p110. ABD, adaptor binding domain (main interaction with p85); RBD, ras binding domain; C2, calcium binding-homology domain. The iSH2 interaction with ABD enhances the stability of p110. Regulatory contacts are indicated with red and purple arrows.

Breakpoint Cluster Region homology domain (BH) in addition to the two SH2 domains and iSH2 found in the smaller isoforms (see Figure 1.3). Both large isoforms of the regulatory subunit, p85α and p85β, are expressed ubiquitously in cells, though p85β to a lesser degree (Hirsch *et al.*, 2007; Ueki *et al.*, 2003). The large isoforms will be the focus of this thesis, specifically p85α.

1.2.2.1.2 Catalytic subunit: p110

As mentioned, the catalytic subunit of PI3K has three isoforms which are encoded on separate genes. *PIK3CA* encodes p110α, *PIK3CB* encodes p110β, and *PIK3CD* encodes p110δ. Both p110α and p110β are ubiquitously expressed; whereas p110δ is expressed in immune cells only and therefore will not be characterized in this thesis (See review Patton *et al.*, 2007 for more about p110δ). The p110 proteins have five domains: the N-terminal adaptor binding domain (ABD) which interacts with the iSH2 of regulatory subunits, the Ras binding domain (RBD), the C2 domain, the helical domain and the kinase domain (Figure 1.3). Structurally, p110α and p110β are very similar, though they diverge from each other in the RBD (Zhang *et al.*, 2011).

The p110α and p110β isoforms can be activated downstream of different signaling pathways. Signals and effects downstream of the PDGFR were found to be impaired by p110α inhibition with neutralizing antibodies, but not by p110β inhibition (Ilic and Roberts, 2010). Conversely, downstream signaling from G-protein coupled receptors (GPCRs) is effected by p110β knockdown only (Jia *et al.*, 2008; Ciraolo *et al.*, 2008). It has been shown, however, that both isoforms have some involvement in insulin signaling (Chaussade *et al.*, 2007; Jia *et al.*, 2008; Ciraolo *et al.*, 2008; Foukas *et al.*, 2006). Therefore, the two isoforms are considered to have partial functional overlap.

1.2.2.1.3 Regulation of PI3K

In resting cells, p85 is bound to p110 and provides inhibition of the kinase by: 1) contacts between the p85 nSH2 domain to the p110 helical and kinase domains, 2) additional contacts between the p85 iSH2 and the p110 C2 domain, and 3) sequestration of p110 in the cytosol, away from its membrane-delimited lipid substrates (Figure 1.3). During growth factor receptor signaling, *i.e.* EGF or insulin-like growth factor-1 (IGF-1) stimulation, the SH2 domains of p85 are recruited to phosphorylated tyrosine residues on EGFR or IGF receptor (Hu

et al., 1992; Yamamoto *et al.*, 1992; Mellor *et al.*, 2012). This brings the catalytic domain in proximity to its lipid substrate PtdIns-4,5-P_2 at the plasma membrane. The nSH2 domain has a greater affinity for pY residues than it does for the helical and kinase domains of p110. Thus, p85 binding to pY residues releases the SH2 domain-mediated inhibition of p85 on p110, activating the kinase (Yu *et al.*, 1998). The phosphatase agonist of PI3K, PTEN, dephosphorylates the lipid second messenger, regulating the time and intensity of the signaling event (De Luca *et al.*, 2012).

The recent solution of the crystal structure of p85 domains with different p110 isoforms elucidated a difference in regulation between catalytic isoforms (Zhang *et al.*, 2011). Both p110α and p110β are regulated by inhibitory contacts made between the iSH2 (p85) and C2 (p110) domain as well as the nSH2 (p85) domain with both the helical and kinase (p110) domains. Regulation of p110β is also dependent on additional contacts with the cSH2 domain of p85. Though the p110β isoform is regulated by a "three brake" mechanism of p85 inhibition, *i.e.* the nSH2, iSH2 and cSH2 contributions, it is not more tightly controlled than p110α because amino acid differences in the p110β C2 domain render the p85 iSH2 inhibition ineffective (Vogt, 2011). Therefore both isoforms are regulated by two inhibitory contacts with the regulatory subunit p85.

1.2.2.1.4 PI3K in cancer

In some cancers, the catalytic activity of p110α is enhanced by mutations E542K, E545K and/or H1047R in the hotspot helical and kinase domains through disruption of p85 inhibitory contacts, releasing p110 from growth factor-dependent regulation by the nSH2 domain (Samuels *et al.*, 2004). In fact, point mutations in the helical and kinase domains accounts for 80% of all oncogenic *PIK3CA* mutations (Samuels and Waldman, 2010). Constitutive activation of p110α can lead to increased downstream signaling in the absence of growth factor, thus conferring a growth advantage. An engineered protein chimera containing full-length p110α and the iSH2 domain of p85 attached N-terminally by a glycine linker was found to be constitutively active (Klippel *et al.*, 1995). Without the inhibitory contacts between the nSH2 domain and the helical and kinase domains, this p110 was both stabilized and disinhibited.

In contrast, overexpression of wild-type p110β was sufficient to induce tumorigenesis, but mutations of the C2 domain of this isoform, *e.g.* mutations that would effectively activate p110α, were not (Kang *et al.*, 2005; Dbouk *et al*, 2010). Additionally, p110β kinase activity, and not the activity of p110α, was necessary for the progression of prostate tumors lacking the tumor suppressor PTEN (Jia *et al.,* 2008). Thus it suggested that p110β is less regulated than p110α, and promotes basal levels of PtdIns-3,4,5-P_3 and downstream signaling in the absence of growth factor.

1.2.2.2 Akt signalling

The serine/threonine Akt is a master regulator of multiple cellular responses including cell survival, cell growth, cell proliferation, and glucose homeostatis due to its substantial repertoire of substrates (Vasudevan and Garroway, 2010; Figure 1.1). Activation of Akt requires both recruitment to the plasma membrane, as mentioned above, and phosphorylation of Thr-308 by phosphoinositide dependent kinase (PDK-1) and Ser-473 by mammalian target of rapamycin complex 2 (mTORC2) (Stokoe *et al.*, 1997; Sarbassov *et al.*, 2005) in response to growth factor binding to RTKs. To promote cell survival, active Akt phosphorylates the pro-apoptotic protein BAD, which then becomes bound and sequestered by 14-3-3 proteins, inhibiting its apoptotic function (Datta *et al.*, 1997; Datta *et al.*, 2000). A second example of Akt-mediated cell survival is the phosphorylation of MDM2, which increases the stability of MDM2 in the nucleus and its E3 ubiquitin ligase activity, leading to the downregulation of p53-mediated apoptosis (Zhou *et al.*, 2001).

Akt affects cell proliferation by promoting the G1-to-S phase cell cycle transition by phosphorylating and inactivating glycogen synthase kinase-3β (GSK-3β), which then can no longer act to downregulate cyclins D1 and E (Diehl *et al.*, 1998; Welcker *et al.,* 2003). The effect of PI3K/Akt signaling on cell growth manifests mainly through mTORC1 which is involved in the increase of protein synthesis (Vivanco and Sawyers, 2002). mTORC1 activation by Akt is indirect. Akt inactivates tuberous sclerosis complex 2 (TSC2) by phosphorylation. TSC2 is a GAP – or GTPase activating protein – to the Ras family member Rheb. Inactivation of TSC2 leads to an increase in active Rheb, which then interacts with and activates mTORC1 (Manning and Cantley, 2007). Many more Akt phosphorylation targets exist in the cell, including kinases, adaptor proteins, and transcription factors such as FOXO1, which can be

found in more extensive Akt reviews such as Manning and Cantley (2007) as well as Vasudevan and Garroway (2010). Down regulation of PI3K/Akt signaling is achieved by dephosphorylation of both PtdIns-3,4,5-P_3 by PTEN in order to stop further activation of Akt, and dephosphorylation of active Akt itself at Thr-308 by protein phosphatase 2A (PP2A), and at Ser-473 by PH-containing leucine-rich repeat protein phosphatase (PHLPP)1 and PHLPP2 (Brognard *et al.*, 2007).

1.3 Endocytosis of activated RTKs

Receptors undergo endocytosis when they are internalized into independent vesicles at the plasma membrane. Known mechanisms of internalization include clathrin-mediated (which will be discussed first) and caveolin-mediated (or clathrin-independent) endocytosis. The first step of clathrin-mediated internalization is the formation of protein complexes, or "nucleation", at the plasma membrane which causes the formation of pits containing specific cargo, such as activated receptors. Some adaptor proteins, such as epsin 1 & 2, epidermal growth factor receptor pathway substrate 15 (EPS15) and FER/CIP4 homology domain only (FCHO) proteins, promote the membrane curvature necessary to form pits by insertion of their wedge shape into the membrane (McMahon and Boucrot, 2011). The multi-subunit adaptor protein, AP-2, coats the cytoplasmic face of the pits and provides an interaction point between plasma membrane lipids, receptor cargo and clathrin. Clathrin "triskelia" subunits assemble to support the curvature of the pits by coating their cytoplasmic surface (McMahon and Boucrot, 2011). The vesicle membrane is pinched off from the plasma membrane by the large GTPase dynamin (Praefcke and McMahon, 2004). It has been recently suggested that asymmetrical membrane protrusions can form a cap over clathrin-coated pits in an alternative method of closure (Shevchuk *et al.*, 2012).

Clathrin-independent endocytosis is less well understood. Plasma membrane domains that contain high concentrations of cholesterol and sphingolipids can deform into pits and have been called caveolae or "little caves" (Andersson, 2012). Caveolae are coated with the hairpin-shaped protein caveolin-1 that interacts with cholesterol (Doherty and McMahon, 2009). These pits have been implicated in a pathway of internalization distinct from the clathrin-dependent pathway. Endocytosis by caveolae is less frequent than clathrin-mediated endocytosis, and some believe that these structures play an important role in stabilizing protein complexes on the

plasma membrane rather than in their internalization (Hansen and Nichols, 2009; Howes *et al.*, 2010). Flotillin proteins are similar in structure to caveolin and may provide a parallel internalization pathway (Andersson, 2012). Dynamin plays an important role in many internalization pathways including clathrin-, caveolae-, and flotillin-mediated endocytosis, but there are some pathways that act independently of dynamin and employ actin instead for membrane scission (Doherty and McMahon, 2009).

Activated RTKs have been generally found in clathrin-coated vesicles after internalization and these seem to be important for downstream signaling (Sorkin and von Zastrow, 2009). A study of transforming growth factor β receptor (TGFβR) endocytosis suggested that the method of receptor internalization affected the outcome of signaling. It has been demonstrated that EGFR is internalized exclusively by clathrin-dependent endocytosis in low ligand concentrations (Sigismund *et al.,* 2008). At high concentrations of EGF, EGFR is internalized via both clathrin and non-clathrin endocytosis (Sigismund *et al.,* 2005). The latter is dependent on cholesterol and ubiquitination of the receptor, and results in receptor degradation (Sigismund *et al.,* 2005). When TGFβR is internalized by clathrin, it leads to downstream signalling, whereas internalization by caveolae leads to receptor ubiquitination and degradation in the lysosome (Di Guglielmo *et al.*, 2003).

The removal of the receptors from the plasma membrane by endocytosis affects their overall signal output by reducing the concentration of receptors available to bind ligand. Also the physical relocation of activated receptors to vesicles within the cytoplasm or "endosomes" results in a bias towards soluble effectors over plasma membrane-associated effectors. Therefore, plasma membrane delimited proteins may only interact with growth factor receptors until they are internalized (Sorkin and von Zastrow, 2009). In this way, endocytosis provides temporal regulation of growth factor signal transduction by limiting the time of interaction between activated receptors and certain effectors. However, it has been shown that signaling from endosomes occurs as well (Vieira *et al.,* 1996). Many effector proteins complex with β-arrestins and/or scaffolding proteins containing a Fab1 YOTB Vac1 EEA1 (FYVE) zinc-finger domain or a PX domain which are specific for the phosphoinositide lipids present on endosomal membranes (Sorkin and von Zastrow, 2009). The early endosome, in which internalized receptors are found, has also been named the "signaling endosome" for this reason. Detection of

components of both PI3K/Akt and Ras/MAPK signaling cascades on endosomes suggests that these pathways remain activated after receptor internalization.

1.4 RTK intracellular trafficking

After internalization, the vesicle containing activated receptors (which may now be called an "early endosome") is uncoated of clathrin or caveolin-1 and adaptor proteins (Stenmark, 2009). Internalized receptors in the early endosome dissociate from their ligand due to the lower pH of the organelle (Cain *et al.*, 1989). The method of internalization and the post-translational modifications of the receptor – including ubiquitination and phosphorylation – determine the fate of the receptor. Possible fates include sorting for recycling back to the plasma membrane or sorting for degradation of the receptor in the lysosome. Receptors can be monoubiquitinated after internalization via clathrin-independent endocytosis which leads to sorting for degradation. Without this monoubiquitination signal, the receptor is recycled (Acconcia *et al.*, 2009). Polyubiquitination of the receptor before clathrin-dependent internalization increases the affinity of adaptor proteins with ubiquitin binding domains such as epsin, leading to more efficient nucleation. The choice of internalization pathway can be regulated by the concentration of ligand, as mentioned in the case of EGF (Sigismund *et al.*, 2008), or through disruption of clathrin-mediated endocytosis by potassium depletion, which prevents clathrin lattice assembly (Vercauteren *et al.*, 2010; Larkin *et al.*, 1986) or by expression of a dominant negative Eps15 (Di Guglielmo *et al.*, 2003).

Receptor trafficking is tailored to specific receptor needs. Some receptors are constitutively internalized (ligand-independent) and recycled to maintain cell sensitivity; *i.e.* the transferrin receptor which is important to maintain cellular iron homeostasis (Wang and Pantopoulos, 2011), the dopamine receptor 2 in neurons (Li *et al.*, 2012), and small amounts (1 – 2%) of epidermal growth factor receptors Her2, Her3 and Her4 (Wiley and Burke, 2001). The trafficking of other receptors is ligand-dependent and may at times be recycled or degraded in order to control their signal output, *i.e.* EGFR (Sigismund *et al.*, 2008) and TGFβR (Di Guglielmo *et al.*, 2003). There is also evidence of basal, ligand-independent receptor degradation through the actions of the small isoforms of ankyrin, Ank105 and Ank120 (Ignatiuk *et al.*, 2006) which may be important in maintenance of steady state levels of receptors, such as PDGFR, on the plasma membrane. Another type of trafficking is the ligand-

dependent recycling of receptors, *i.e.* dopamine receptor 2, through perinuclear recycling endosome for functional resensitization of the receptor (Li *et al.*, 2012). The early trafficking steps of receptors through the early endosome are common regardless of the pathway, whereas later steps require the sorting into different Rab-protein containing endosomes (Leonard *et al.*, 2008).

1.4.1 Rab proteins

Rab proteins (so named due to their homology to Ras: Ras-related in brain) are involved in the intracellular trafficking of vesicles. The evolution of distinct organelles within a cell suggests the necessity for trafficking cargo between these organelles and the plasma membrane. Rab proteins have been demonstrated to be involved in every step of vesicle trafficking from internalization, to vesicle coating (with clathrin and AP-2) and uncoating, to vesicle motility and to the fusion of the incoming membrane with its target organelle (Stenmark, 2009; McMahon and Boucrot, 2011). In growth factor receptor signaling attenuation, the trafficking of activated receptors through the early endosome to either the lysosome where they are degraded, or back to the plasma membrane requires multiple Rab proteins (Stenmark, 2009). Different Rab proteins are associated with specific vesicle trafficking pathways including: endocytosis to early endosomes (Rab5, Figure 1.4 A and B), early endosome recycling to the plasma membrane (Rab4, Figure 1.4 C), recycling endosome to plasma membrane (Rab11, Figure 1.4 D), late endosome to lysosome (Rab7, Figure 1.4 F), and late endosome to the trans-Golgi network (Rab9, not pictured) (Seachrist and Ferguson, 2003; Zerial and McBride, 2001). The human genome encodes 60 Rab proteins which are part of the Ras superfamily of small GTPases.

Ras proteins, as described in section 1.2.1.1, incorporate into the plasma membrane via a post-translational cysteine farnesylation of the C-terminal C-A-A-X motif (A is an aliphatic amino acid, X is any amino acid except for leucine; Ahearn *et al.*, 2011). While Rab proteins have structural similarity to Ras, they do not contain the farnesylation motif, but instead a dual geranylgeranyl motif, C-X-C or X-X-C-C at their C-terminus, which is recognized by Rab escort protein (REP) which is in turn recognized by Rab geranylgeranyl transferase (Rab GGTase or GGT-II) (Pfeffer and Aivazian, 2004; Leung *et al.*, 2006). The doubly geranyl-

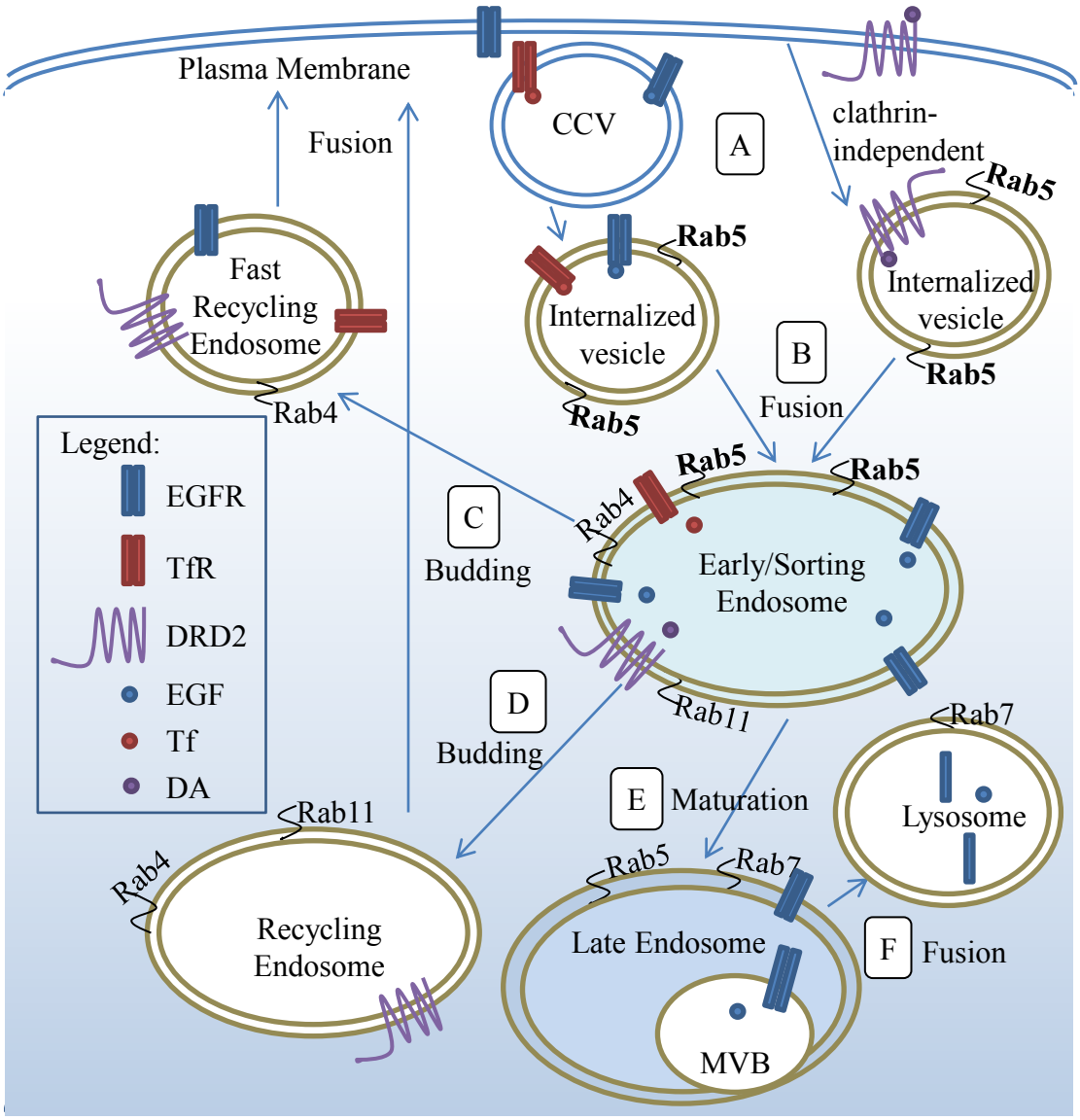

Figure 1.4 Endocytic trafficking by Rab proteins. **A.** Receptors are internalized at the plasma membrane via a clathrin-dependent (CCV, clathrin-coated vesicle) or clathrin-independent mechanism. The resulting internalized vesicles are coated with Rab5 which recruits effector proteins to alter the lipid composition of the membrane. **B.** Internalized vesicles fuse together to form early endosomes through actions of EEA-1 and SNARE proteins (not shown). Within the early endosome, the receptors dissociate from their ligand and are sorted for further trafficking into Rab microdomains. **C.** Receptors sorted for fast recycling (2-5 mins after internalization) bud off the endosome in Rab4-positive vesicles and are returned to the plasma membrane. **D.** Slower recycling of receptors (12-30 mins) occurs in the recycling endosome which depends on Rab4 and Rab11. **E.** Early endosomes mature into late endosomes through the actions of Mon1 and the recruitment of Rab7 activating proteins. Receptors destined for degradation are internalized in multi-vesicular bodies (MVB) within the lumen of the late endosome. **F.** Late endosomes fuse with lysosomes and receptors are degraded. EGF, epidermal growth factor; EGFR, receptor; Tf, transferrin; TfR, receptor; DRD2, dopamine receptor 2; DA, dopamine.

geranylated Rabs are chaperoned by either REP or by a GDP dissociation inhibitor (GDI) which bind to and mask the hydrophobic geranylgeranyl moieties allowing the complex to exist in the cytosol (Leung *et al.*, 2006; Figure 1.5).

During receptor endocytosis, the Rab-GDP:GDI complex is recruited to its target membrane by a GDI displacement factor (GDF) (Pfeffer and Aivazian, 2004). Displacement of the GDI by GDF frees the isoprenyl group which may then be incorporated into the target membrane. So, unlike membrane delimited Ras, GDP-bound Rab proteins move on and off membranes through the concerted actions of GDI and GDF. Once the Rab geranylgeranyl group is incorporated into the membrane, the Rab activation cycle resembles that of Ras. Rab protein nucleotide exchange is facilitated by a GEF and GTP hydrolysis is enhanced by a GAP. A study of fluorescent lipidated Rab proteins demonstrated that GDI affinity for Rab-GTP was several orders of magnitude lower than for Rab-GDP (Wu *et al.,* 2010) making the deactivation of the Rab protein a prerequisite for displacement from the membrane by GDI.

Rab GTPases act by recruiting effector proteins to a specific endosome at the proper time. An additional level of organization is achieved by Rab "microdomains" on an endosome, where different Rab proteins co-exist within the same organelle, but remain enriched in discrete domains of the membrane (Zerial and McBride, 2001) (Figure 1.4, early endosome). The coordination of all trafficking events within a cell requires a complement of functional Rab proteins. Rab effector protein binding sites are only presented in the proper orientation in the GTP-bound Rabs and are unique in sequence or orientation from one Rab protein to another (Mishra *et al.*, 2010). Protein complexes on vesicles and endosomes are therefore organized by the specific Rab available on the surface and only recruited when that Rab is in its active form.

1.4.1.1. Rab5

Rab5 has three subgroup isoforms (A, B and C) with 81-90% sequence identity (Wilson and Wilson, 1992) which are encoded by separate genes. *RAB5A* is located on chromosome 17, *RAB5B* is on chromosome 2 and *RAB5C* is on chromosome 11 (Barbosa *et al.,* 1995). The abundance of each Rab5 isoform is cell-type dependent (Chiariello *et al.,* 1999; Chen *et al.*, 2009). All Rab5 isoforms co-localize with internalized transferrin and are involved in endocytic trafficking (Bucci *et al.*, 1995). Differential phosphorylation of Rab5 isofroms has been

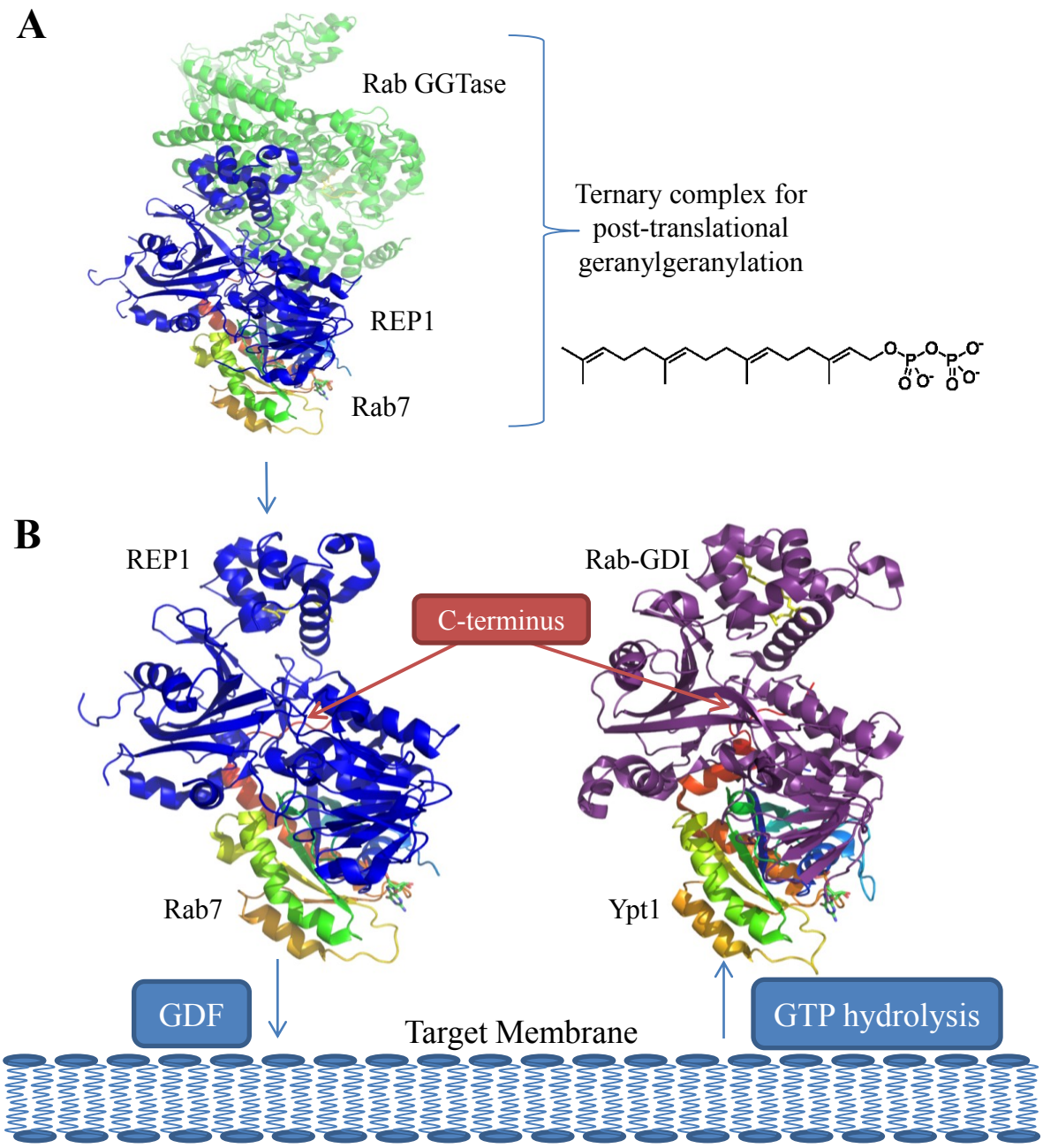

Figure 1.5 Rab protein geranylgeranylation and membrane recruitment cycle. A. Alignment of crystal structures of the Rab7: Rab escort protein 1 (REP1, PDB ID: 1VG0; *blue*) complex with Rab geranylgeranyl transferase (Rab GGTase, 1LTX; *green*). REP1 recognizes the C-terminal C-X-C or X-X-C-C motif of the Rab, binds to it and recruits Rab GGTase which transfers two geranylgeranyl groups (*right*) to the Rab. **B.** The isoprenylated Rab exists in complex with either REP1 or guanine dissociation inhibitor (GDI, 2BCG; *purple*) in the cytoplasm in absence of receptor signaling and endocytosis. The hydrophobic C-terminal geranygeranylation (indicated with red arrows) is masked by REP1 or GDI. During receptor endocytosis, a GDI displacement factor (GDF) removes the bound GDI and facilitates Rab protein recruitment to the target membrane, where it can be activated. At the end of their activation cycle, GDP-bound Rab proteins can be removed from the membrane by GDI.

reported where Rab5B is phosphorylated by cdc2 kinase, Rab5A by ERK (Chiariello *et al.*, 1999). Rab5A siRNA knockdown and Rab5A overexpression have a greater influence on EGFR trafficking in HeLa and DU145 cells compared to the other Rab5 isoforms (Chen *et al*., 2009). Because of its importance in RTK trafficking, Rab5A (which will hence be designated only as "Rab5") is the focus of this thesis.

Rab5 is a typical Rab protein that cycles between nucleotide-bound states and membrane-bound to cytoplasmic locations, providing both spatial and temporal regulation of early endosomal trafficking. Interaction with a GDF brings inactive Rab5 from the cytoplasm to the plasma membrane, in response to growth factor stimulation, where it may be activated. The Rab5-GEF Ras and Rab interactor 1 (Rin1) is activated downstream of EGFR (Barbieri *et al.*, 2003) through binding of the Rin1 SH2 domain to phosphorylated tyrosine residues of the receptor. Other Rab5 GEFs exist, including Rabex-5 (Horiuchi *et al.,* 1997), alsin (Topp *et al.,* 2004) and GAPex-5 (also called RME-6, RAP-6 and GAPVD1 because it has dual GEF and GAP activity) (Su *et al.,* 2007). Though the GEFs have the overlapping function of activating Rab5, they may be specific to one isoform of Rab5 or act in different circumstances. After upstream receptor signaling, Rin1 is thought to be the first activator of Rab5, linking endocytosis to the activation of receptors (Jozic *et al.,* 2012). On early endosomes, the binding of the Rab5 effector Rabaptin-5 induces a positive feedback loop of Rab5 activation by the recruitment of Rabex-5 (a binding partner of Rabaptin-5) and allows for the enrichment of active Rab5 on early endosomes, counteracting the intrinsic GTPase activity of Rab5 (Horiuchi *et al.,* 1997; see Figure 1.6). Regulatory proteins of Rab5 are summarized in Table 1.1.

The role of active Rab5 is to recruit effector proteins that bind specifically to Rab5-GTP. Active Rab5 is found at the plasma membrane as well as on early endosomal membranes (Ali *et al.*, 2004). Rab5 has been associated with cargo selection into clathrin-coated membrane invaginations as well as clathrin-independent receptor internalization by macropinocytosis (or fluid-phase endocytosis; "cell drinking") through its effector Rabankyrin-5 (Schnatwinkel *et al.*, 2004). Another important Rab5-mediated process is the modification of phosphatidylinositols on the early endosomal membrane by the concerted activity of Rab5 effectors. PI3K (section 1.2.2.1), phosphatidylinositol 4`-phosphatase and phosphatidylinositol 5`-phosphatase enrich the early endosome with PtdIns-3-P (Shin *et al.,* 2005) by generating and dephosphorylating the

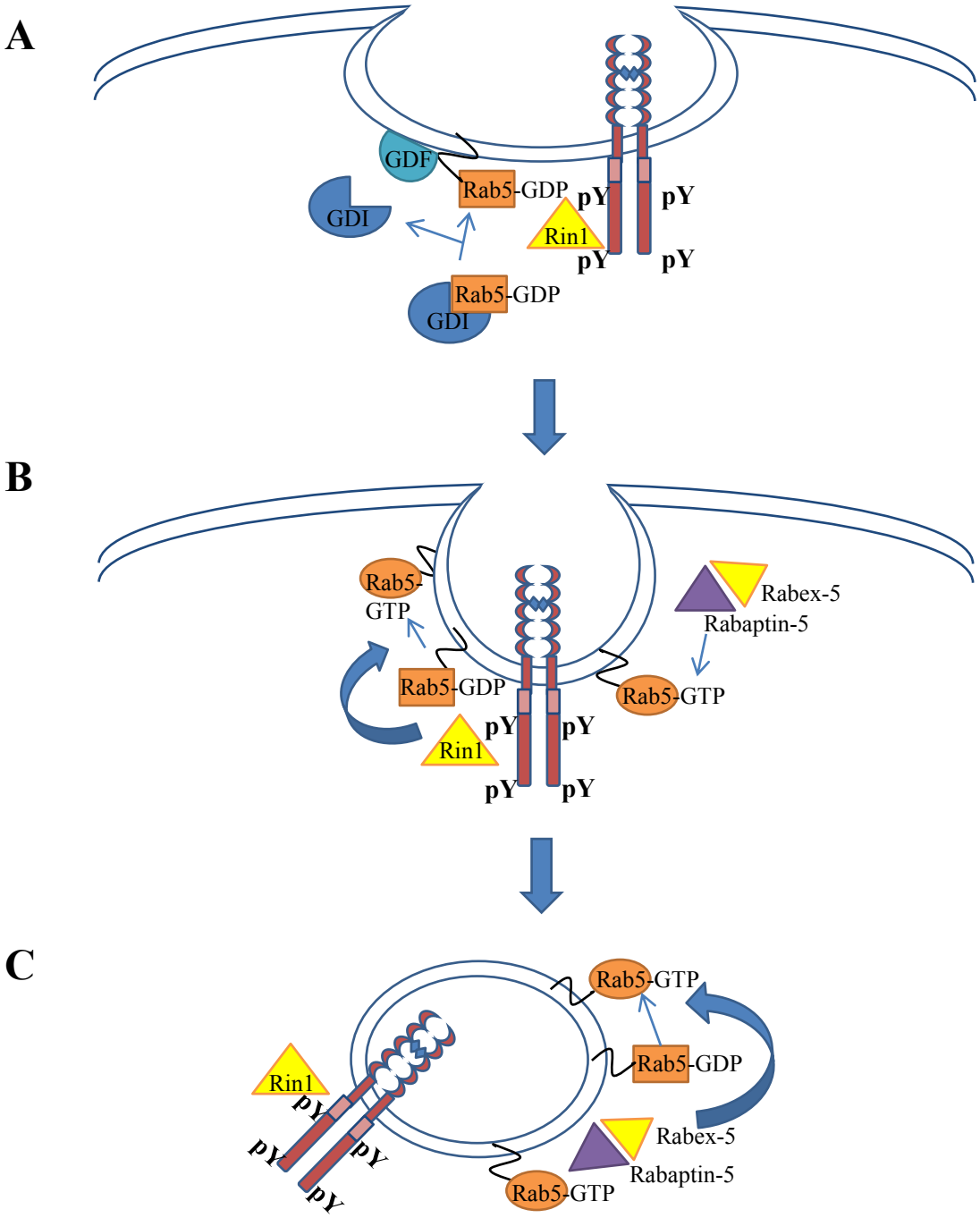

Figure 1.6 Rab5 activation by different GEFs. A. Membrane recruitment of Rab5 by GDF displacement of GDI. **B.** Receptor-interacting GEF Rin1 activates Rab5 by exchanging bound GDP for GTP. Rab5-GTP recruits effector proteins such as Rabaptin-5 which bind to specific epitopes on active Rab5. **C.** Positive feedback loop whereby Rabex-5, which is recruited by active Rab5 through its binding partner Rabaptin-5, enhances Rab5 GDP for GTP exchange.

Table 1.1 Regulatory proteins of Rab5.

Protein	Function	Reference
Rin-1	GEF, downstream of receptor signalling	Barbeiri, *et al.,* 2003; Jozic *et al*., 2012
Rabex-5	GEF, positive feedback on early endosomes	Horiuchi *et al.,* 1997
Alsin	GEF	Topp *et al.,* 2004
GAPex-5	GEF/GAP	Su *et al.,* 2007
Tuberin	GAP	Xiao *et al.,* 1997
RabGAP-5	GAP, arginine finger is R165	Haas *et al.,* 2005
PRC17	GAP, arginine finger is R107	Pei *et al.,* 2002
p85	GAP, arginine finger is R274	Chamberlain *et al.,* 2004
RN-tre	GAP, arginine finger is R150, also acts on Rab41	Lanzetti *et al.,* 2000; Haas *et al.,* 2005

PtdIns-3,4,5-P_3 lipid product, respectively (Figure 1.7). In addition, the class III PI3K, Vps34, directly generates PtdIns-3-P from PtdIns (Shin *et al.,* 2005; Figure 1.7). Rab5 protein effectors with FYVE domains, *i.e.* EEA-1 and Rabenosyn-5, interact with both Rab5 and PtdIns-3-P on early endosomes to form a tether between two early endosomes. The proximity of the two vesicles allows membrane anchored proteins called soluble N-ethylmaleimide-sensitive attachment protein receptors (SNAREs) to interact *in trans* with high affinity, effectively mediating the fusion of vesicle membranes in what is called homotypic or lateral fusion (Woodman, 2000).

Expression of a dominant negative mutant of Rab5, *i.e.* Rab5-S34N which selectively binds GDP, results in the inhibition of both early endosomal homotypic fusion and receptor internalization by macropinocytosis (Barbieri *et al.,* 2000). In its inactive conformation, Rab5 cannot recruit the phosphatidylinositol modifying enzymes nor the FYVE-domain containing proteins required to bring early endosomes together. Thus, SNARE proteins cannot promote the homotypic fusion important for receptor cargo sorting in the early/ "sorting" endosome because their interaction requires the juxtaposition of the membranes to be fused (Woodman, 2000). Expression of Rab5-Q79L, which lacks GTPase activity such that it is locked in an active Rab5-GTP conformation, in contrast, results in the formation of enlarged early endosomes (Barbieri *et al.,* 2000) due to increased early endosome fusion.

Several GTPase activating proteins of Rab5 have been discovered and include proteins tuberin (Xiao *et al.,* 1997), RabGAP-5 (SGSM3) (Haas *et al.,* 2005), PRC17 (TBC1D3) (Pei *et al.,* 2002) and p85 (Chamberlain *et al.,* 2004). All of these proteins have been shown to increase the rate of GTP hydrolysis compared to purified Rab5 alone. Additionally, the GAP activity of most of these proteins, except tuberin which was not tested, was abolished after mutation of a specific arginine residue, the catalytically important arginine finger (Table 1.1). The significance of having multiple GAPs for Rab5 is unknown, but may be a form of redundancy to ensure the appropriate inactivation of Rab5. The specificity of the aforementioned GAPs toward Rab5 isoforms has not been investigated.

The crystal structure of Rab5 has been determined, alone as well as in complex with some of its effectors (Zhu *et al.,* 2003; Terzyan *et al.,* 2004; Zhu *et al.,* 2004; Eathiraj *et al.,* 2005; Mishra *et al.,* 2010). The most studied effector of Rab5 is EEA-1, which is important for

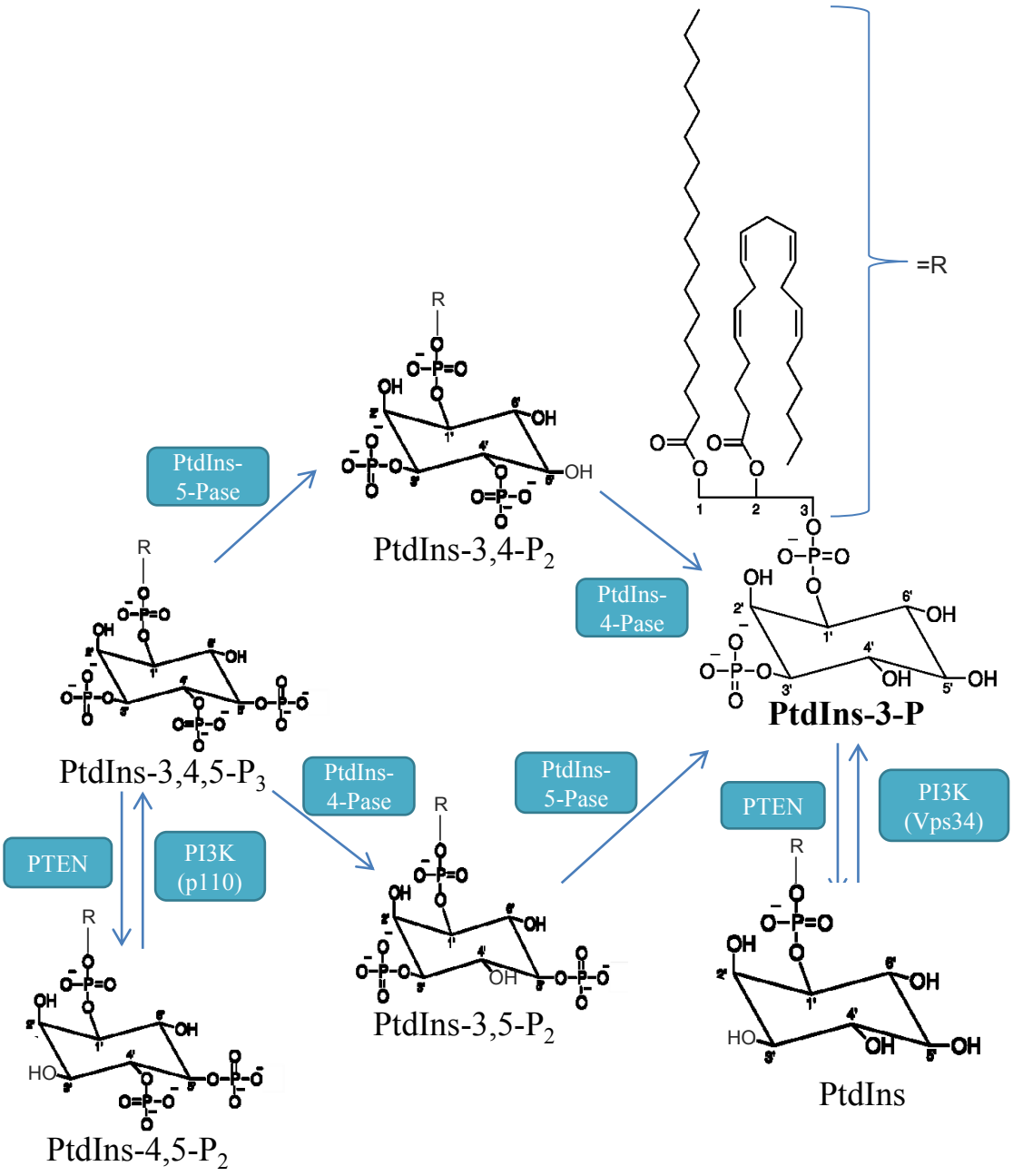

Figure 1.7 Generation of phosphorylated phosphatidylinositol signaling intermediates. Phosphatidylinositol (PtdIns) is a phospholipid component of the plasma membrane. Kinases and phosphatases act on the 3`, 4`and 5`hydroxyl groups to increase or decrease, respectively, protein affinity for the phospholipid. From the right, PtdIns-4,5-$P_2$ is phosphorylated by phosphatidylinositol-3`-kinase catalytic subunit p110, making PtdIns-3,4,5-P_3. This phosphorylation is antagonized by phosphatase PTEN. PtdIns-3,4,5-P_3 recruits cytoplasmic proteins with a PH domain. Sequential dephosphorylation by PtdIns-4-Pase and PtdIns-5-Pase, either order, leads to the accumulation of PtdIns-3-P on endosomal membranes. Proteins with a FYVE finger domain interact with PtdIns-3-P and act to tether endosomal membranes together. Another method of PtdIns-3-P generation is through phosphorylation of PtdIns by Vps34, another phosphatildylinositol-3`-kinase. Lipid group (R) is as indicated in the figure (*right*).

docking or tethering the internalized vesicles with the early endosome. It is known that EEA-1 interacts with both Rab5-GTP as well as PtdIns-3-P lipid, the latter through its FYVE-finger domain. A similar interaction is seen with Rab5 and Rabenosyn-5, which also has a FYVE domain. Because these proteins are effectors, they recognize an epitope on Rab5 which is unavailable in its GDP-bound inactive state.

Crystal structures of Rab5 in complex with an effector require the protein to be in its active GTP-bound state. Since Rab5 has intrinsic GTPase activity, crystals are either prepared in the context of a GTPase-deficient mutant of Rab5 (*e.g.* Q79L) or, more commonly, with a non-hydrolysable GTP-analogue (Terzyan *et al.,* 2004; Zhu *et al.,* 2004). Examples of these GTP analogues include GTPγS (Guanosine 5′-[gamma-thio] triphosphate), which replaces a γ-phosphate group oxygen with a sulfur atom, GppCp (Guanosine 5′-[β, γ methyleno]-triphosphate) and GNP (Guanylyl 5′-[β, γ] imidodiphosphate) which replace the β-γ bridge oxygen with either carbon or nitrogen, respectively (Figure 1.8). By replacing GTP with one of these analogues, the hydrolysis reaction is impeded, in the case of GTPγS, or inhibited, keeping wild-type Rab5 in its active conformation. These minor changes in the structure of the nucleotide may affect some Rab5 contacts with its effectors, compared to what occurs *in vivo*, but this is the compromise for having a stable active-state Rab protein for binding studies.

1.4.1.2 Rab4 and Rab11 recycling pathways

Rab4 and Rab11 are involved in the recycling pathway of RTK trafficking (Stenmark, 2009). Both proteins can be found associated with the early endosomal membrane, though Rab4 can be found within Rab4/Rab5 microdomains as well as Rab4/Rab11 microdomains (Zerial and McBride, 2001). Rab4 is essential for rapid recycling of cargo back to the plasma membrane, whereas Rab11 is involved in a slower recycling process that involves sorting through a recycling endosome before returning cargo to the plasma membrane (Stenmark, 2009).

Recycling receptors back to the plasma membrane allows them to be activated again, and is important for sustained signaling especially when growth factor concentration is limiting. Rab4 is critical for the constitutive recycling important for maintaining steady-state levels of dopamine receptor 2 and transferrin receptors (Li *et al.,* 2012). Rab11-positive recycling endosomes are found near the nucleus and are important for dopamine-stimulated recycling of

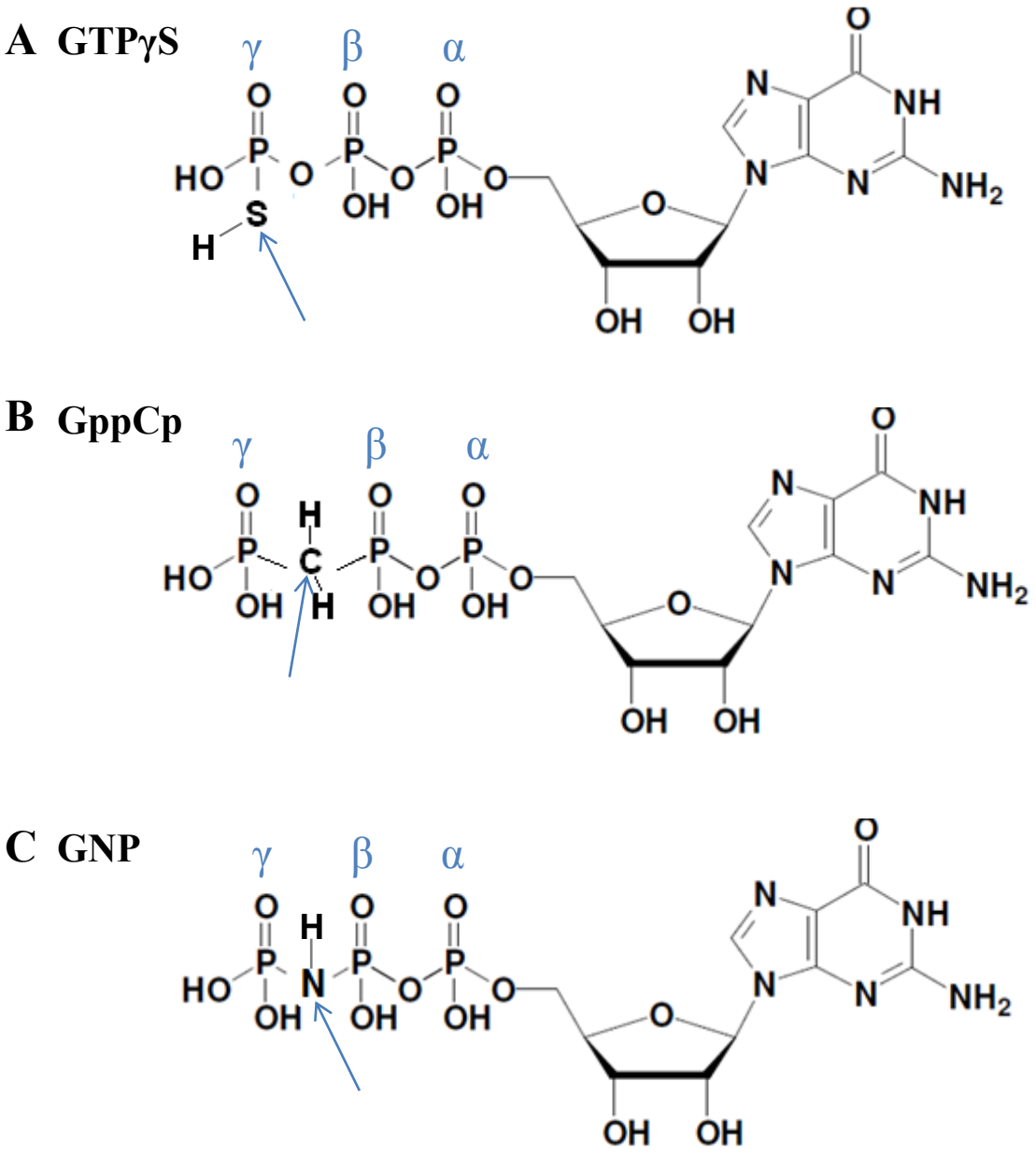

Figure 1.8 Non-hydrolysable GTP analogues. A. GTPγS (Guanosine 5′[gamma-thio]-triphosphate. **B.** GppCp (Guanosine 5′[β, γ methyleno]-triphosphate, figure from www.jenabioscience.com. **C.** GNP (Guanosine 5′[β, γ]- imidotriphosphate). Modifications of the nucleotide are indicated with blue arrows.

the dopamine receptor 2, as shown in studies using dominant negative Rab11 mutants in cultured mouse striatal medium spiny neurons (Li *et al.*, 2012). Through total internal reflection fluorescence microscopy (TIRFM) it has been discovered that Rab-11 is also implicated in the exocytosis of cargo in recycling endosomes, *i.e.* transferrin receptor, at the plasma membrane through fusion steps analogous to Rab5-dependent fusion of early endosomes (Takahashi *et al.*, 2012). The regulation of internalized receptor recycling seems to be determined by ligand binding and involves one of two routes: ligand-independent Rab4-mediated fast recycling or ligand-dependent Rab-11-mediated slow recycling through the recycling endosome.

1.4.1.3 Rab protein domains and conversion of endosomes

Some Rab5 effector proteins also have affinity or a separate binding site for Rab4, which explains their combined microdomain on early endosomes. One such effector is Rabaptin-5 which binds both Rab5 and Rab4 via separate domains (Somsel-Rodman and Wandinger-Ness, 2000). In bringing Rab5 and Rab4 together in complex, Rabaptin-5 connects endocytosis with the recycling network. No such interactivity has been described between Rab5 and Rab11.

It is thought that some endosomal compartments undergo conversion or "maturation" as the lipid identity and associated coat-proteins are altered and replaced. The theory is compelling at least for early to late endosomal maturation, which has been used as a model for Rab-mediated endosome conversion (Spang, 2009). The switch protein Mon1 is recruited to the early endosome and displaces Rabex-5, disrupting the Rab5 positive activation feedback loop. Mon1 also recruits the homotypic fusion and vacuole protein sorting (HOPS) complex, which is responsible for nucleotide exchange and activation of Rab7 (Poteryaev *et al.*, 2010). The Rab7-GTP concentration increases due to the recruitment of HOPS and active Rab5 is reduced in time due to the activity of GAPs, therefore converting Rab identity of the early endosome (Rab5-enriched) into a late endosome (Rab7-enriched). In the case of Rab4 or Rab11 recycling endosomes, it is believed that vesicle budding from early endosomes to a separate endosome occurs, rather than maturation.

1.5 GAP proteins

GAPs provide two functions: a conserved arginine finger and stabilizing interactions with the switch regions of small monomeric GTPases (Fidyk and Cerione, 2002). GAPs may be multi-domain proteins that have a GAP, BH, or Tre-2/Bub-2/Cdc16 (TBC) domain. Conserved among these domains is the presence of a catalytic arginine finger. This arginine residue acts in three ways to enhance GTP hydrolysis. First, the backbone carbonyl forms a hydrogen bond with glutamine 61 of Ras (equivalent to Q79 of Rab5), which is known to draw the polar charge of the electrophilic water by hydrogen bonding (Figure 1.9). Second, the guanidinium functional group forms hydrogen bonds with oxygens of the α-phosphate, the α-β bridge, the γ-phosphate and/or the β-γ bridge oxygen, stabilizing the transition-state (Figure 1.9). Third, the insertion of arginine into the nucleotide binding pocket displaces 5 water molecules, therefore decreasing the entropy of the reaction by as much as 40 kJ/mol (Kotting *et al.,* 2007).

Most studies of GAP activity have been explored in the context of Ras, and though much of what has been learned may be true for Rab protein regulation as well, not all will be transferrable. For example, many Rab GAPs contain a conserved TBC domain which functions through a two-finger mechanism: an arginine finger and a glutamine finger, though some unconventional TBC domain-containing proteins act through a single arginine finger (Pan *et al.,* 2006). There are 44 predicted TBC-containing proteins in the human genome; of these, 19 TBCs whose substrates have been elucidated. Nineteen other RabGAPs have been identified (Frasa *et al.,* 2012).

Switch stabilization of small GTPases during GTP hydrolysis may also contribute to the effectiveness of a particular GAP. Because of the mobility of the switch region loops in the GDP conformation in most small GTPases, stabilization of these regions is a conserved function in the GAPs that regulate them. Mutation of arginine fingers to alanine in the GAPs p85 and p50rhoGAP reduced overall GAP function, but did not abolish it (Leonard *et al.,* 1998; Chamberlain *et al.,* 2004). In the co-crystal structure of Cdc42-p50rhoGAP contacts are made between the switch regions of Cdc42 and residues N414 and N422 of p50rhoGAP (Nassar *et al.,* 1998). Mutation of these residues on p50rhoGAP greatly reduced its activity (Fidyk and Cerione, 2002) suggesting that contacts between switch regions of small GTPases and their GAPs are catalytically important.

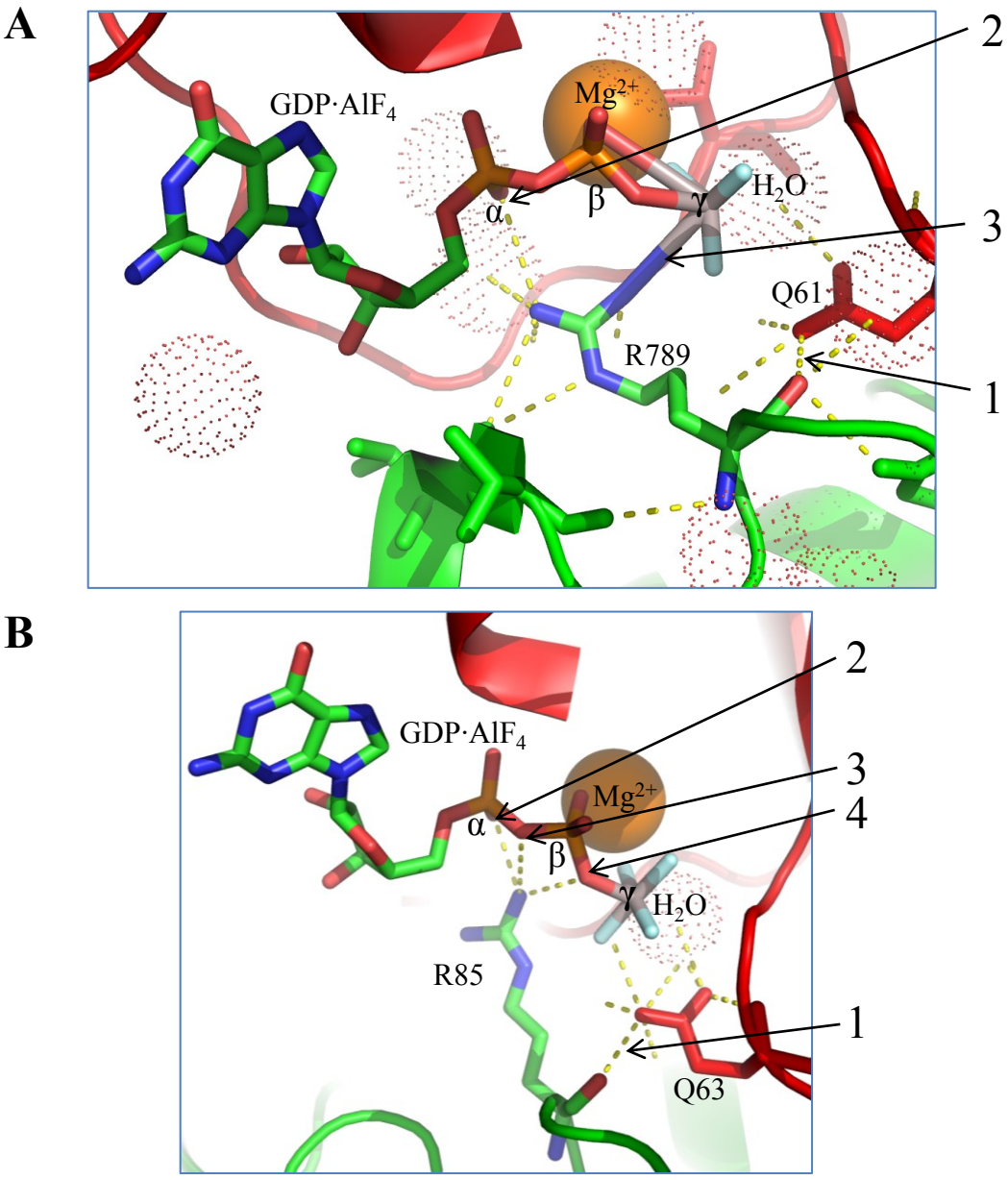

Figure 1.9 Arginine finger mechanism of action. A. Co-crystal structure of Ras (*red*) and p120rasGAP (*green*) with GDP·AlF_4 (PDB ID: 1WQ1). The arginine finger of p120rasGAP, R789, enhances GTP hydrolysis by hydrogen bonding with Ras Q61 (indicated by arrow 1), which coordinates a water molecule, and by forming a hydrogen bond with the α-phosphate oxygen (arrow 2) and a covalent bond with γ-Al fluoride (arrow 3) to stabilize the transition state. **B.** Co-crystal structure of Rho (*red*) and p50rhoGAP (*green*) with GDP·AlF_4 (PDB ID: 1TX4). The arginine finger of p50rhoGAP, R85, employs a similar hydrogen bonding pattern with Rho Q63 (arrow 1), the α-phosphate (arrow 2) the α-β bridge (arrow 3) and the β-γ bridge (arrow 4) oxygens.

More than one GAP can regulate Rab5. Since Rab5 is an important component of the endocytic machinery it may have redundant regulators. Alternatively, the differential expression and subcellular distribution of GAPs, through other protein or lipid binding domains, may ensure that Rab5 inactivation occurs on distinct intracellular membranes in a timely manner (Frasa *et al.,* 2012). Tuberin was the first described Rab5 GAP (Xiao *et al.,* 1997). RN-tre was determined to have Rab5 GAP activity through its TBC domain (Lanzetti *et al.,* 2000), though in HeLa cells it predominantly regulates Rab41 (Haas *et al.,* 2005). PRC17, also known as TBC1D3, was identified as a gene amplified in prostate cancers and a protein overexpressed in both prostate and breast cancers. Its Rab5 GAP activity was determined to drive tumorigenicity in those cells (Pei *et al.,* 2002). Other described Rab5 GAPs include RabGAP5, and p85. Some GAPs have activity towards more than one small GTPase target *in vitro, i.e.* TBC1D1 which regulates Rab2A, Rab8A, Rab8B, Rab10, and Rab14, though the *in vivo* relevance is unknown (Roach *et al.,* 2007). Therefore, some of Rab5 GAPs mentioned may have additional Rab protein targets (including the different isoforms of Rab5) and could be important for Rab protein downregulation in a specific cellular context.

1.5.1 Role for p85 in the regulation of Rab proteins

Though it is known as a regulatory subunit of PI3K, p85α has also been shown to have catalytic activity as a GAP towards Rab4, Rab5 (as mentioned previously), Rac1, Cdc42 and to a lesser extent Rab6 *in vitro* (Chamberlain *et al.,* 2004) through its BH domain. The smaller isoforms of PI3K regulatory subunits do not contain the BH domain, and do not have GAP activity. The arginine finger of p85 has been identified as R274 (Chamberlain *et al.,* 2004). Mutation of arginine 274 to alanine reduces GAP activity of purified p85 *in vitro* by 95% (Chamberlain *et al.,* 2004). Though mutations in the BH domain are uncommon in cancers, p85-R274A was able to drive tumorigenesis in a xenograft mouse model (Chamberlain *et al.,* 2008) by increased and sustained MAPK activation (Chamberlain *et al.,* 2004). The transforming phenotype of p85-R274A cells was reversed by the co-expression of dominant negative mutant Rab5-S34N, suggesting that the disruption of GAP activity towards Rab5 (and therefore increased Rab5-GTP) was the mechanism by which cells were transformed (Chamberlain *et al.,* 2008).

Interaction between Rab5 and PI3K has been investigated. Both the regulatory (p85) and catalytic (p110β) subunits have been found to bind to the small GTPase (Chamberlain *et al.*, 2004; Chirstoforidis *et al.*, 1999; Kurosu and Katada, 2001). Specifically, GST pull-down assays have demonstrated GST-Rab5 binding to p85 regardless of its nucleotide-bound status, *i.e.* Rab5-GDP or Rab5-GTPγS (Chamberlain *et al.*, 2004). Through yeast two-hybrid (Kurosu and Katada, 2001) and affinity columns (Christoforidis *et al.*, 1999) the binding of Rab5 to the p110 β isoform has been shown. This interaction occurs only when Rab5 is in its active conformation (Christoforidis *et al.*, 1999), which can be approximated by binding to non-hydrolysable GTP analogues such as GTPγS. The binding site between p110β and Rab5-GTP has been narrowed down to residues 136-270 and 658-759 on the p110β protein (Kurosu and Katada, 2001).

1.5.2 Non-catalytic involvement of p110 in trafficking

The drug wortmannin is a pan-PI3K inhibitor which also affects early endosome morphology (Mills *et al.*, 1999). At 100 nM, the inhibitor reduces PI3K activity by up to 80% (Martys *et al.*, 1996) and its effect on downstream signaling can be evaluated by probing whole cell lysates with phospho-specific Akt antibodies. In many cell types, wortmannin treatment induces the formation of enlarged cytoplasmic vesicles (Chen and Wang, 2001a; Houle and Marceau, 2003) where endocytosed receptors are found. In wortmannin-treated cells, the degradation of receptors is sometimes increased, as in the case of bradykinin receptor and induced, in the case of the transferrin receptor (Houle and Marceau, 2003; Martys *et al.*, 1996; Chen and Wang, 2001a). The enlarged vesicles are not affected by the replenishment of PI3K products, namely PtdIns-3-P, PtdIns-3,4-P_2 and PtdIns-3,4,5-P_3 in wortmannin-treated cells (Chen and Wang, 2001b), suggesting that although wortmannin inhibits PI3K lipid kinase activity, p110 also has a role in endocytic trafficking which is being disrupted by the drug. Similar enlarged early endosomes can be seen when the active conformation mutant Rab5-Q79L is expressed in cells (Barbieri *et al.*, 2000; Chen and Wang, 2001a) as mentioned in section 1.4.1.1. Also, the wortmannin-induced formation of enlarged vesicles is inhibited by expression of Rab5-S34N (Houle and Marceau, 2003; Hunyady *et al.*, 2002; Chen and Wang, 2001a, b). Therefore, a Rab5-mediated function of receptor trafficking requires a kinase-independent function p110.

Genetic knock-out of either *PIK3CA* (p110α) or *PIK3CB* (p110β) results in early embryonic death in mice, but knock-ins of catalytically dead p110β lead to survival in mice, though their growth lagged behind wild-type p110β-expressing mice (Ciraolo *et al.*, 2008). Additionally, endocytic trafficking of both transferrin and EGFR were altered when p110β was knocked out or expressed at lower levels (Ciraolo *et al.* 2008; Jia *et al.*, 2008) but they were restored to normal by the re-expression of the kinase-dead mutant p110β. These data support the idea that p110β has some function within the endocytic pathway that is unrelated to its kinase activity.

We postulate that p85 and p110β act together to provide the catalytic arginine finger and the switch stabilization features of a GAP, respectively, in order to inactivate Rab5 and shut down receptor trafficking. This cooperative heterodimer model of GAP activity is extremely rare and has not been described in the literature for Rab proteins. Some GAPs have been shown to act as homo- and hetero-dimers for other GTPases. For example, regulators of G-protein coupled receptor signaling (RGS) can form complexes with the subunits of the heterotrimeric G-protein coupled receptors (GPCRs) to promote GAP activity (Snow *et al.*, 1998). Another example is CAPRI, a GAP with activity towards Ras and Rap1, which alters its substrate specificity by Ca^{2+}-dependent homodimerization (Dia *et al.*, 2011). Also, plant-specific Rho (ROP) GAPs have also been found to act as homodimers (Schaefer *et al.*, 2011). However, in the regulation of Rab GTPases, GAPs are normally monomeric (Frasa *et al.*, 2012; Paduch *et al.*, 2001).

In order to assess the validity of the p85/p110 heterodimeric GAP model, the binding sites between these two proteins and Rab5 should be determined. Residues which bind and stabilize the switch regions of Rab5 have not been identified in the structure of p85, and may be provided by its binding partner, p110β. The binding sites of p85 and p110β on the Rab5 protein were sought using site-directed mutation and pull-down experiments. Non-binding mutants generated in this thesis (i.e. p110βΔRab5 and/or Rab5Δp110β) will be used in future research to test if there is p85/p110β cooperation in regulating the GTPase activity of Rab5.

2.0 HYPOTHESIS AND OBJECTIVES

2.1 Rationale

The regulation of the nucleotide bound status of Rab5 requires both GEFs and GAPs (Paduch *et al.*, 2001; Stenmark, 2009; McMahon and Boucrot, 2011). Our lab has identified the regulatory subunit of PI3K, p85, to be a GAP for Rab5 (Chamberlain *et al.,* 2004). Mutation of its arginine finger greatly reduced GAP activity but did not abolish it (Chamberlain *et al.*, 2004). Other studies have shown that a second function of GAP proteins is to provide stabilizing contacts to the mobile switch regions of small GTPases (Fidyk and Cerione, 2002). No such interaction has been identified between p85 and Rab5, as p85 binds to both Rab5-GDP and Rab5-GTP (Chamberlain *et al.,* 2004) despite their differences in switch region conformation. A binding partner of p85, p110β, binds to Rab5 in its GTP-bound state only (Christoforidis *et al.*, 1999; Kurosu and Katada, 2001). Therefore, this thesis proposes that p85 and p110β act together to perform the two functions of a GAP: p85 providing the catalytic arginine finger and p110β providing the switch region stabilization. The regulation of p85 and p110β towards Rab5 can be evaluated by disruption of contact regions between Rab5 and p85 as well as Rab5 and p110β. In order to disrupt binding, the regions of contact between the proteins must first be identified.

2.2 Hypotheses

The hypotheses of this work were two-fold: I) The binding of p85 to Rab5 is conformation-independent and involves Rab5 amino acids outside of the switch regions. II) The binding of p110β to Rab5 is conformation dependent and involves Rab5 amino acids within the switch I (AA 42-52) and/or switch II (AA 77-95) regions of Rab5.

2.3 Objectives

The objectives of this thesis were:

1) To determine the p85 binding site on Rab5 by pull-down experiments with wild-type FLAG-p85 and immobilized Rab5 non-switch region mutants.
2) To determine the p110β binding site by pull-down experiments with Myc-iSH2-p110β and immobilized Rab5 switch region mutants.
3) To determine the Rab5 binding site on p110β by pull-down experiments using immobilized wild-type Rab5 and Myc-iSH2-p110β mutations in the Ras-binding domain.

3.0 MATERIALS AND METHODS

3.1 Materials

3.1.1 Mammalian cells

COS-1 *Cercopithecus aethiops* (green monkey) SV40 transformed kidney cells from the American Type Culture Collection (#CRL-1650) were used in transient transfections to overexpress FLAG-p85 and Myc_3-iSH2-p110α/β protein.

3.1.2 Yeast strains

Yeast two-hybrid experiments were performed using two strains of *Saccharomyces cerevisiae*: EY111 (*MATα, his3, trp1, ura3::LexA8op-lacZ, ade2::URA3-LexA8op-ADE2 leu2::LexA6op-LEU2*) and EY93 (*MATa, ura2, his3, trp1, leu2, ade2::URA3*) (Barreto *et al.*, 2009) both generously provided by Dr. Ronald Geyer (University of Saskatchewan).

3.1.3 Bacterial cells and culture

DNA amplification was performed within the *Escherichia coli* (*E. coli*) strain TOP10 [F^-, *mcr*A, D(*mrr-hsd*RMS-*mcr*BC), f80*lac*ZDM15 D*lac*X74, *deo*R, *rec*A, *ara*D139 D(*ara-leu*)7697, *gal*K, *rps*L(StrR), *end*A1, *nup*G] (Invitrogen). GST-fusion proteins were overexpressed in protease-deficient BL21 [*E. coli B,* F-, *dcm, ompT, hsdS(rb-mb-), gal*] cells (Amersham). Both bacterial strains were grown in Millar's Luria Bertani broth (LB, Sigma-Aldrich), supplemented with 100 µg/mL ampicillin (Sigma-Aldrich), at 37°C in a shaking incubator.

3.1.4 Antibodies

All antibodies were purchased from Santa Cruz Biotechnology, with the exception of anti-FLAG-M2 (Sigma-Aldrich Canada, Ltd.; Oakville, ON) and anti-p85 nSH3 (Millipore; Billerica, MA). Secondary antibodies were goat anti-mouse or goat anti-rabbit conjugated to infrared dye (LI-COR Biosciences; Lincoln, NB) and were visualized using LI-COR imaging and Odyssey software V3.0. All antibodies used are summarized in Table 3.1.

Table 3.1 Primary and secondary antibodies used to probe protein blots.

Antibody Name, species	Company and Cat. #	Figure(s)	Concentration used
Anti-FLAG (M2), mouse	Sigma-Aldrich, F3165	4.1, 4.4, 4.5	10 µg/mL
Anti-PI3K p85 N-SH2, mouse	Millipore, 05-217	4.1, 4.8	1 µg/mL
Anti-Rab5 (FL-215), rabbit	Santa Cruz Biotechnology, SC-28570	Not shown	10 µg/mL
Anti-Myc-C (A14), rabbit	Santa Cruz Biotechnology, SC-789	4.9, 4.11, 4.13	10 µg/mL
IRDye 680 Anti-Mouse, goat	LI-COR Biosciences, 926-32220	4.1, 4.4, 4.5, 4.8	0.132 µg/mL
IRDye 680 Anti-Rabbit, goat	LI-COR Biosciences, 926-32221	4.9, 4.11, 4.13	0.132 µg/mL
IgG AC (normal), mouse	Santa Cruz Biotechnology, SC-2343AC	4.8	10 µg/ 0.5 mL
Myc mAb (agarose conjugated), mouse	Santa Cruz Biotechnology, SC-14428AC	4.8	10 µg/ 0.5 mL

3.1.5 Plasmids and vectors

Both p85α (human) and Rab5A (dog) cDNAs were subcloned separately into pGEX6P1 vector (Amersham). All GST-Rab5 mutants were generated within this construct, which has two amino acid substitutions (S3N, N210S) compared to human Rab5. The human cDNA of Rab5A was subcloned into the vector pGEX3X, which is similar to pGEX6P1 except it contains a Factor Xa cleavage site instead of a PreScission protease cleavage site in the multiple cloning site (Amersham). The p110 protein chimeras were generated in the $pMyc_3$-$p110\alpha_{mouse}/p110\beta_{human}$ plasmid (Pastor, 2004; James, 2005) which was derived from the pRC/CMV vector (Invitrogen). The yeast two-hybrid bait plasmid pEG202 allows the constitutive expression of LexA-fusion protein as well as the auxotrophic selectable marker, histidine. The yeast two-hybrid pJG4-5 prey plasmid allows the expression of a galactose-induced B42-fusion protein as well as the constitutive expression of the auxotrophic selectable marker, tryptophan. Both plasmids were provided by Dr. Ronald Geyer (University of Saskatchewan).

3.1.6 Primers

Table 3.2. Primers for GST-Rab5 mutagenesis and pMyc$_3$-iSH2-p110beta mutagenesis. All primers were custom-ordered through Invitrogen Life Technologies. Primers were used for mutagenesis in sense/antisense pairs with the sense strand as indicated below with mutant codon underlined.

Mutagenesis Primers	
Primer Name	**Sequence**
GST-Rab5 S84A	CGA TAC CAT GCC CTA GCA CCA ATG
GST-Rab5 S84L	GAA CGA TAC CAT CTC CTA GCA CCA ATG
GST-Rab5 S84E	CAA GAA CGA TAC CAT GAG CTA GCA CCA ATG TAC
GST-Rab5 S84R	CAA GAA CGA TAC CAT AGG CTA GCA CCA ATG TAC
GST-Rab5 E106A	C ACA AAT GAG GCG TCC TTT GCA AG
GST-Rab5 N113A	GCA AGA GCA AAA GCT TGG GTT AAA GAA C
GST-Rab5 N113RE	GCC AGA GCC AAA TTG TGG GTT AAA GAA C
GST-Rab5 F145A	GA GCT GTC GAT GCC CAG GAA GCA C
GST-Rab5 E172A	G AAT GTA AAT GCA ATA TTC ATG G
GST-Rab5 E172R	G AAT GTA AAT CGA ATA TTC ATG GC
GST-Rab5 M175A	GAA ATA TTC GCG GCA ATA GCT
GST-Rab5 K179A	GCA ATA GCT GCA AAG TTG CCA
GST-Rab5 K180A	CA ATA GCT AAA GCG TTG CCA AAG
GST-Rab5 K179E+K180E	C ATG GCA ATA GCT GAA GAG TTG CCA AAG
GST-Rab5 Q44E	GTG AAG GGC GAA TTT CAT GAA
GST-Rab5 H46A	GGC CAA TTT GCT GAA TTT CAA GAG
GST-Rab5 E47A	GGC CAA TTT CAT GCA TTT CAA GAG AG
GST-Rab5 I53A	GAG AGT ACC GCA GGG GCT GC
GST-Rab5 F57A	CC ATT GGG GCT GCT GCT CTA ACC C
GST-Rab5 W74A	G TTT GAA ATA GCG GAT ACA GCT GG
GST-Rab5 E80R	CA GCT GGT CAA CGA CGA TAC CAT AG
GST-Rab5 R81E	GCT GGT CAA GAA GAA TAC CAT AGC C
GST-Rab5 Y82A	GGT CAA GAA CGA GCC CAT AGC CTA GC
GST-Rab5 H83E	CAA GAA CGA TAC GAG AGC CTA GCA CC
GST-Rab5 L85A	CGA TAC CAT AGC GCA GCA CCA ATG TAC
GST-Rab5 M88A	GC TTA GCA CCA GCG TAC TAC AGA GG
GST-Rab5 Y89A	C TTA GCA CCA ATG GCC TAC AGA GGA GC
GST-Rab5 R91E	CCA ATG TAC TAC GAA GGA GCA CAA GC
p110betahuL232A	C CAA AAA CGT GCG ACT ATT CAT GG
p110betahuI234A	CGT TTG ACT GCT CAT GGG AAG G
p110betahuE238R	CAT GGG AAG AGA GAT GAA GTT AGC C
p110betahuD239R	GGG AAG GAA CGT GAA GTT AGC CCC
p110betahuY244A	GTT AGC CCC GCT GAT TAT GTG TTG C

Table 3.3 Other primers. All primers were custom-ordered through Invitrogen Life Technologies. All sequencing primers are mentioned first, followed by special primers that include: the NheIGly7 primers used for the generation of the glycine linker (glycine codons underlined) of $pMyc_3$-iSH2-p110, the PCR primers for the amplification of p85 iSH2 domain (p85 codons underlined) for $pMyc_3$-iSH2-p110, and primers for amplification of full-length p85 (p85 codons underlined) and full-length Rab5 (Rab5 codons underlined) for homologous recombination.

Primer Name	Sequence
Sequencing Primers	
5′GST	TTT GCA GGG CTG GCA AGC
5′Myc-seq	GGA TCT GCT GAG CGA GCA G
5′pEG202 seq	GGG CTG GCG GTT GGG GTT ATT C
5′pJG4-5 seq	GGA CAG GAG ATG CCG ATG GA
5′b110seq114	CAA GAA GTT GTG ACC CAG G
5′b110seq272	TGT GTG ATG AAC AGA GCC C
5′b110seq435	GCA TTA TCC TGT AGC GTG G
5′b110seq561	TTT GCG ACA AGA CTG CCG AGA G
5′b110seq816	GAC ACT CCA AAT GTT GCG
3′b110seq875	GGC ATC TTT GTT GAA GGC
5′p110seq1	ATG CCT CCA CGA CCA TCT
5′p110seq401	CAG AAG TCC AAG ACT TTC
5′p110seq801	AGT CAG TAC AAG TAC ATA
5′p110seq1203	CCT TTG CCT TTC AAT CTG
5′p110seq1604	GCA CCC GGG ACC CAC TAT
5′p110seq2005	TGG CAT TTA AAA TCT GAG
5′p110seq2401	TTT AAA AAT GGC GAC GAC
5′p110seq2808	TGG GCA CTT TTT GGA TCA
Special Primers (Linkers and PCR)	
5′NheIGly7	CT AGC GGT GGA GGA GGT GGT GGA GGT A
3′NheIGly7	CT AGT ACC TCC ACC ACC TCC TCC ACC G
5′NheIp85iSH2	GCA GCT AGC TTA TAT GAA GAA TAT ACC CG
3′NheIp85iSH2	CCA GCT AGC TTT AAT GCT GTT CAT ACG TTT G
5′BamHI-pEG202-p85	GTT ATT CGC AAC GGC GAC TGG CTG GAA TTC CCG GGG ATC CGT AGT GCC GAG GGG TAC CAG
3′NotI-pEG202-p85	GGA ATT AGC TTG GCT GCA GGT CGA CTC GAG CGG CCG CCA TTA TCG CCT CTG CTG CGC GTA
5′EcoRI-pJG4-5-Rab5	TAC CCT TAT GAT GTG CCA GAT TAT GCC TCT CCC GAA TTC GCT AGT CGA GGC GCA ACA AGA
3′XhoI-pJG4-5-Rab5	TGA CCA AAC CTC TGG CGA AGA AGT CCA AAG CTT CTC GAG TTA GTT ACT ACA ACA CTG ATT

3.1.7 Other reagents and supplies

The non-hydrolyzable GTP analogues used were GTPγS from Sigma-Aldrich and GppCp from Jena Bioscience. Both were obtained as a sodium salt and dissolved in ddH_2O. All other reagents and chemicals used were purchased from Sigma-Aldrich or VWR and were of analytical grade or higher unless otherwise specified.

3.2 Methods

3.2.1 Generation of Myc_3-iSH2-p110α and Myc_3-iSH2-p110β

3.2.1.1 Addition of a glycine linker

Myc-tagged p110 (α and β) constructs were already present in the laboratory (made by Chris Pastor and Kristy James, respectively). Two designed primers which encode seven glycine residues flanked by *Nhe*I restriction site sticky ends (see Table 3.3) were used to add a glycine linker N-terminally to p110. Each primer (0.3 mM) was phosphorylated by 10 U of T4 polynucleotide kinase (New England Biolabs or NEB) in the presence of 1 µM ATP, at 37°C for 1 hour. The T4 polynucleotide kinase was heat-inactivated by incubation at 75°C for 10 min. The two phosphorylated primers were pooled and annealed by heating in boiling water and allowing them to cool slowly to room temperature. Two µg of the plasmid, pMyc_3-p110 (α or β) was digested with 10 U of *Nhe*I (NEB) in One-Phor-all buffer (United States Biochemical/Affymetrix) for 1 hour at 37°C. The digested plasmid was treated with shrimp alkaline phosphatase (SAP; Fermentas) for 1 hour at 37°C, and then SAP was heat-inactivated by incubation at 75°C for 10 min. The phosphorylated annealed glycine linker oligonucleotides (6.66 pmol) were ligated into the SAP-treated plasmid (45 ng) using 1 µL Quick ligase (NEB) in 20 µL at room temperature for 20 min. The ligated DNA was transformed into TOP10 competent cells (Hanahan *et al.*, 1991), which were grown on LB plates with ampicillin (100 µg/mL) selection. Plasmid DNA from the resulting colonies was isolated with QIAgen Spin Miniprep Kit (QIAgen) and sent to DNA Services in the Plant Biotechnology Institute for sequencing with the 5`Myc-seq primer (Table 3.3). The second *Nhe*I site was intentionally not maintained by including an imperfect sequence within the glycine linker oligonucleotides.

3.2.1.2 Addition of iSH2 encoding region of p85

The region encoding the iSH2 domain of p85α was amplified from the pGEX6P1-p85α vector by PCR with KOD polymerase (Novagen). The primers used were specific to regions of p85 encoding amino acids 466 to 567 and incorporated an *Nhe*I restriction site at both ends of the insert (see Table 3.3, special primers). The thermocycler program used was as follows: 1) initial melting: 98°C for 1 min, 2) melting and annealing/extension: 20 cycles of 98°C for 15 sec and 68°C for 10 sec, 3) final extension: 68°C for 10 sec. The amplified fragment was purified from the PCR reaction using a clean-up kit (QIAgen) and digested by *Nhe*I for 1 hour at 37°C. The digested fragment was removed from buffer and enzyme using the clean-up kit. The fragment was ligated into the *Nhe*I-digested and SAP-treated pMyc$_3$-Gly$_7$-p110 plasmids (α and β) using Quick ligase as before (3.2.1.1). The plasmids were sequenced using the 5`Myc-seq primer and primers for full-length p110β or p110α (Table 3.3, sequencing primers) to ensure proper orientation of ligated fragments and to ensure that no mutations were added to the sequence during the procedure.

3.2.2 Site-directed mutagenesis of GST-Rab5 and Myc$_3$-iSH2-p110β

Twenty-eight Rab5 mutations were generated within the background of pGEX6P1-Rab5 and five p110β mutations were made in the background of pMyc$_3$-iSH2-p110β through site-directed mutagenesis with *Pfu* polymerase (Invitrogen) in a thermocycler. The reaction mixture contained 5 µL of the *Pfu* buffer (10X) with $MgSO_4$ provided, 0.05 mM dNTPs, 10-200 ng of template DNA, 125 ng of each sense/antisense mutagenic primer (See Table 3.2, mutagenesis primers) and 2.5 U of *Pfu* polymerase in a 50 µL reaction volume. The program used was as follows: 1) initial melting: 95ºC for 30 sec, 2) melting, annealing and extension: 18 cycles of 95ºC for 30 sec, 55ºC-67ºC (depending on the primer Tm) for 1 min and 72ºC for 11 min 15 sec (pGEX6P1-Rab5) or 5 min 30 sec (pMyc$_3$-iSH2-p110β), 3) final extension: 72ºC for 5 min.

The reaction products were digested with 10 U *Dpn*I (New England Biolabs) for 1 hour at 37ºC to selectively nick the methylated parental wild-type plasmid DNA which had been isolated from *E. coli*. The samples were transformed into TOP10 competent cells, which were grown on LB plates with ampicillin (100 µg/mL) selection. Plasmid DNA from the resulting colonies was isolated with a QIAgen Spin Miniprep Kit (QIAgen) and sent to DNA Services in

the Plant Biotechnology Institute for sequencing with the 5`GST primer (pGEX6P1-Rab5) or 5` b110seq114 primer (pMyc$_3$-iSH2-p110β) to confirm the mutation.

3.2.3 Yeast two-hybrid analysis of LexA-p85wt and B42-Rab5wt

3.2.3.1 PCR amplification of p85 and Rab5 encoding regions

The full-length p85α human cDNA was amplified by PCR from pGEX6P1-p85 with primers encoding 42 bases of pEG202 vector DNA and 21 bases specific to p85 (see Table 3.3, special primers) using *Pfu* polymerase in a thermocycler. The program used is as follows: 1) initial melting: 95°C for 4 min, 2) melting, annealing and extension: 35 cycles of 95°C for 30 sec, 80°C for 30 sec and 72°C for 5 min, 3) final extension: 72°C for 10 min. Similarly, the full-length Rab5A human wild-type cDNA was amplified from pGEX3X-Rab5 with Rab5 specific primers extended by 39 bases of pJG4-5 sequence (Table 3.3, special primers).

3.2.3.2 Homologous recombination of yeast two-hybrid plasmids and p85 or Rab5

The full-length p85 and Rab5 inserts were incorporated into *Bam*HI/*Not*I and *Eco*RI/*Xho*I sites of the plasmids pEG202 and pJG4-5, respectively by homologous recombination within the yeast cell environment. Yeast competent cells were generated through the Gietz and Schiestl procedure (2007) whereby a 50 mL overnight culture of a selected yeast colony was grown to an OD_{600nm} of 0.6, harvested and washed with 25 mL ddH_2O by centrifugation at 3000 x *g* for 5 min at 20°C. The pelleted cells were resuspended in 0.5 mL of 100 mM lithium acetate and aliquoted into 10 x 50 µL samples.

Both insert and plasmid DNA was transformed into yeast competent cells using the lithium acetate transformation procedure (Gietz and Schiestl, 2007). Briefly, a sample of competent cells were pelleted at 13000 x *g* for 15 sec and the supernatant was replaced by the reaction mixture containing: 260 µL of 50% (w/v) polyethylene glycol 3350, 36 µL 1 M lithium acetate, 50 µL of 2 mg/mL single-stranded DNA, 0.5 µg plasmid DNA and 1 µg PCR insert. The mixture and cells were vortexed and incubated at 30°C for 45 min, and then heat shocked for 20 min at 42°C. The cells were pelleted, resuspended in ddH_2O and plated on auxotrophic selective plates SDH^- (pEG202) or SDW^- (pJG4-5) and incubated at 30°C for three days.

The plasmids were isolated from the resulting colonies and subjected to colony PCR, where the extracted plasmid DNA was used as a template for the amplification of the gene of interest (p85 or Rab5 in this case) by KOD polymerase and primers (Table 3.3). The PCR

conditions were as follows: 1) initial melting: 98°C for 1 min, 2) melting, annealing and extension: 30 cycles of 98°C for 15 sec, 80°C for 2 sec and 72°C for 20 sec, 3) final extension: 72°C for 5 min. Confirmation of incorporation of the gene of interest into the plasmid was achieved by sequencing through the multiple cloning sites of both pEG202 and pJG4-5 using the sequencing primers in Table 3.3.

3.2.3.3 Yeast two-hybrid assay for p85wt and Rab5wt interaction

Yeast strain EY111 competent cells were transformed with the LexA-p85 bait plasmid using the lithium acetate transformation (Gietz and Shiestl, 2007). Similarly, the EY93 strain was transformed with the B42-Rab5 prey plasmid. Both strains were incubated on rich media plates [YPDA: 1% (w/v) yeast extract, 2% (w/v) peptone, 80 mg/L adenine and 2% (w/v) dextrose] at 30°C for 3 days. Colonies were isolated, lysed in 0.1 M NaOH and boiled in SDS sample buffer. The extracted protein was subjected to SDS-PAGE, transferred to nitrocellulose and probed for p85 and Rab5 expression by western blot. Those that were expressing high levels of either LexA-p85 (~110 kDa) or B42-Rab5 (~37 kDa) were grown in culture overnight and then mated on a YPDA plate. After three days at 30°C, the resulting diploid colonies were assessed for protein expression by immunoblotting with anti-p85 or anti-Rab5 as before. Those that expressed both proteins were then spotted onto selection media plates; first SDH^-W^- (sugar source is dextrose, lacking histidine and tryptophan), SGH^-W^- (sugar source is galactose, lacking histidine and tryptophan), then $SGH^-W^-L^-A^-$ (galactose, lacking histidine, tryptophan, leucine and adenine), $SDH^-W^-L^-A^-$ (dextrose, lacking histidine, tryptophan, leucine and adenine) and $SGH^-W^-L^-A^-$Xgal (galactose, lacking histidine, tryptophan, leucine and adenine with Xgal) to assess the expression of reporter genes (for leucine, alanine and beta-galactosidase) driven by p85:Rab5 interaction.

3.2.4 Expression and purification of GST-Rab5 and GST-p85 proteins

DNA encoding GST-Rab5 or GST-p85 was transformed into protease-deficient BL21 cells. For protein overexpression, 1 L LBA was inoculated with a 5 mL overnight culture of BL21 expressing GST-p85 or GST-Rab5 and grown at 37°C to an OD_{600nm} of 0.6. Protein expression was induced by Isopropyl β-D-1-thiogalactopyranoside (0.3 mM, Calbiochem) at room temperature overnight with shaking. Cells were pelleted at 6000 x *g* at 4°C for 15 min and

resuspended on ice in 5 mL of LBA. Aliquots of 100 mL equivalents (or $1/10^{th}$ of the cells) were pelleted again; the supernatant was removed and stored at -80°C until needed.

To purify the GST-fusion protein, an aliquot of cells was resuspended in 1 mL phosphate buffered saline (137 mM NaCl, 2.7 mM KCl, 4.3 mM Na_2HPO_4, 1.4 mM KH_2PO_4) + 10 µg/mL aprotinin (Calbiochem), 10 µg/mL leupeptin and 1 mM AEBSF [4-(2-Aminoethyl) benzenesulfonyl fluoride]. Lysis of cells was achieved by incubation with 1 mg/mL lysozyme on ice of 30 min and sonication (3 x 10 seconds at setting 1.5). After sonication, a 10 min incubation with DNase (100 U, room temp) was performed to reduce viscosity. Triton X-100 (to 1%) was added to the tubes and then the cell debris was pelleted in a microcentrifuge for 10 min at 16100 x *g* at 4°C. The supernatant containing the fusion protein was passed through a 0.45 µM filter (Nalgene) to remove additional cell debris and contaminants. Glutathione-Sepharose beads (Amersham) (100 µL of a 50% suspension) were added to the filtered lysate and allowed to bind at 4°C for 1 hour. The beads were pelleted by centrifugation (2300 x *g*, 1 min) and washed three times with 500 µL PBS, before being resuspended (50 µL beads) in 450 µL of PBS.

Protein concentration of a 10 µL aliquot of beads was determined by boiling the beads for 5 min in sodium dodecyl sulfate (SDS) sample buffer [10% (w/v) glycerol, 5% (v/v) 2-mercaptoethanol, 2.3% (w/v) SDS, 0.0625 M Tris, pH 6.8, 0.02 mg/mL bromophenol blue] for 5 min, pelleting the beads, and performing a Lowry assay (Sigma-Aldrich) on the supernatant containing the fusion protein.

Purification of p85 protein from GST-p85 bound to glutathione-Sepharose beads was achieved using 3C Prescission protease. In this case, the entire volume of culture (1 L) was lysed at once. The filtered lysate was added to 2 mL of a 50% suspension of glutathione-Sepharose beads and incubated for 1 hour at 4°C. The beads were pelleted and washed 5 times in Prescission Lysis Buffer [(PLB): 50 mM Tris-HCl pH 7.0, 150 mM NaCl, 1 mM Ethylenediaminetetraacetic acid (EDTA)]. The 3C Prescission protease (100 µL in 900 µL PLB) was added to the beads and allowed to cleave the protein overnight at 4°C with agitation. The beads were pelleted and the supernatant containing the cleaved protein was collected. Washes with PLB were performed until the OD_{280nm} was less than 0.2. All washes containing p85 protein were pooled.

3.2.5 Protein visualization

3.2.5.1 Coomassie blue staining

Proteins were resolved by sodium dodecyl sulfate polyacrylamide gel electrophoresis (SDS-PAGE, 7.5-15% acrylamide, EM Science) (Laemmli, 1970) and Coomassie blue staining [0.14% (w/v) Coomassie Blue R-250 (Bio-Rad), 41.4% (v/v) methanol, and 5.4% acetic acid]. Unbound Coomassie blue was removed by washing gels with destain solution [41.4% (v/v) methanol, 5.4% (v/v) acetic acid]. A single band of 50 kDa was expected for GST-Rab5 fusion proteins and additional bands were considered contamination from other cellular proteins or proteolytic products of GST-Rab5. For p85 purified as GST-p85 and cleaved with 3C Prescission protease, a single band of ~85 kDa was expected.

3.2.5.2 Western blotting

For western blot analysis (immunoblot), proteins resolved by SDS-PAGE were transferred to a nitrocellulose membrane (Whatman) in transfer buffer [48 mM Tris-HCl pH 9.2, 0.038% (w/v) SDS, and 20% (v/v) methanol) using an Owl Panter Semi-Dry Electroblotter (VWR). The apparatus was layered as follows: three pieces of 3MM filter paper (Whatman) pre-soaked in transfer buffer, SDS-PAGE gel, one nitrocellulose membrane pre-hydrated in H_2O, three more pre-soaked 3MM filter papers. Any air bubbles between the layers were removed by rolling a tube over the layers. A constant current of 400 mA was applied to transfer proteins from the gel to the nitrocellulose for 15 min/gel.

The nitrocellulose membrane (blot) was incubated in blocking solution [5% (w/v) Carnation skim milk powder (Safeway) in PBS] for 1 hour at room temperature while rocking. The blot was incubated with 5 mL primary antibody solution for 1 hour at room temperature. The blot was washed three times for 5 minutes in PBS. The appropriate secondary antibody (anti-mouse for FLAG and p85 blots, anti-rabbit for Myc blots) was prepared in 5 mL blocking solution. The blot was incubated with secondary antibody for 1 hour at room temperature. The blot was washed as before and scanned using the LI-COR Odyssey Infrared Imager (LI-COR Biosciences) and analyzed with the Odyssey V3.0 software and Microsoft Excel.

3.2.5.3 Protein visualization software

To visualize the orientation of Rab5 amino acid side chains of the GDP-bound crystal structure in comparison to the GTP-bound structure, the program Protein Workshop was used (Moreland *et al.*, 2005). Figures 4.3, 4.10, and 4.12 were generated with this software using the crystal structure information deposited in the Protein Data Bank (www.rcsb.org) for Rab5-GDP (PDB ID: 1TU4) and Rab5-GNP (PDB ID: 1R2Q).

The structural alignments of proteins in Table 3.4 were generated using the program PyMOL (The PyMOL Molecular Graphics System, Version 1.4.1 Schrödinger, LLC.).

Table 3.4 Protein data used in structural alignments.

Figure	Protein A (PDB ID)	Aligned with Protein B and C (PDB ID)
1.2	Ras-GDP (SP21)	-
1.2	Ras-GNP (4Q21)	-
1.5	REP1:Rab7 (1VG0)	RabGGTase:REP1 (1LTX)
1.5	RabGDI:Ypt1 (2BCG)	-
1.9	Ras:p120rasGAP (1WQ1)	-
1.9	Rho:p50rhoGAP (1TX4)	-
4.14	p110β:ci-p85β (2Y3A)	p110α:ni-p85α (3H1Z)
5.2	Cdc42:p50rhoGAP (1AM4)	Rab5-GNP (1R2Q) and p85 BH domain (1PBW)
5.2	Rho:p50rhoGAP (1TX4)	Rab5-GNP (1R2Q) and p85 BH domain (1PBW)
5.3	Cdc42:p50rhoGAP (1AM4)	p85 BH domain (1PBW)
5.3	Rho:p50rhoGAP (1TX4)	p85 BH domain (1PBW)
5.4	Ras:p110γ (1HE8)	Rab5-GNP (1R2Q) and p110β:ci-p85β (2Y3A)

3.2.6 Mammalian cell culture

COS-1 cells were grown in Dulbecco's Modified Eagle Medium (DMEM; Gibco) supplemented with 10% fetal bovine serum (FBS; Gibco) at 37°C + 5% CO_2.

3.2.6.1 COS-1 lipofectamine transfection

Transfection of COS-1 cells was performed at 40% confluency, as determined visually by light microscopy. Lipofectamine (18 µL; Invitrogen) and DNA (6 µg) were added to separate 600 µL samples of OPTI-MEM (Gibco) and then mixed together and incubated for 15 min at room temperature. Cells were washed with serum-free DMEM prior to transfection. The OPTI-MEM solution with DNA and lipofectamine was diluted by the addition of 4.8 mL of serum-free DMEM and added to cells. Transfection media remained on cells for 5 hours at 37°C + 5% CO_2. After 5 hours, 6 mL of DMEM + 20% FBS were added and the cells were grown overnight at 37°C + 5% CO_2. The media was changed to DMEM + 10% FBS and the cells were grown for an additional 48 hours.

3.2.6.2 Cell lysis procedure

Cells were placed on ice and washed with PBS. One mL of cell lysis buffer (50 mM HEPES pH 7.5, 150 mM NaCl, 10% glycerol, 1% Triton X-100, 1.5 mM $MgCl_2$, 1 mM EDTA, 10 mM NaPPi, 100 mM NaF, + 10 µg/mL aprotinin, 10 µg/mL leupeptin and 1 mM AEBSF) was used to induce cell lysis for 5 mins. Plates were scraped with a spatula to remove all cells and transferred to Eppendorf tubes. Cell lysate was centrifuged at 16100 x *g* for 10 min at 4°C, to pellet cell debris. Supernatant was stored at -80°C until needed.

Total protein concentration was determined by Lowry assay of 25 µL aliquots. The presence of overexpressed protein of interest was observed by western blotting for either the FLAG/Myc tag or the protein itself, in the case of p85. For Myc_3-iSH2-p110β mutants, pull-down experiments required consistent protein concentration between mutant and wild-type lysates. Therefore, 10 µL of each Myc_3-iSH2-p110β (wt and mutant) lysate was subjected western blotting and their intensities were quantified as arbitrary units using Odyssey software V3.0 and Microsoft Excel. Normalization of relative expression to Myc_3-iSH2-p110βwt as well as total protein concentration required the dilution of some Myc_3-iSH2-p110β mutant lysates with untransfected COS-1 lysate.

3.2.7 Pull-down binding assay using immobilized GST-Rab5 (wt or mutant) and p85 or FLAG-p85 or Myc_3-iSH2-p110

Ten µg of GST-Rab5 protein already attached to beads was stripped of nucleotide by incubation for 30 min at room temperature with buffer containing EDTA [20 mM Tris-HCl pH 7.5, 50 mM NaCl, 1 mM dithiothritol (DTT), 5% glycerol, 0.1% Triton X-100, 10 mM EDTA pH 8.0, 10 µg/mL aprotinin, 10 µg/mL leupeptin], which chelates the Mg^{2+} ion necessary for proper nucleotide binding. Beads were pelleted and the supernatant was aspirated. The desired nucleotide, e.g. GDP, GTPγS or GppCp, was added (200 nM) to the beads in nucleotide loading buffer containing Mg^{2+} (20 mM Tris-HCl pH 7.5, 50 mM NaCl, 1 mM DTT, 5% glycerol, 0.1% Triton X-100, 10 mM $MgCl_2$, 10 µg/mL aprotinin, 10 µg/mL leupeptin) and incubated at room temperature for 30 minutes. Beads were pelleted and the supernatant was aspirated. The beads were then incubated for 30 min either with 25 µL FLAG-p85 cell lysate, diluted in 75 µL nucleotide loading buffer, or with normalized Myc_3-iSH2-p110 cell lysate in nucleotide loading buffer to a total protein concentration of 130 µg and total volume of 500 µL. The beads were washed 4 times with 400 µL 1% Nonidet P-40 buffer (50 mM Tris pH 7.5, 150 mM NaCl, 1% Nonidet P-40) and bound proteins were eluted in SDS sample buffer. The protein containing buffer was subjected to SDS-PAGE and immunoblot assay to detect bound FLAG-p85 (FLAG), p85 (p85) or Myc_3-iSH2-p110 (Myc).

Purified p85 protein pull-down assays required a blocking step after nucleotide binding. The nucleotide loading buffer with 10% bovine serum albumin (BSA) and 10% skim milk powder (Carnation, Safeway) added was used for this step. Beads were incubated with the blocking solution for half an hour before addition of p85, and the blocking solution was not removed during the p85 incubation step. Purified p85 was added to a final concentration of 37.5 ng/µL (in PLB).

3.2.7.1 Statistical evaluation of data

Blots were scanned directly using the LI-COR Odyssey Infrared Imager (LI-COR Biosciences). The bands visualized using Odyssey software V3.0 were quantified and given arbitrary intensity units using Microsoft Excel. Background intensity or GST negative control lane intensity, when relevant, was subtracted from all sample bands. Protein expression in Myc_3-iSH2-p110-expressing cell lysates was normalized to the wild type protein, which was assigned a value of 1. The amount of FLAG-p85, p85wt or Myc_3-iSH2-p110β bound to GST-Rab5 fusion proteins in each pull-down experiment was normalized to either wild-type Rab5-GTPγS (100%) or Rab5wt-GDP (100%) depending on bound nucleotide. Data from three or more independent experiments were combined as mean ± SD, as indicated in each figure legend. P-values to assess statistically significant differences were obtained using Prism software (GraphPad Prism 4.00, San Diego, CA) using a one-way ANOVA and Dunnett's multiple comparison test.

3.2.9 Co-immunoprecipitation analysis of FLAG-p85 and Myc_3-p110 or Myc_3-iSH2-p110

COS-1 cells were cultured and co-transfected with FLAG-p85 and Myc_3-p110 or Myc_3-iSH2-p110 as described in section 3.2.6.1. Cells were lysed in 1 mL cell lysis buffer (see section 3.2.6.2) and centrifuged for 10 min at 16100 x *g*. The entire lysate was precleared of non-specific binding proteins using agarose conjugated (AC) mouse IgG antibodies (Table 3.1) and protein A Sepharose beads (10 µg) for 1 hour at 4°C with rocking. The antibodies were pelleted at 4°C, 16100 x *g* and the supernatant divided into two samples. The precleared lysate samples were incubated with protein A Sepharose beads (10 µg) and either AC Myc antibody or AC mouse IgG antibody for 1 hour at 4°C with rocking. The beads with bound antibodies and associated proteins were pelleted at low speed (500 x *g*) for 2 min and washed three times with 1 mL 1% Nonidet P-40 buffer. The samples were resolved on two SDS-PAGE gels and both were subjected to western blot analysis. One blot was probed for Myc_3-p110 or Myc_3-iSH2-p110 with anti-Myc antibody; the other was probed for p85 with anti-p85 antibody.

4.0 RESULTS

4.1 Pull-down experiments with Rab5, Rab4 and Rab11 and p85

Previous work had shown that p85 has GAP activity towards Rab5 and Rab4, but it has no GAP activity towards Rab11 (Chamberlain *et al.*, 2004). GAP function involves the insertion of an arginine finger into the nucleotide binding site of the Rab protein. Interestingly, p85 bound to both active and inactive forms of Rab5 (Chamberlain *et al.*, 2004). This suggested that the binding site for p85 on the Rab5 protein is likely to be outside of the switch regions of Rab5 that remain in similar conformations for both Rab5-GDP and Rab5-GTP. Being members of the same superfamily of Rab GTPases, Rab5, Rab4 and Rab11 have very strong sequence identity. Therefore to investigate p85 binding, a pull-down experiment was performed with p85 and each of Rab5, Rab4 and Rab11 in both active and inactive forms. It was hypothesized that, because p85 was a poor GAP towards Rab11, binding between the two proteins would be very low.

Each of Rab5A, Rab4 and Rab11 was generated as a GST-fusion protein, overexpressed in BL21 *E. coli* cells and purified by binding to glutathione-Sepharose beads. To discriminate between GDP- and GTP-bound conformations of the Rab proteins, and their effects on binding to p85, each Rab was stripped of bound nucleotide by incubation with an EDTA-containing buffer, as described previously (Hart *et al.*, 1994) followed by reloading the nucleotide binding site of the Rab with either GDP or a non-hydrolysable GTP-analogue, GTPγS, in a Mg^{2+}-containing buffer. This method, which does not ensure 100% of desired GDP- or GTP-bound Rab, can at least provide a majority of the desired conformation to allow discrimination between the two in the pull-down assays performed in this thesis.

The p85 used in the binding experiments was provided by COS-1 (green monkey kidney) cell lysate transiently expressing exogenous FLAG-tagged p85. The use of cell lysate for binding studies allowed for other cellular proteins to compete for binding to the purified Rab proteins. Endogenous p85 was also expressed, but at a much lower concentration, and could also compete for Rab5 binding. The FLAG-p85 lysate was added to the GST-Rab protein beads after loading with nucleotide and was allowed to bind for 30 minutes. The samples were then washed three times with 1% Nonidet P-40 containing buffer, subjected to SDS-PAGE and

transferred to a nitrocellulose membrane. The resulting blots were probed with anti-FLAG antibody, so endogenous p85 binding was not considered.

The binding of FLAG-p85 to Rab4 and Rab11 was less than Rab5 (Figure 4.1). Specifically, Rab4 showed nearly half as much FLAG-p85 binding as compared to Rab5, though there was some variability in the assay (Figure 4.1 B, see SD) The reduction in FLAG-p85 binding to Rab4 compared to Rab5 was unexpected because the GAP activity of p85 was nearly equal towards both proteins (Chamberlain *et al.,* 2004). As expected by the lack of GAP activity of p85 towards Rab11, little or no binding was observed between the proteins *in vitro* (Figure 4.1 A and B). With an average binding intensity that was 7% of Rab5wt-GDP and 1% of Rab5wt-GTPγS, the data demonstrates that Rab11 is a not a likely binding partner for p85.

Pull-down assays using purified p85wt were also performed (Figure 4.1 A, *lower*). The addition of unrelated proteins (BSA, skim milk casein and whey proteins) was utilized as a "blocking step" to control for non-specific interaction with purified p85. The amount of p85 binding to Rab4 was even less in these experiments compared to Rab5 binding in both activation states. Purified p85 showed little to no binding to Rab11 in its inactive state, whereas it bound to Rab11-GTPγS at similar levels to that of Rab4-GTPγS. The reproducibility of these results was very low using purified p85, and since more steps were required to make the purified protein, FLAG-p85 from cell lysates was used for the rest of the p85 binding studies. These Rab binding data became the basis for my mutational analysis of the binding site on Rab5 for p85.

4.2 Sequence alignment between Rab5, Rab4 and Rab11

The amino acid sequence of human Rab5A (NP_004153.2) was aligned to both human Rab4 (NP_004569.2) and human Rab11 (NP_004654.1) using ClustalW (v1.83) to identify residues that may be involved in p85 binding (Figure 4.2). Theoretically, because Rab5 and Rab4 both bind to p85, they should both present a p85 binding motif on their structures, whereas Rab11, which does not bind to p85, should not have the binding site. Amino acids were selected based on their conservation between the p85 binding Rabs and the presence of non-conservative residues in the equivalent position of the Rab11 sequence. This first set of selected residues was then subjected to additional criteria, including surface accessibility and conservation of orientation in the GDP- and GNP- bound Rab5 crystal structures (Figure 4.3).

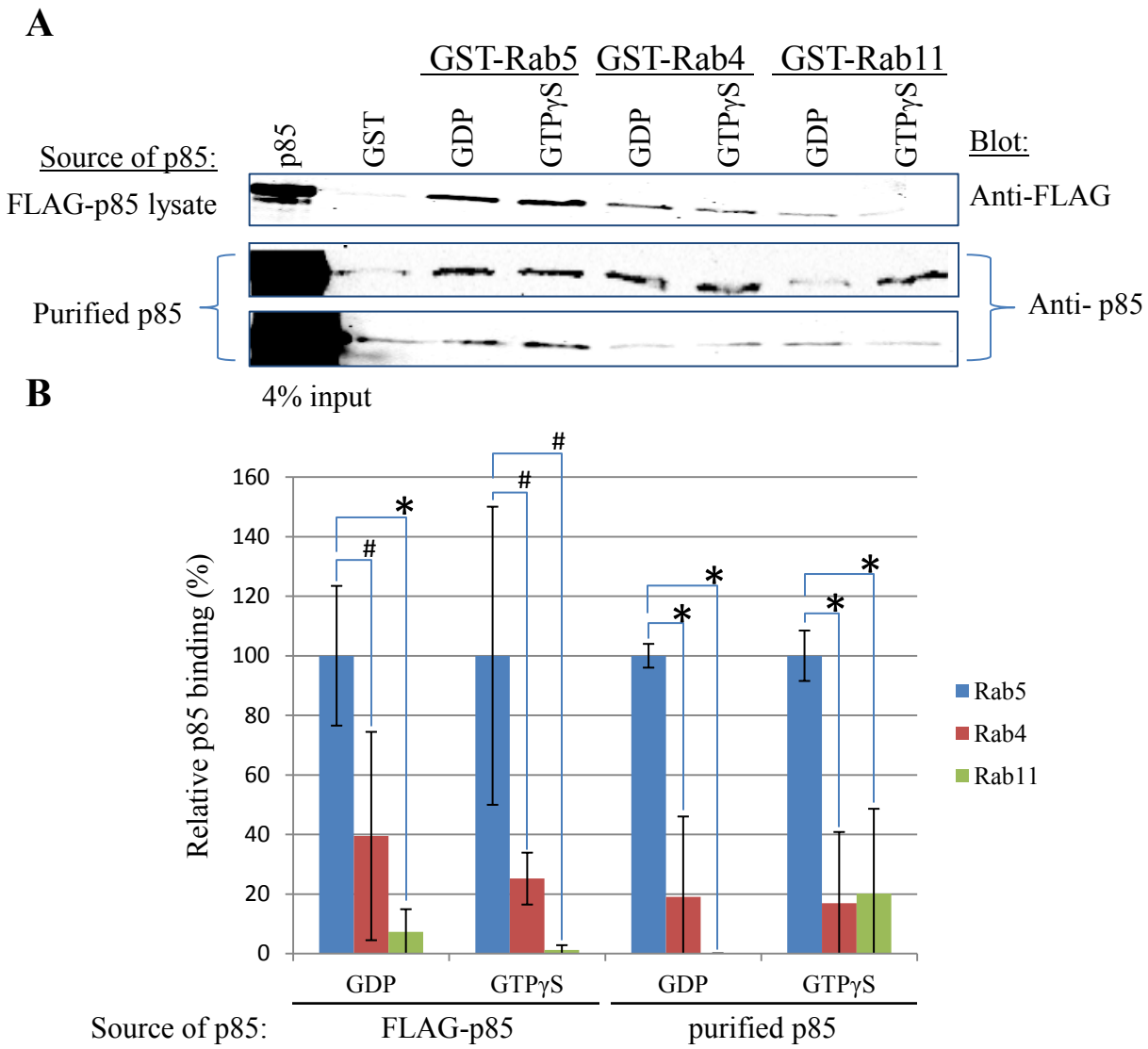

Figure 4.1 FLAG-p85 binding to GST- Rab5, Rab4 but not Rab11. **A.** Pull-down assay where 10 µg of GST, GST-Rab5, GST-Rab4 or GST-Rab11 were immobilized on glutathione Sepharose beads and loaded with either GDP or GTPγS. Samples were incubated with FLAG-p85 expressing COS-1 cell lysates or purified p85 protein, as indicated, for 30 min and then washed. Samples were subjected to SDS-PAGE and protein was transferred to a nitrocellulose membrane. Bound p85 was detected with an anti-FLAG antibody (*upper*) or an anti-p85 antibody (*lower*). An infrared dye conjugated secondary antibody was used for visualization of bands using the LI-COR Odyssey scanner and software (V3.0). **B.** Quantification of bound p85 from three separate experiments as performed in A. Intensity measured in arbitrary units, GST band was subtracted from each lane and all bands were normalized to Rab5. Mean +/- SD. (#) $P < 0.05$; (*) $P < 0.01$, based on the results of four separate one-way ANOVAs (FLAG-p85 GDP: $F = 10.89$, degrees of freedom = 8; FLAG-85 GTPγS: $F = 9.252$, df = 8; purified p85 GDP: $F = 25.48$, df = 7; purified p85 GTPγS: $F = 13,71$, df = 8), Dunnett's multiple comparison test.

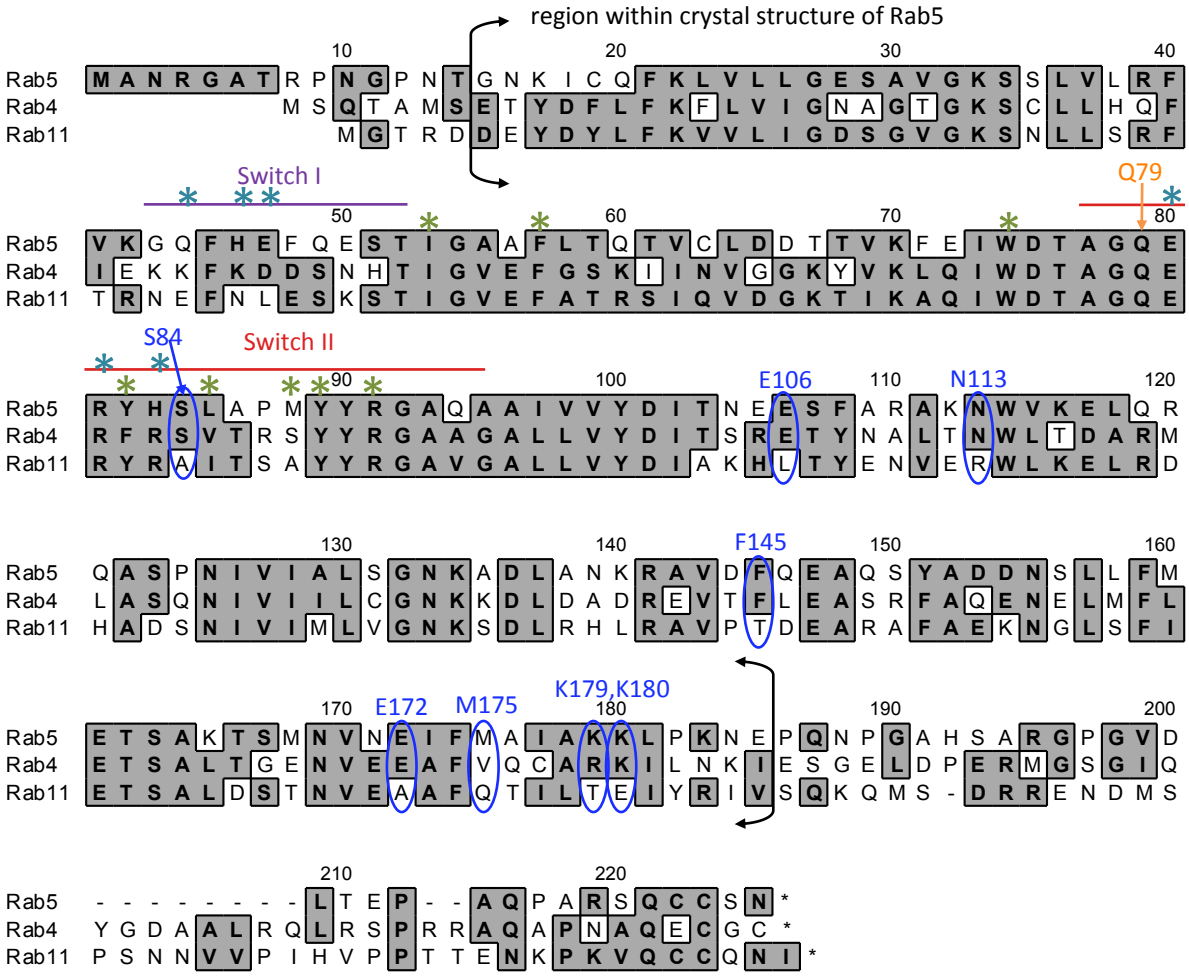

Figure 4.2 Amino acid sequence alignment of Rab5, Rab4 and Rab11. The sequence alignment was generated in ClustalW (v.1.83) with human Rab5 (NP_004153.2), Rab4 (NP_004569.2), and Rab11 (NP_004654.1). Conserved residues are shaded in grey. Curved arrows indicate the limits of the sequence included in the crystal structure of Rab5. Switch I is labelled in purple and switch II in red. Q79, which catalyzes the intrinsic hydrolysis of GTP, is indicated in orange. Amino acids circled in blue were chosen for site-directed mutagenesis and pull-down assays with p85 based on the conservation between Rab5 and Rab4, but not Rab11. Teal and green stars indicate amino acids mutated for disruption of p110β binding.

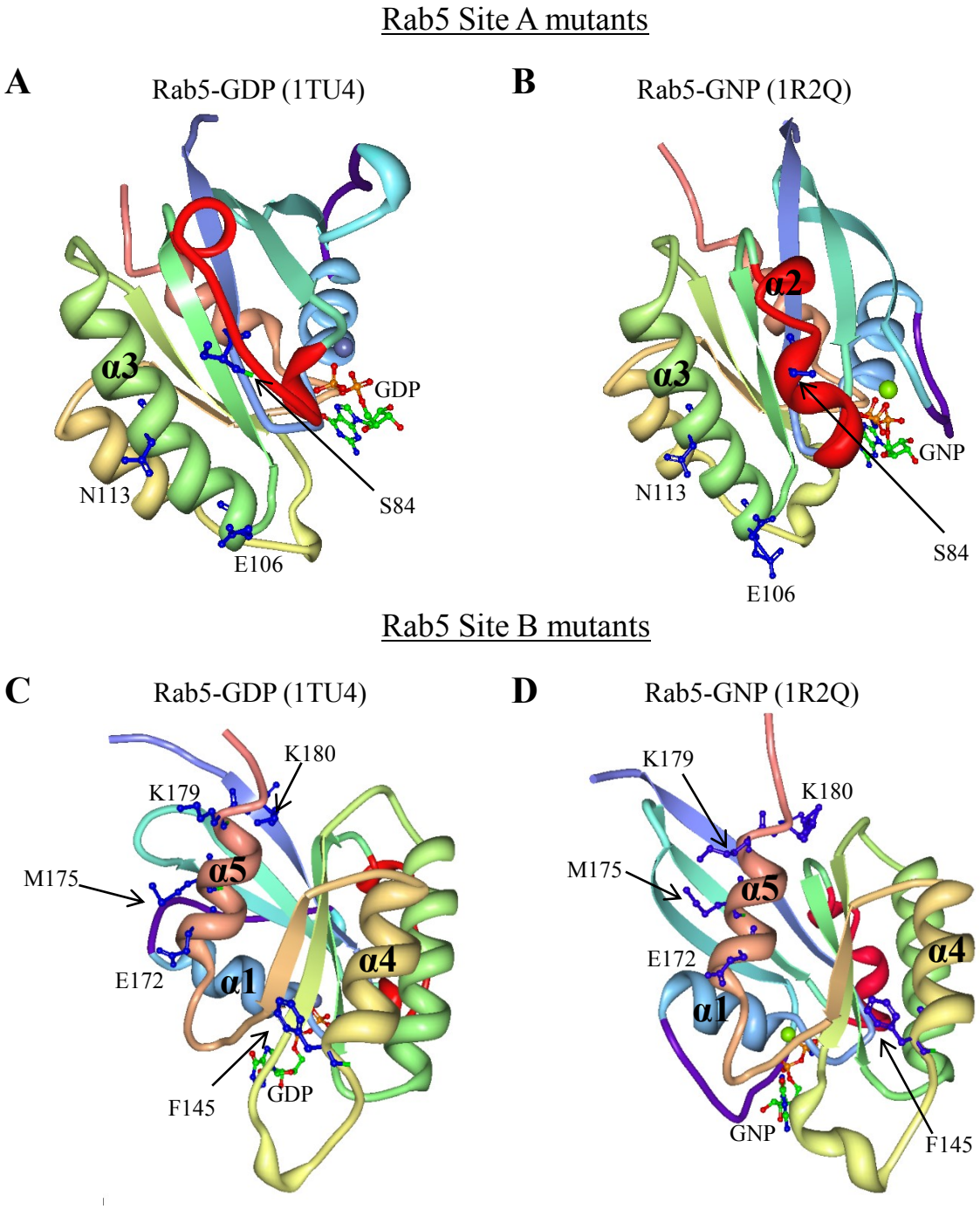

Figure 4.3 Residues that may bind p85 on crystal structures of Rab5 in both GDP and GNP bound conformations. Structures of Rab5-GDP (PDB ID: 1TU4) **A, C** and Rab5 bound to GNP (a non-hydrolysable GTP analogue; see Figure 1.8 for structure) (PDB ID: 1R2Q) **B, D** with highlighted blue residues selected for mutation to disrupt p85 binding based on their conservation between Rab5 and Rab4 sequences but not in Rab11. Site A Rab5 mutation residues are shown in panels A and B, whereas site B mutation residues are shown in panels C and D. Conventional numbering of alpha-helices is indicated. Images generated in Protein Workshop (Moreland *et al*., 2005).

The crystal structure has been solved for Rab5 in its GDP- bound inactive state as well as Rab5 bound to non-hydrolysable GTP analogues and transition state analogues (Zhu *et al.*, 2003; Terzyan *et al.*, 2004; Zhu *et al.*, 2004; Eathiraj *et al.*, 2005). These crystals were derived from a modified Rab5 protein lacking its very N- and C-terminal residues. The 14 N-terminal residues and residues 186-215 of the C terminus were therefore eliminated from our analysis (Figure 4.2, curved arrows) since it was not clear where they would be positioned in the folded Rab5 structure. The putative p85-binding residues from the sequence alignment were located on the crystal structure of Rab5 (PDB ID: 1TU4 and 1R2Q) and assessed for accessibility for binding and conservation of orientation between active and inactive structures (Figure 4.3).

The eight amino acids that fulfill these criteria were as follows: S84, E106, N113, F145, E172, M175, K179 and K180. Although S84 was within the switch II region, it was also selected for mutation based on its sequence conservation between Rab5 and Rab4 and divergence with the Rab11 sequence. It was noted that the residues were found clustered on two faces of the crystal structure of Rab5, therefore two putative "binding sites" were tested, site A and site B. Residues were assigned to either site A or B depending on which face of Rab5 they resided (Figure 4.3 A and B vs. C and D). A list of all mutations made to Rab5 can be found in Table 4.1.

4.3 Pull-down experiments with FLAG-p85 and Rab5 mutants

4.3.1 Rab5 site A mutant binding studies

The amino acids of Rab5 site A included S84, E106, and N113. Mutation of individual residues to alanine can be used to assess their involvement in the binding site between two proteins, but only when the side chain of that amino acid is involved in forming contacts with the binding partner. It would not be useful, in this case, if p85 is interacting with the backbone of any of the chosen Rab5 amino acids, nor if their binding is influenced by many residues providing small forces. Charge reversal or hydrogen bond disrupting mutations can sometimes provide enough repulsive force to reduce or inhibit binding even though many other residues are also involved in the interaction. According to this rationale, the identified residues of Rab5 were mutated to alanine and, in the case of N113, to glutamic acid for a more drastic change in amino acid structure and charge.

Table 4.1 Mutations of Rab5 amino acids based on sequence alignment. Putative p85 binding site A consisted of amino acids identified as conserved between Rab5 and Rab4 but different in Rab11, and having similar conformations in the crystal structure of both GDP- and GTP-bound Rab5, which were outward facing on the "front" face (according to Figure 4.3). Mutations to alanine or a residue of opposite charge are indicated. Putative p85 binding site B residues were chosen using the same criteria and are found on the opposite face of Rab5 to site A. Binding to p110β was assessed with Rab5 mutations of amino acids within the switch regions that have large conformational differences between GDP and GTP bound structures of Rab5, and that do not affect nucleotide binding. Additional mutations were made to amino acids important in binding Rab5 effectors EEA-1 and Rabenosyn-5, many of which are found in the switch II region.

p85 binding	**p85 binding**	**p110β binding**	**p110β binding**	**p110β binding**
Site A	Site B	Switch I	Switch II	Effector binding
S84A	F145A	Q44E	E80R	I53A
E106A	E172A	H46A	R81E	F57A
N113A	E172R	E47A		W74A
N113E	M175A		(Y82A)	Y82A
	K179A		H83E	
	K180A		S84A	
	K179+180E		(L85A)	L85A
			(M88A)	M88A
			(Y89A)	Y89A
			(R91E)	R91E

Table 4.1 Mutations of Rab5 amino acids based on sequence alignment. Putative p85 binding site A consisted of amino acids identified as conserved between Rab5 and Rab4 but different in Rab11, and having similar conformations in the crystal structure of both GDP- and GTP-bound Rab5, which were outward facing on the "front" face (according to Figure 4.3). Mutations to alanine or a residue of opposite charge are indicated. Putative p85 binding site B residues were chosen using the same criteria and are found on the opposite face of Rab5 to site A. Binding to p110β was assessed with Rab5 mutations of amino acids within the switch regions that have large conformational differences between GDP and GTP bound structures of Rab5, and that do not affect nucleotide binding. Additional mutations were made to amino acids important in binding Rab5 effectors EEA-1 and Rabenosyn-5, many of which are found in the switch II region.

p85 binding	**p85 binding**	**p110β binding**	**p110β binding**	**p110β binding**
Site A	Site B	Switch I	Switch II	Effector binding
S84A	F145A	Q44E	E80R	I53A
E106A	E172A	H46A	R81E	F57A
N113A	E172R	E47A		W74A
N113E	M175A		(Y82A)	Y82A
	K179A		H83E	
	K180A		S84A	
	K179+180E		(L85A)	L85A
			(M88A)	M88A
			(Y89A)	Y89A
			(R91E)	R91E

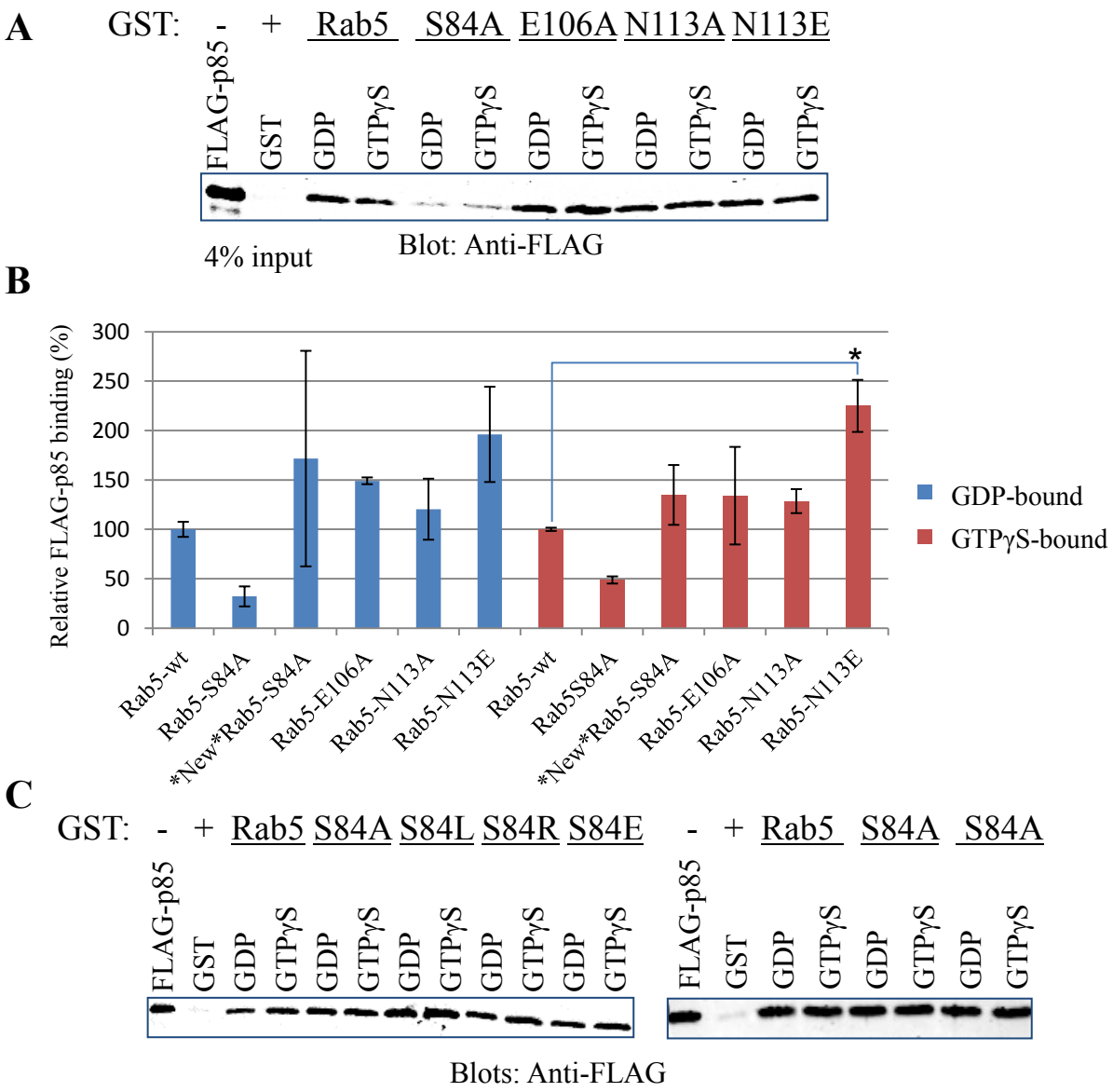

Figure 4.4 No reduction in FLAG-p85 binding to Rab5 site A mutants. A. GST, GST-Rab5 wt and mutant (as indicated) fusion proteins (10 µg) immobilized on glutathione Sepharose beads were loaded with either GDP or GTPγS and incubated with FLAG-tagged p85 from transfected COS-1 lysate. Bound p85 was detected using an immunoblot analysis with an anti-FLAG antibody. **B.** Quantification of pull-down binding data (n=3), intensity measured in arbitrary units and normalized to Rab5-wt; mean SD. Statistical analysis of GDP-bound Rab5 and mutants: one way ANOVA (F = 4, df = 17); GTPγS one-way ANOVA (F = 14.13, df = 17), (*) P <0.01, Dunett's multiple comparison test. Only statistically significant P values are indicated. **C.** Pull-down immunoblot results of GST-Rab5, wt and mutants (as indicated), fusion proteins loaded with either GDP or GTPγS and binding carried out as in A.

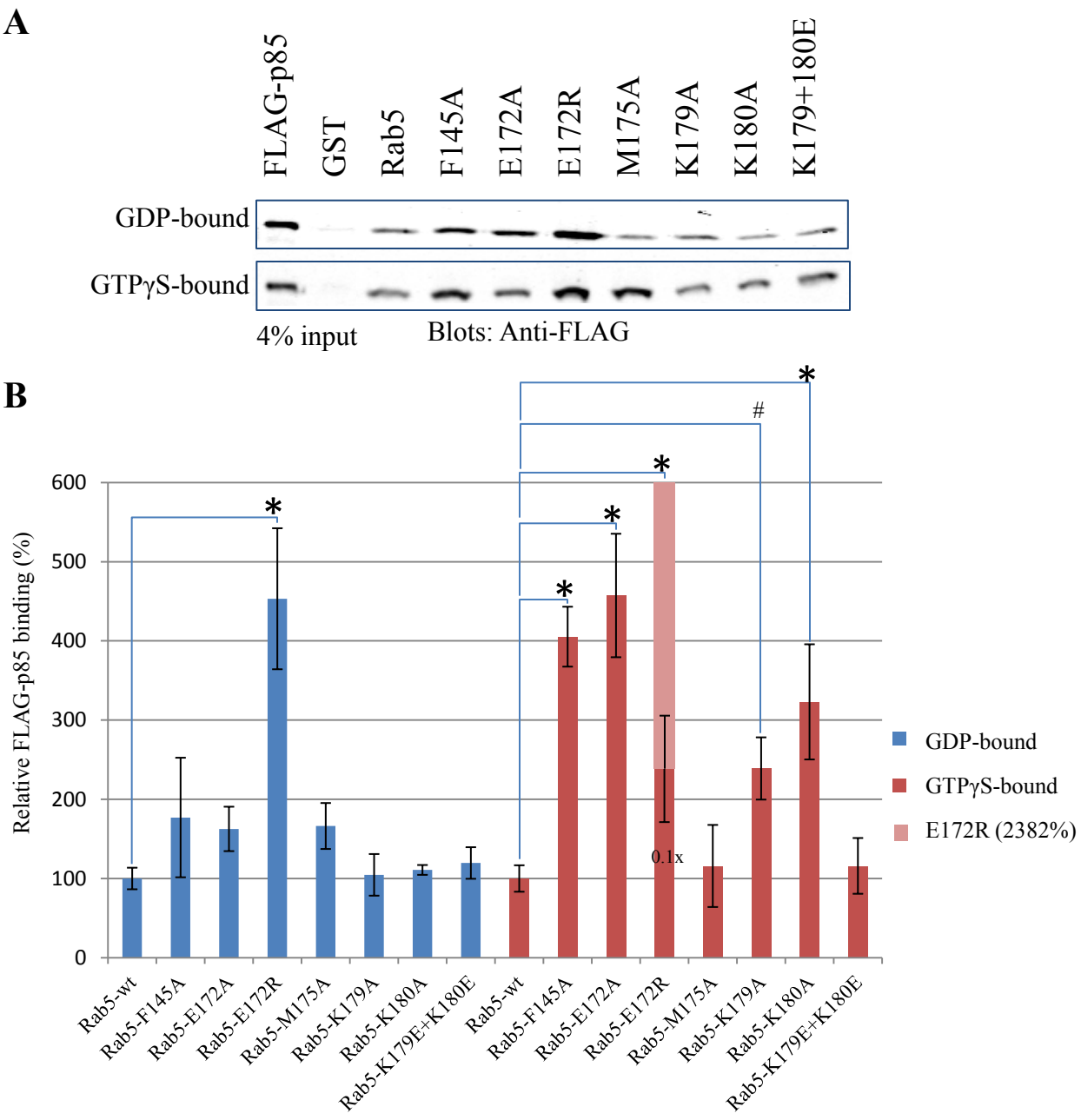

Figure 4.5 No reduction in FLAG-p85 binding to Rab5 site B mutants. A. GST, GST-Rab5 wt and mutant (as indicated) fusion proteins (10 µg) immobilized on glutathione Sepharose beads were loaded with either GDP or GTPγS and incubated with FLAG-p85 from transfected COS-1 lysate. Bound FLAG-p85 was detected using an immunoblot analysis with an anti-FLAG antibody. **B.** Quantification of pull-down binding data (n=3), intensity measured in arbitrary units and normalized to Rab5wt; mean SD. Rab5-E172R-GTPγS is shown at 0.1x (*red*) so that the error bar is visible on the graph (actual value is 2382%). Statistical analysis: GDP one-way ANOVA (F=19.75, df=23); GTPγS one-way ANOVA (F=611.3, df=23), $P<0.05$ (#), $P<0.01$ (*), Dunett's multiple comparison test. Only statistically significant P values are indicated.

4.4 Yeast two-hybrid experiment

There was inconsistency in the data obtained from the pull-down experiments. It was suggested that a yeast two-hybrid assay might provide more clear results. Yeast two hybrid experiments use the binding of two proteins of interest to bring the GAL4 transcription activation domain (B42) and the DNA binding domain (LexA) together to initiate the transcription of reporter genes (see Figure 4.6). A library of B42-Rab5 fusion protein random mutants was to be screened for the ability to bind p85 by mating with yeast expressing the LexA-p85wt fusion protein. Any colonies unable to grow on selection media plates would therefore be traced back to the original B42-Rab5 yeast colony and sequenced. It was considered an unbiased way to identify amino acids on Rab5 important in binding p85.

For the wild-type experiment, Rab5A human cDNA was inserted into the yeast prey vector by homologous recombination. The prey vector was induced by galactose and encodes a B42 transcription activation domain fusion protein and a nuclear localization signal (Figure 4.6). The p85 human cDNA was similarly inserted into the yeast bait vector which encodes for a LexA-fusion protein (containing the DNA-binding domain). The bait and prey vectors were transfected into two different strains of yeast: EY111 and EY93, respectively. The two strains were mated on YPDA non-selective plate and then assessed for protein expression after growth in galactose-containing liquid media. Both LexA-p85 and B42-Rab5 (inducible) were being expressed (data not shown).

The selection media lacked essential amino acids that the yeast could not synthesize: histidine (H^-), tryptophan (W^-), or the genes under control of the GAL4 promoter: leucine (L^-), adenine (A^-) and beta-galactosidase. Growth in $(HW)^-$ media and plates suggests that both vectors are present in the cell because they confer the ability to synthesize histidine (bait vector) and tryptophan (prey vector). Growth in L^- or A^- or both $(LA)^-$ media suggests that the B42 activation domain fusion protein was brought into proximity with the LexA-fusion protein due to Rab5:p85 binding and drove the expression of the leucine and/or adenine synthesis genes. When the cells were grown in $SG(HWLA)^-$ liquid media the cells grew, but when they were plated on the same media no colonies grew. The additional selection of Xgal + plates is the most stringent and growth on these plates suggests that the protein interaction is very strong.

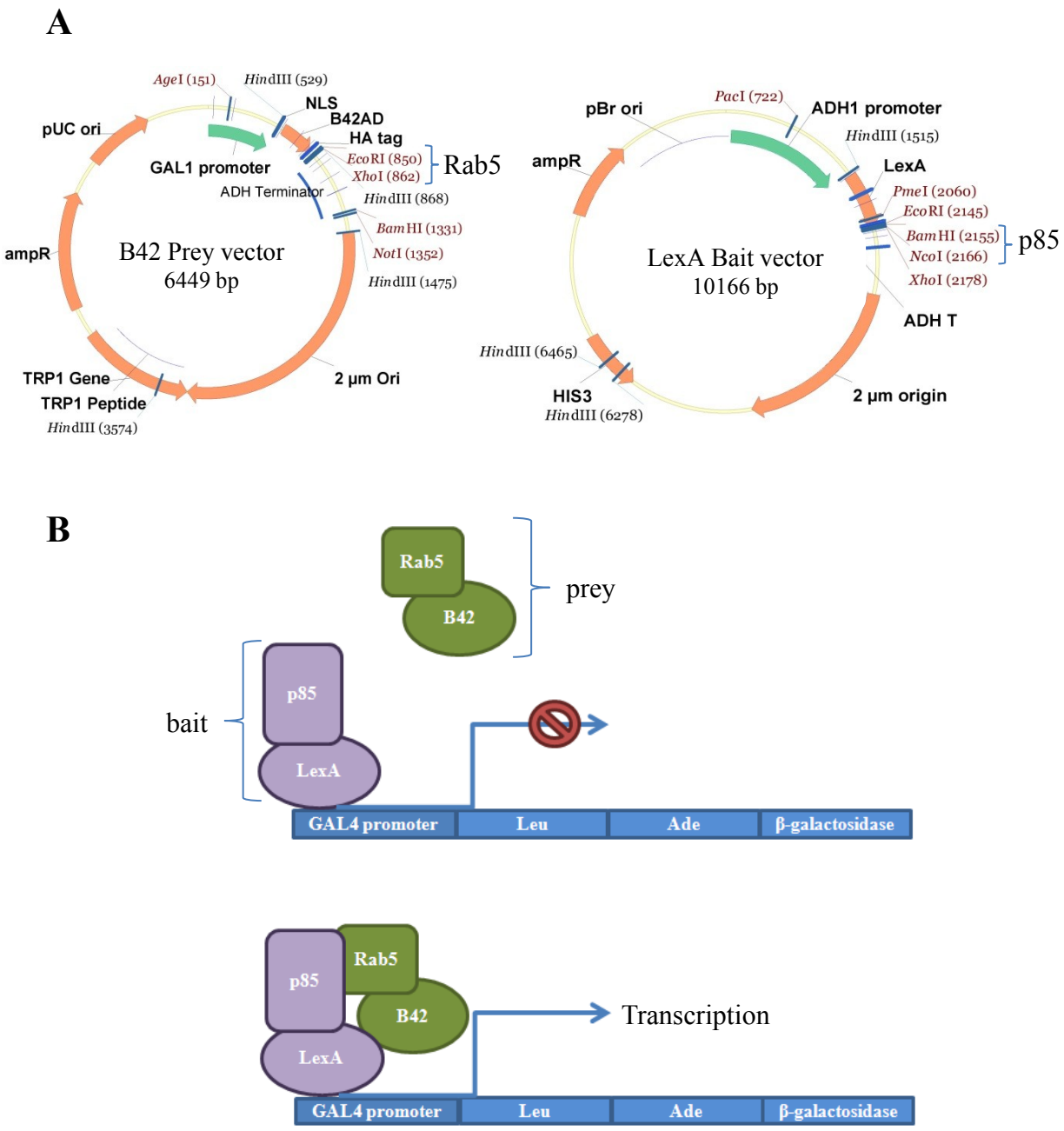

Figure 4.6 Yeast two-hybrid experimental design. A. Vector maps of the B42-Rab5 "prey" vector (*left*) which encodes a galactose induced B42 activation domain fusion protein with an N-terminal nuclear localization signal and the *TRP1* gene which enables the yeast to grow in tryptophan-free media and the LexA-p85 "bait" vector (*right*) which encodes a LexA DNA binding domain fusion protein and the *HIS3* gene which confers the ability to grow on histidine-free media. **B.** Mechanism of protein binding selection: the transcription of leucine, adenine and β-galactosidase genes is controlled by the GAL4 promoter and occurs when LexA-p85 and B42-Rab5 are brought together through the binding of their fusion proteins, p85 and Rab5 in this case.

The cells did not grow on any of the binding selection plates. The binding between Rab5 and p85 was not stable enough for the cells to endure the selection media. Therefore, this approach was not pursued any further.

4.5 Identification of p110β binding surface on Rab5

4.5.1 Generation of p110 for binding studies

Previous studies had shown that p110β, but not p110α, bound specifically to Rab5-GTPγS, but not Rab5-GDP (Christoforidis *et al.,* 1999). In this objective, the p110β binding site on Rab5 was to be determined. The identification of the p110β binding site on Rab5 required a source of stable p110 protein. This stable p110 must also be free of bound p85. In cells p110 is constitutively bound to p85 (Geering *et al.,* 2007), whose interaction prevents the protein from being degraded (Yu *et al.,* 1998). However, since p85 also binds to Rab5, its presence in the binding experiments with p110 would confuse the results.

A construct given to our lab from L.T. Williams, which encoded full-length cDNA of p110α attached at its N-terminus by a 7 glycine linker to the iSH2 domain of p85 (Figure 4.7 A, *upper*), was considered for expression of stabilized p110. There was also a C-terminal Myc tag for easy detection because there are few good p110 antibodies. The L.T Williams lab had shown previously that this protein chimera is constitutively active because it lacks the inhibitory contacts from p85 yet retains the stabilizing iSH2 (p85)-ABD (p110) contacts (Hu *et al.,* 1995). Expression of this construct in COS-1 cells was not detectable with the suggested antibodies, nor with several other anti-Myc antibodies tested (data not shown). Therefore, two similar constructs were generated which contained a total of three N-terminal Myc tags for better detection, the p85 iSH2 domain (amino acids 466-567) linked via a 7 glycine linker to p110α or p110β (Figure 4.7 A, *lower*). The synthesis of the two constructs required multiple rounds of subcloning and sequencing because the cohesive ends of the inserts could be incorporated in two orientations (see Figure 4.7 B). Both chimeric proteins expressed well in COS-1 cells and were readily detectable by immunoblotting (Figure 4.8).

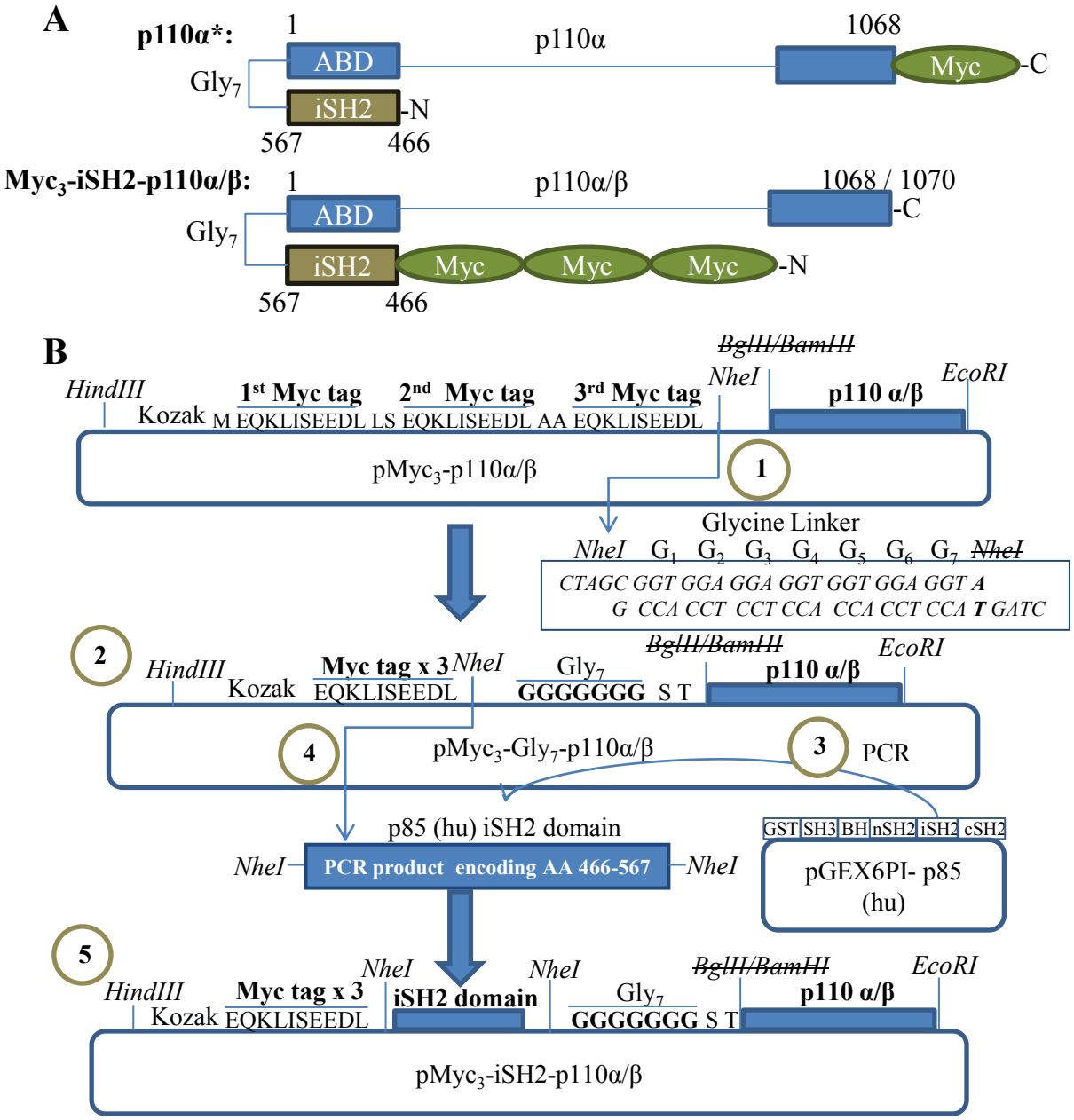

Figure 4.7 Construction of p110α and p110β proteins which do not bind p85. A. Comparison of our construct (*lower*) to the one made by L.T. Williams in 1995 (*upper*). Numbers indicate amino acids. ABD, adaptor binding domain; iSH2, inter-SH2 domain from p85 which binds p110. **B.** Diagram of the steps to build construct from **A: 1**. Insert linkers encoding a 7 glycine residue peptide into *NheI* site of pMyc$_3$p110 vectors previously made in the lab for both p110β and p110α. **2.** Sequence construct DNA with 5`Myc sequencing primer and selection of clone with appropriate orientation of glycine linker sequence. **3.** Amplify region encoding the iSH2 domain from p85 cDNA by PCR. **4.** Insert region encoding iSH2 domain into the same *NheI* site of the plasmid. **5.** Sequence construct again, to ensure correct orientation of iSH2-encoding region and through entire gene of p110.

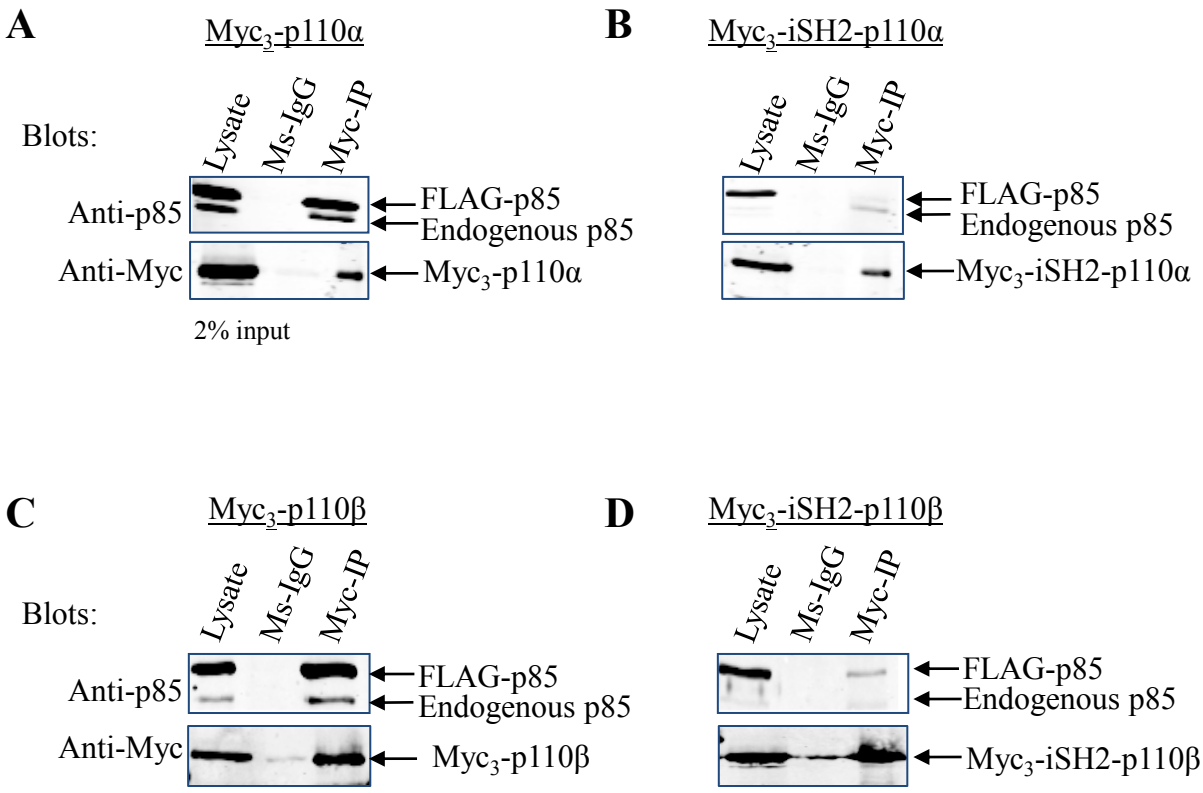

Figure 4.8 Chimeric Myc_3-iSH2-p110α/β proteins do not bind well to p85 *in vivo.* COS-1 cells were co-transfected with FLAG-p85 and Myc-p110 or Myc-iSH2-p110 constructs, as indicated, and lysed. Cell lysate was pre-cleared with agarose-conjugated (AC) mouse IgG antibody. The unbound supernatant was incubated with either AC anti-Myc antibody or AC mouse IgG antibody (control). The beads with bound antibody and associated proteins were washed and samples were boiled in SDS to remove protein from beads. Samples were subjected to SDS-PAGE. Resulting gels were transferred to nitrocellulose and co-immunoprecipitation of FLAG-p85 and endogenous p85 with Myc-p110 or Myc_3-iSH2-p110 was assessed by immunoblotting with anti-p85 and anti-Myc antibodies as indicated. Loading pattern was as follows: 2% input lysate, ½ volume of control mouse IgG IP, 2% Myc IP (probed for Myc); and 2% input lysate, ½ volume control IP, 98% Myc IP (probed for p85). Typical result shown for one of three independent experiments.

4.5.2 Co-immunoprecipitation of Myc_3-iSH2-p110 proteins with p85

It was hypothesized that the iSH2 domain within the construct would saturate the binding site for p85 on p110, thus isolating p110 from the endogenously expressed p85 in cell lysates. To test this hypothesis, a Myc immunoprecipitation was performed and the resulting blot was probed with p85 antibodies and Myc antibodies as a control (Figure 4.8). Both endogenous p85 and exogenous FLAG-p85 were expressed in COS-1 cells along with either Myc_3-p110 (alpha or beta) or Myc_3-iSH2-p110 (alpha or beta). The cells expressing the normal Myc-p110 protein were found to be in complex with both p85 and FLAG-p85 (Figure 4.8 A and C). The p110α iSH2-containing construct, however, showed little or no binding to FLAG-p85 and greatly reduced binding to endogenous p85 (Figure 4.8 B). Myc_3-iSH2-p110β showed the reverse: little or no binding to endogenous p85 and greatly reduced FLAG-p85 binding (Figure 4.8 D). These results illustrate that Myc_3-iSH2-p110β can be expressed in mammalian cells and does not require endogenous p85 binding for stability. Therefore the constructs were a good source of p110β and control p110α for binding to Rab5 mutants *in vitro.*

4.5.3 Pull-down experiments with Myc_3-iSH2-p110 and Rab5 mutants

The initial wild-type binding experiments were performed with four Rab5 controls: Rab5wt-GDP, Rab5wt-GppCp, Rab5 GTPase-deficient mutant Q79L and dominant negative mutant S34N. It was found that only Rab5-GppCp was able to bind significant amounts of the Myc_3-iSH2-p110β protein (Figure 4.9). It was expected that Rab5-Q79L-GppCp would bind to Myc_3-iSH2-p110β because it was locked in the GTP-bound conformation, but it was later determined that the residue Q79 was part of the binding site for p110β on Rab5; therefore its mutation reduced binding. The Myc_3-iSH2-p110α protein showed little or no binding to any form of Rab5, consistent with previous published work (Christoforidis *et al.*, 1999). These results indicated that Myc_3-iSH2-p110β bound specifically to Rab5-GppCp and was suitable for experiments to test p110β binding to Rab5 mutants.

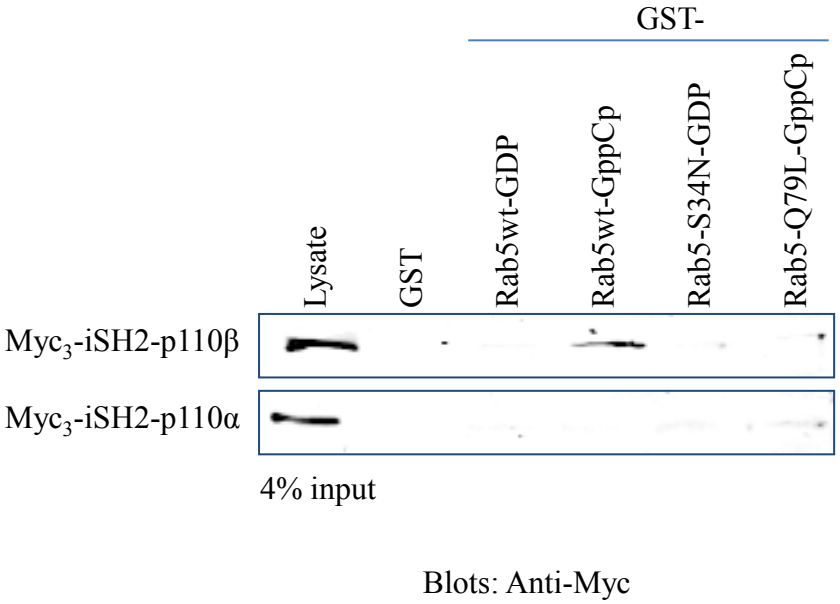

Figure 4.9 Rab5-GTP binds to Myc_3-iSH2-p110β but not Myc_3-iSH2-p110α. pull-down assay where GST, GST-Rab5wt bound to GDP or GppCp (a non-hydrolysable analogue of GTP), GST-Rab5-S34N (a mutant locked in the inactive conformation), or GST-Rab5-Q79L (active conformation mutant) were incubated with a chimeric Myc_3-iSH2-p110α or Myc_3-iSH2-p110β protein (which contains the iSH2 domain of p85) from COS-1 lysate. pull-down analyses were carried out as in Figure 4.1 and were immunoblotted with anti-Myc antibodies to detect bound Myc_3-iSH2-p110 proteins.

Amino acids in the Rab5 switch regions were chosen for mutation and testing for binding with p110β based on their accessibility in the GNP (a non-hydrolysable GTP-analogue)-bound crystal structure and their different conformation in the GDP crystal (Figure 4.10). The residues originally to be characterized were Q44, H46, and E47 in switch I and E80, R81, H83 and S84 in switch II. Some were mutated to alanine and others to a residue of opposite charge (see Table 4.1). Many of the pull-down experiments were conducted alongside Myc_3-iSH2-p110α as a negative control, but after three experiments it was decided that there was no binding to Myc_3-iSH2-p110α with any of the Rab5 mutants, and the experiments continued with the GST beads and the Rab5wt-GDP as negative controls.

Mutations in the switch I region, Q44E and H46A did not significantly affect p110β binding to Rab5 (Figure 4.11). The E47A mutant showed a slight reduction in binding. The E80R and H83E mutations of Rab5 were promising candidates of the p110β interaction-site, as they significantly reduced binding with p110β (Figure 4.11, 4.12 and Table 4.2), and showed little or no binding to p110α (not shown). However, it was possible that the charge-reversal mutations could be destabilizing the structure of Rab5. Therefore, other more modest mutations were tested, such as mutation to alanine for many of the amino acids investigated.

Rab5 amino acids involved in the binding-site to other Rab5 effectors (*i.e.* Rab5-GTP binding proteins) such as EEA-1, Rabaptin-5 and Rabenosyn-5 may also play a role in p110β binding. Therefore, eight additional mutations of Rab5 were chosen for p110β binding experiments: I53A, F57A, W74A, Y82A, L85A, M88A, Y89A and R91E; several of which were in switch II (AA 77-95). All of these mutants showed some reduction in p110β binding (Figure 4.11, 4.12 and Table 4.2). Of these, M88A, Y82A and I53A showed the most reduction of p110β binding. Thus, the Rab5 surface required for p110β binding was successfully identified (Figure 4.12 B).

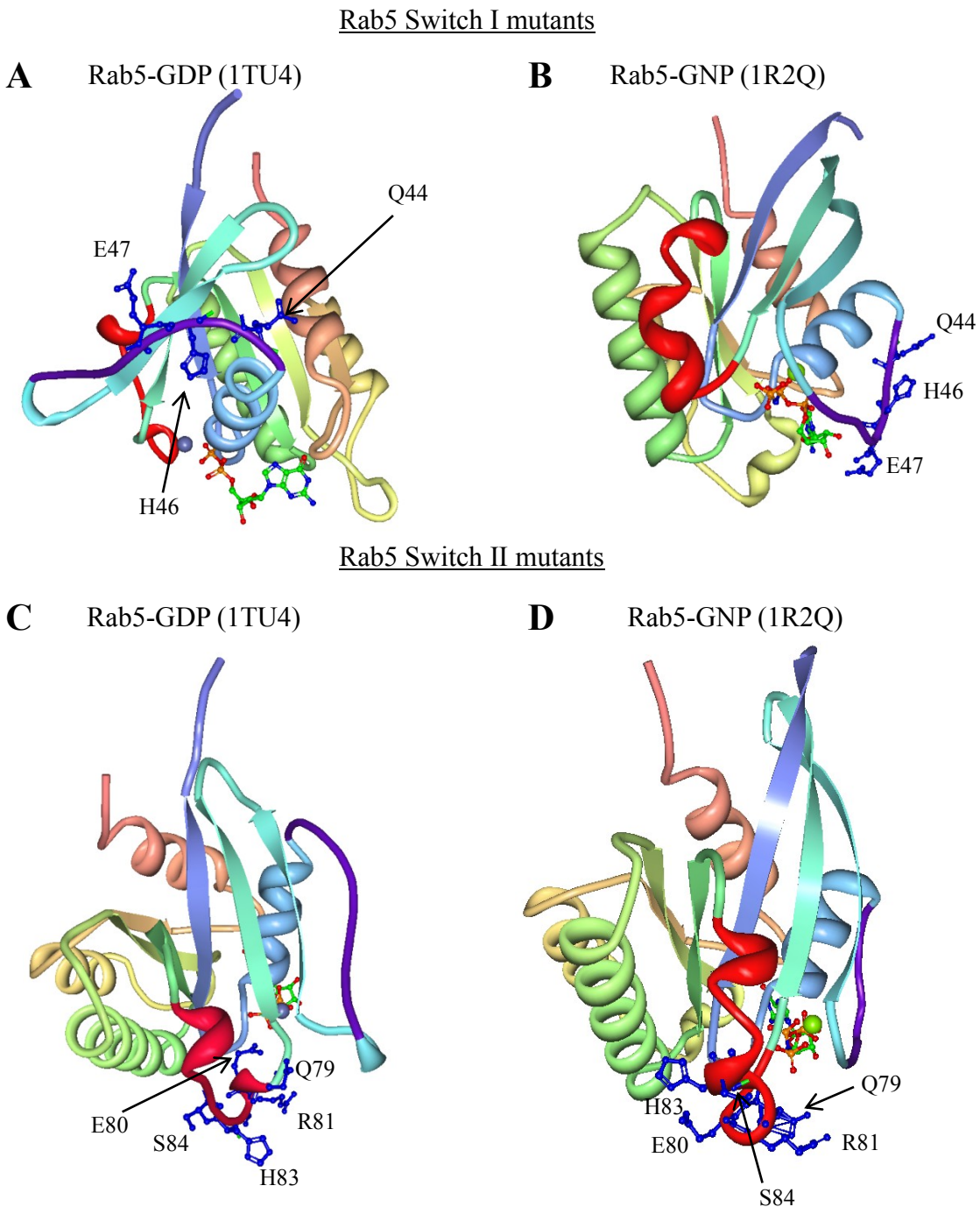

Figure 4.10 Residues that may bind p110β on crystal structures of Rab5 in both GDP and GNP bound conformations. Residues (*blue*) selected in the switch regions which have different conformations between GDP (1TU4) **A, C** and GNP(1R2Q) -bound Rab5 structures **B, D** and are facing outwards from Rab5 in the GNP-bound structure.

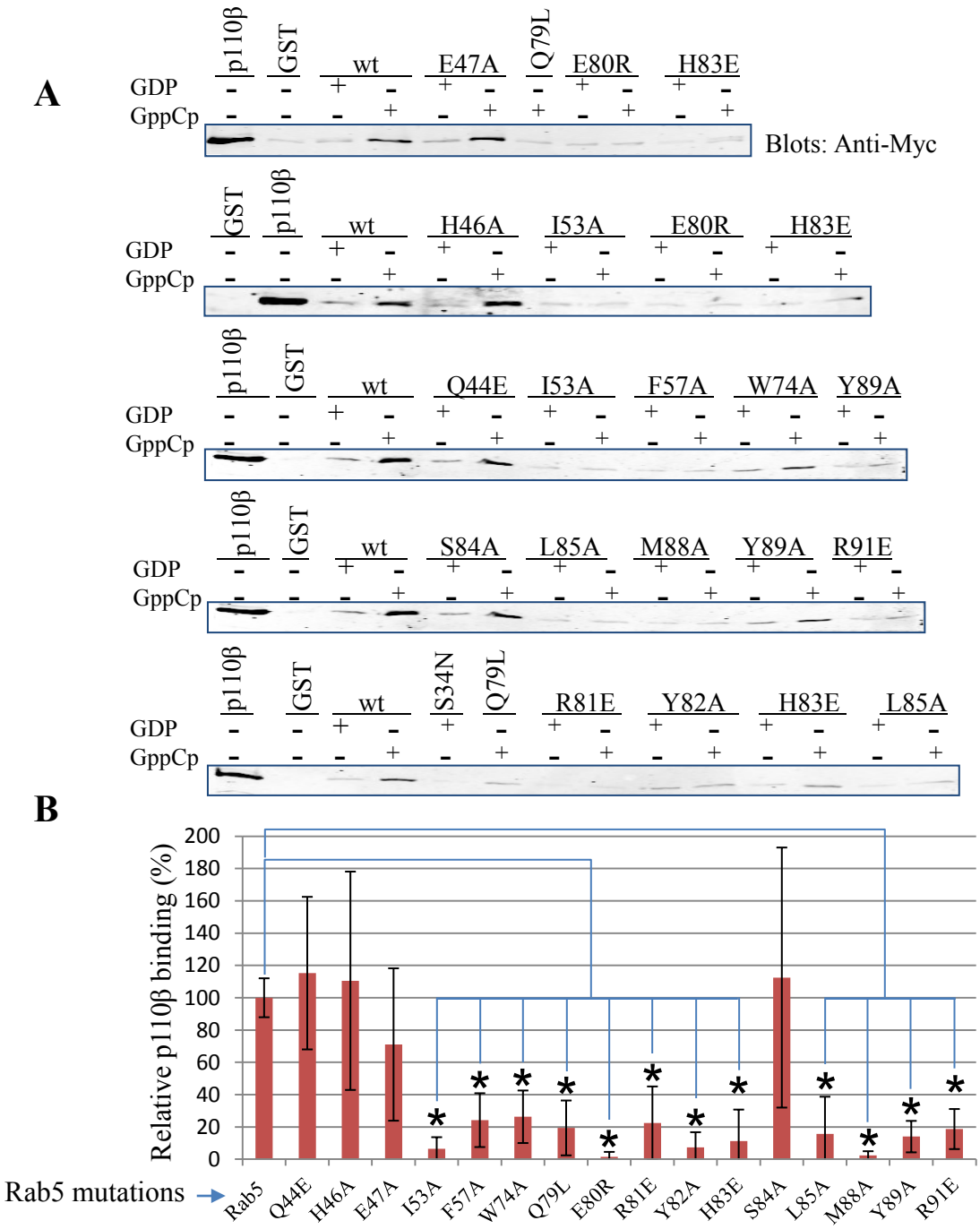

Figure 4.11 Myc$_3$-iSH2-p110β does not Bind to Rab5 switch II region mutants. A. GST, GST-Rab5 wt and mutant (as indicated) fusion proteins (10 µg) immobilized on glutathione Sepharose beads were loaded with either GDP or GppCp and incubated with Myc$_3$-iSH2-p110β from transfected COS-1 lysates. Bound Myc$_3$-iSH2-p110β was detected using an immunoblot analysis with an anti-Myc antibody. **B.** Quantification of pull-down binding data from A. Intensity of GppCp-bound mutant lanes was measured in arbitrary units and normalized to that of Rab5wt-GppCp; mean SD. (*) $P<0.01$, one way ANOVA (F = 10.96, df = 104), Dunnett's multiple comparison test. Only statistically significant P values are indicated. Also see Figure 4.12 & Table 4.2 for additional results.

A

Little or No Effect Switch I & II (> 70% binding)	Slight Reduction Switch I (30% reduction)	Reduction Switch II (>75% reduction)	Reduction Non-switch (>75% reduction)
Q44E (n=3)	E47A (n=7)	Q79L (n=6)	I53A (n=6)
H46A (n=7)		E80R (n=8)	F57A (n=5)
S84A (n=7)		R81E (n=5)	W74A (n=5)
		Y82A (n=4)	
		H83E (n=9)	
		L85A (n=10)	
		M88A (n=4)	
		Y89A (n=5)	
		R91E (n=4)	

B

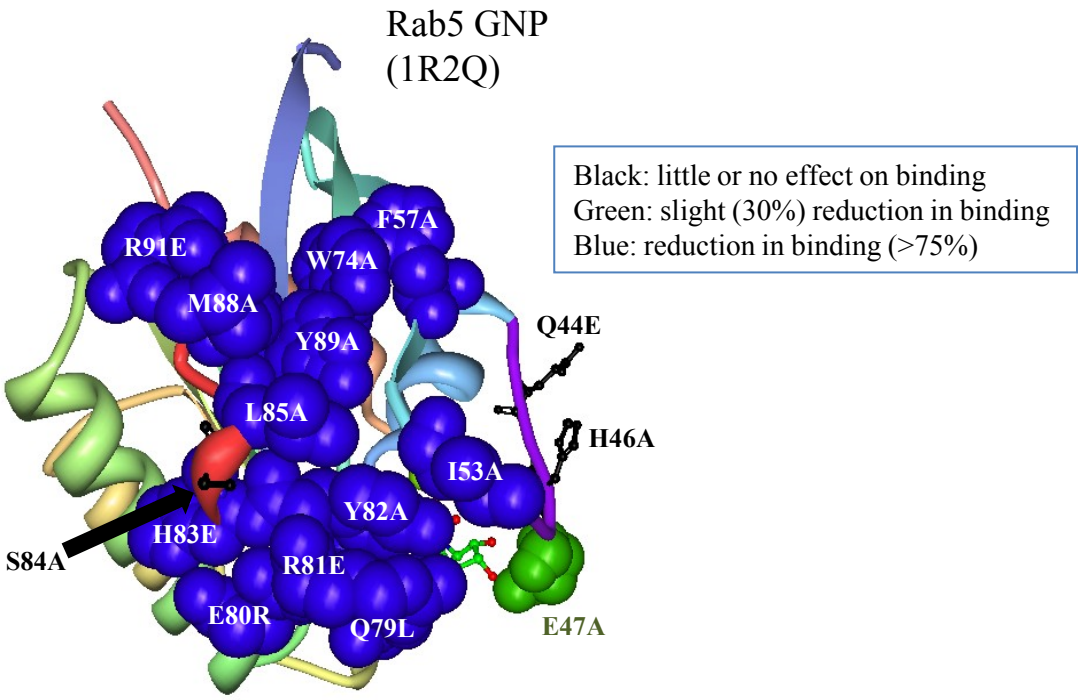

Figure 4.12 Rab5 mutations that affect p110β binding. A. Table of Rab5 mutations organized by their effect on Myc_3-iSH2-p110β binding. Experiments were carried out with different Rab5 mutant combinations so the number of replicates for each mutant is indicated in brackets. **B.** Rab5-GNP structure (1R2Q) displaying the mutated amino acids that had little or no effect on Myc_3-iSH2-p110β binding (*black*), reduced Myc_3-iSH2-p110β binding slightly (*green*), or greatly reduced binding (*blue*).

Table 4.2 Myc3-iSH2-p110β experiments. Experiments are represented by numbers along the top row. Each row depicts the amount of p110 binding in the GppCp bound form of a Rab5 mutant. Hierarchy of binding as follows: - (little or no binding), +/- (small amount of binding), + (binding observed), ++ and +++ (means substantial binding was observed). Blank spaces mean the mutant was not tested in that particular experiment. Arrows indicate the experiments that were represented in Figure 4.11.

Mutation	pull-down Experiment with Myc_3-iSH2-p110β																
	1	2	3	4	5	6	7	8	9	10	11	12	13	14	15	16	17
S34N									-							-	
Q44E									++		++	++					
H46A	+++		+++	+++	+++	+++	+++	+++									
E47A	+	+++	+++	+++		+	++	+									
I53A					-	-	-	+		-	-						
F57A									+	-/+	-	-					
W74A									+	-	+	+	+				
Q79L	-	-					+/-	+	+							+	
E80R	-	-	-	-	-	-		-				-					
R81E													-	-	-	-	+/-
Y82A														-	-	+/-	-
H83E		-	-	+	-	-	-						+	-		+	
S84A	+++		+/-		+++	+++	+++	+++							++		
L85A			-	+	-	-	-	++					-	-		-	+/-
M88A					-	+/-	-	-									
Y89A						+	-	+			-	+/-					
R91E					+	+	+	+									
wt	+++	++	+++	+++	+++	+++	+++	+++	+++	+++	+++	+++	+++	+++	+++	++	+++

4.6 Identification of Rab5 binding site with the p110β RBD domain

Previous studies have shown that p110 has a Ras Binding Domain (RBD: AA 196-286; Figure 4.13 A) through which it interacts with the small GTPase Ras. Considering that Rab5 is also a small GTPase and has some structural similarity to Ras, it has been proposed that p110β binds to Rab5 via the same domain. This theory has been affirmed by deletion mutations of p110β followed by pull-down experiments, and has been narrowed down to the Rab5 binding site to amino acids 136-270 of p110β (Kurosu and Katada, 2001). To determine the precise amino acids involved in Rab5 binding, a structural alignment between the RBDs of p110α (which does not bind Rab5-GTP) and p110β was performed with the assistance of Dr. Stanley Moore (Figure 4.14).

The crystal structure of p110β had been solved in complex with the p85 cSH2 and iSH2 domains (PDB: 2Y3A) but the p110β amino acids 234 to 240 were disordered (Zhang *et al.*, 2011). Alignment of the amino acid sequence demonstrated marked divergence between p110β RBD consensus sequence (AA 200-260) and that of p110α (Figure 4.13 B). Despite this, the residues surrounding the disordered region overlay well in the structural alignment (Figure 4.14). Five amino acids in the p110β RBD were identified to be distinct in both identity and positioning from p110α (in parentheses): L232 (T), I234 (S), E238 (S), D239 (S) and Y244 (G) though no conformational information was available for I234, E238 or D239. These amino acids were assessed for sequence conservation in p110β from 4 different species, rat, mouse, human and cow (Figure 4.13 B). Four of the residues were conserved among all species analyzed, while Y244 was conserved in human and bovine sequences only. These five amino acids were mutated separately within the full-length Myc-iSH2-p110β protein.

Pull-down experiments were performed with wild-type Rab5 in either GDP or GppCp bound states (Figure 4.13 C). The p110β mutants D239R and L232A mutants showed Rab5-GppCp binding comparable to p110βwt. p110β-E238R and -Y244A showed little or no binding to any form of Rab5, while p110β-I234A also had reduced binding. These results suggest that the Rab5:p110β binding interface contains residues I234, E238 and Y244 but not L232 or D239 within the RBD of p110β.

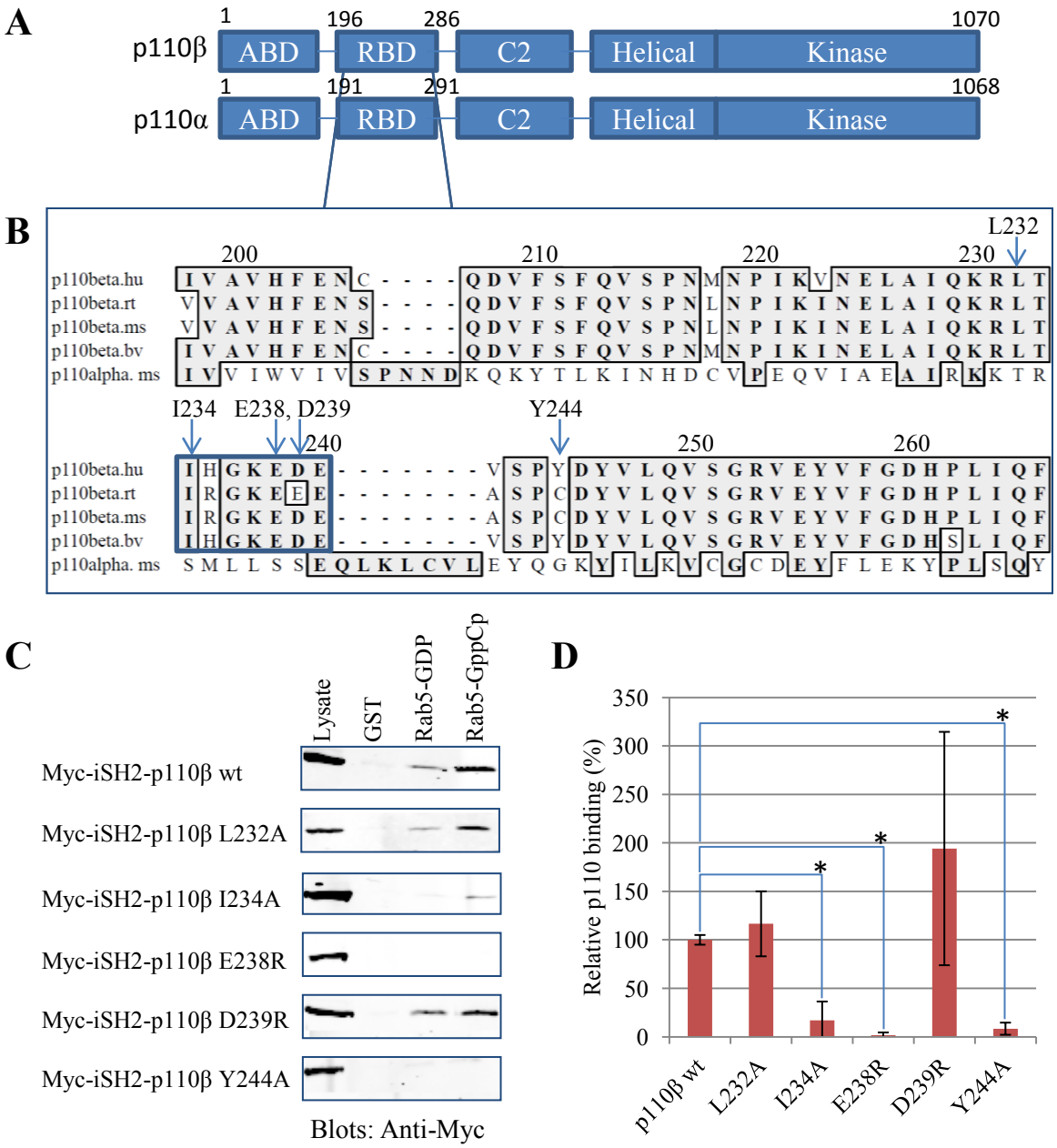

Figure 4.13 Identification of the Rab5 binding site within p110β. A. Domain representation of p110β and p110α (as indicated). ABD, adaptor binding domain; RBD, Ras Binding Domain; C2; helical and kinase domains. **B.** Sequence alignment of p110β from 4 species and p110α, mouse using ClustalW (v1.83). Residues not found in the p110β crystal structure are indicated by a blue box. Arrows indicate residues that were chosen for mutation. **C.** pull-down assay where GST-Rab5 was loaded with either GDP or GppCp and incubated with each Myc_3-iSH2-p110β mutant (as indicated) and analyzed as before. Blots are representative of 3 independent binding experiments. **D.** Quantification of pull-down binding data from **C**; intensity measured in arbitrary units and normalized to Myc_3-iSH2-p110βwt binding to Rab5GppCp; mean SD. (*) $P<0.01$, one way ANOVA ($F = 44.89$, degrees of freedom = 17), Dunnett's multiple comparison test.

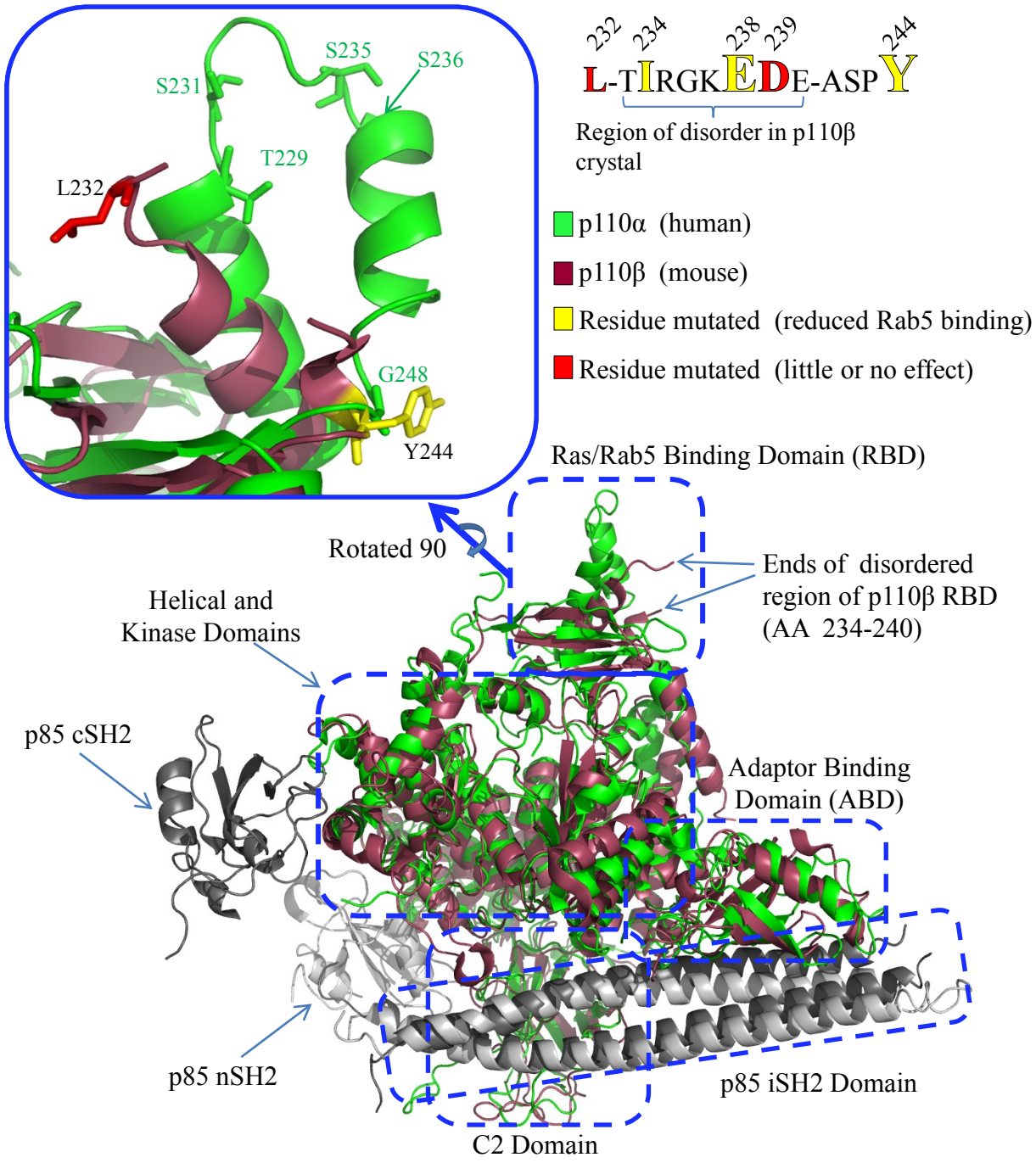

Figure 4.14 Structural alignment of p110β-cip85β and p110α-nip85α. *(lower)* Structural alignment of the p110βwt and p110α (H1047R) full length protein crystals containing either the C-terminal SH2 (cSH2) and iSH2 domains of p85β or the N-terminal SH2 (nSH2) and iSH2 domains of p85α, respectively. Structure formatted in PyMOL (V.1.4.1, Schrödinger, LLC). Domains of p110 and p85 are indicated by dashed blue boxes. p110β-cip85β (PDB ID: 2Y3A) in dark red and dark grey; p110α-nip85α (PDB ID: 3HIZ) in green and silver. *(upper)* RBD magnified domain with mutated amino acids indicated in either red (little or no effect on Rab5 binding) or yellow (reduction in Rab5 binding). p110β residues not present in structure are listed to the right.

5.0 DISCUSSION

5.1 Experiments to determine the binding site of p85 on Rab5

5.1.1 p85 regulation of and binding to Rab5 and Rab4

Rab proteins have critical roles in protein trafficking between different intracellular compartments including during endocytosis of activated surface receptors. As such, their activities are tightly regulated to protect growth factor receptors from undergoing inappropriate endocytic trafficking. The GAP p85 is especially relevant to the regulation of receptor trafficking dynamics because it inactivates both Rab5 and Rab4 (Chamberlain *et al.*, 2004). Rab5 is involved in the movement of activated receptors from early to sorting endosomes by regulating the fusion of early endosomes. Rab4 is involved in the recycling pathway of intracellular vesicle trafficking where internalized receptors on early/sorting endosomes are returned to the plasma membrane. Once recycled, receptors can resume interaction with their extracellular ligand, eliciting cellular effects by downstream protein signaling cascades. Alternatively, some receptors can be diverted from early/sorting endosomes to lysosomes and result in receptor degradation to terminate signaling events. If both Rab5 and Rab4 trafficking steps are overactive by disruption of their regulation, receptors could be repeatedly activated without proper signal attenuation which requires their degradation. Overactive growth factor signaling pathways is a major cause of tumorigenesis (Samuels and Waldman, 2010; Takeuchi and Ito, 2011; Bartholomeusz and Ganzalez-Angulo, 2012).

The binding between p85 and Rab5 has been investigated previously (Chamberlain *et al.*, 2004). It was determined that p85, which had GAP activity towards Rab5, bound to both active GTP- and inactive GDP-bound states of Rab5. The binding of p85 to other Rab proteins had not been determined, although p85 had GAP activity towards both Rab4 and, to a lesser extent, Rab6, but not to Rab11 (Chamberlain *et al.*, 2004). Through pull-down experiments with purified Rab proteins Rab5, Rab4 and Rab11 it was investigated whether p85 binding and GAP activity were correlated. In section 4.1, it was clearly shown that p85 bound to both Rab5 and Rab4 in either activation state, but had little or no binding to Rab11. Therefore, the binding of p85 was consistent with its GAP activity towards Rab proteins.

There were some differences in pull-down experiment results with Rab5 when using purified p85 and FLAG-p85 from lysate. It would be expected that the purified p85 protein would have increased binding to its substrates over the FLAG-p85 expressed in lysate because in lysate other proteins can compete for binding, including endogenous p85, whereas purified p85 had little or no contaminating proteins to compete for binding. However, the results of the pull-down experiments with Rab4 suggested that purified p85 bound less to Rab4 than FLAG-p85 from lysate (Figure 4.1). It is possible that the FLAG-p85 expressed in mammalian cells was folded in a different conformation that led to more productive binding as compared to bacterially expressed and purified p85. Another possibility is that post-translational modifications occurring in mammalian cells impacts p85:Rab4 binding. Rab11 had little or no binding with FLAG-p85 from lysate. Increased p85 binding to Rab11-GTPγS was observed when using purified p85, though it did not bind Rab11-GDP. Mammalian FLAG-p85 transfected cell lysates were used for subsequent binding experiments to control for differential folding in bacterial cells and/or post-translational modifications of p85 that may be important for Rab protein binding.

Rab5 showed good binding to FLAG-p85 in both its GDP and GTPγS bound forms (Figure 4.1), consistent with previous observations (Chamberlain *et al.*, 2004). The difference in FLAG-p85 binding between Rab5 activation states varied between experiments. In the Rab5, Rab4, and Rab11 experiments, FLAG-p85 bound more to Rab5wt-GTPγS than to Rab5wt-GDP (Figure 4.1 A, *upper*) whereas, in the experiments with the mutations of site A and B residues, FLAG-p85 bound more to Rab5wt-GDP (Figures 4.4 and 4.5).

Overall, p85 and FLAG-p85 bound to Rab4 about half as much as to Rab5 (Figure 4.1), which suggests that p85 may have a preference to bind Rab5 in the cell, and may exert a stronger effect on Rab5 regulation compared to Rab4. However, there are many other factors that may influence the p85:Rab4 interaction *in vivo*, such as proximity of the two proteins or competition between Rab5 and Rab4 for binding p85. If GAP activity of p85 is predominantly involved in Rab5 regulation, its disruption should have a greater impact on Rab5-mediated trafficking of receptors to the early endosome than on Rab4-mediated receptor recycling to the plasma membrane. The GAP-deficient p85-R274A mutant was investigated previously

(Chamberlain *et al.*, 2004; Chamberlain *et al.*, 2010), but the magnitude of its effect on Rab5 compared to Rab4 was not measured or apparent.

5.1.2 Pull-down experiments with FLAG-p85 and Rab5 mutants

A sequence alignment between Rab4, Rab5 and Rab11 was used to identify residues that could be involved in p85 binding (Figure 4.2). Eight residues (S84, E106, N113, F145, E172, M175, K179 and K180) were selected based on their conservation in Rab4 and Rab5 and divergence in the Rab11 sequence. Pull-down experiments were performed with Rab5 proteins, with mutations in the eight chosen amino acids, to test two putative binding sites for p85, arbitrarily termed site A and site B.

In the site A experiments (S84A, E106A, N113A, N113E), there was one mutation of Rab5 within the switch II region, *e.g.* S84A, which reduced binding to p85 in three experiments (Figure 4.4). It is still unknown what caused the S84 mutant to have reduced binding to p85, but it is known that the protein used in the three experiments were from the same preparation of Rab5-S84A. Therefore, additional testing of different preparations of this mutant (as well as other mutations of this residue) was deemed sufficient to assess its importance in p85 binding, and ultimately eliminate S84 as a candidate involved in the p85:Rab5 binding interface.

Rab5 mutants bearing substitution within site B, *e.g.* F145A, E172A, E172R, K179A and K180A, had different effects on p85 binding when bound to GDP or GTPγS (Figure 4.5). An increase in FLAG-p85 binding could mean that the side chain of the mutated residue is normally disruptive to p85:Rab5 binding, or that it constrains Rab5 in a less productive shape for p85 binding that the mutation releases. Therefore, it is possible that the Rab5 amino acids residing near those whose mutation increased FLAG-p85 binding may be involved in the binding site. Mutation of residues next to E172, for example, may decrease p85 binding to Rab5. Another possibility is that the binding site of p85 on Rab5 is mainly non-polar and the removal of large or charged functional groups, and their replacement with a methyl group (from mutation to alanine), would increase affinity of p85 for Rab5 and possibly expand the binding site between the proteins. Incongruent with this theory is the fact that a charge reversal caused the greatest increase in binding, namely E172R. Interpretation of the data suggests that residues in site B of Rab5 are not normally involved in p85 binding, though their mutation may provide additional contacts to expand the existing binding site on Rab5.

It was decided to perform pull-down binding studies with FLAG-p85 from lysate instead of purified p85 protein, although that may not have been the best choice because p110 (alpha or beta) binding to FLAG-p85, as well as the competition with endogenous p85, may have impacted the results. If p110β was bound to FLAG-p85 during the pull-down experiments, for example, any Rab5 mutation-induced reduction of p85 binding could have been masked by p110β:Rab5 binding – which would artificially increase the FLAG-p85 signal. However, by the time this became apparent, most of the experiments had already been completed.

5.1.3 Rab5 binding to p85 using yeast two-hybrid experiments

The mutation of carefully selected amino acids did not resolve the p85 binding site on Rab5, so yeast two-hybrid experiments were pursued as a non-biased method to identify Rab5 amino acids involved in binding to p85. Yeast two-hybrid experiments are useful to identify binding partners of a bait protein from a large library of prey proteins. With the use of replica plating and plasmid DNA sequencing, one can also screen for non-binding proteins based on the lack of growth in selection media as compared to a positive control. A library of B42-Rab5 proteins randomly mutated by an error-prone DNA polymerase was to be tested for binding with p85. Non-binding mutant expressing colonies would not grow in selection media and would be traced back to the original plate and sequenced.

The yeast two-hybrid experiment with wild type Rab5 and p85, however, was not successful. Though both proteins were expressed in the diploid yeast colonies in galactose media (data not shown), it seemed that their interaction was not strong enough, or perhaps not stable enough, to drive the transcription of the reporter genes. It is possible that, by growing the yeast on media lacking both adenine and leucine, as well as containing X-gal, the stringency for interaction was too high. Perhaps if each of the markers were selected for separately, first looking for adenine gene expression, then leucine, it would have been less stressful for the yeast.

Another possible difficulty with the yeast two-hybrid experiments might have been the structure of the fusion proteins. Both Rab5 and p85 were expressed in yeast as B42 and Lex-A fusion proteins, respectively, attached at the N-terminus of the protein of interest. The folding of the fusion proteins may have masked the binding site of either Rab5 or p85, resulting in their inability to bind each other. One way to assess the effects of folding on the ability of the fusion

proteins to interact would be to reverse the order of proteins expressed, so that Lex-A or B42 are expressed as the second protein attached C-terminally to p85 and Rab5, respectively. The B42 protein has a nuclear localization signal that would also have to remain at the N-terminus. While being tethered to other proteins, the freedom of movement in space of Rab5 and p85 was restricted, and may have been the reason that they did not interact in the yeast two-hybrid experiments.

5.1.4 The p85 binding site on Rab5: other possibilities and future studies

The original hypothesis of the p85 binding experiments hinged on the fact that p85 bound to all conformations of Rab5. This result suggested that residues involved in binding would be positioned similarly and available for binding in both active and inactive forms, so binding should not be conformation dependent. However, this hypothesis was reconsidered after testing mutations of Rab5 amino acids with conserved orientation between active and inactive states for p85 binding, which did not resolve the binding site on Rab5. It is possible that the Rab5 residues involved in p85 binding could differ between activation states and that two binding sites could exist on Rab5 that both bind p85. This project did not determine the binding site of p85 on Rab5.

The p85 mutant R274A does not bind to Rab5-GTP, suggesting that the arginine residue may be critical for Rab5 interaction (Chamberlain *et al.*, 2004). As mentioned in section 1.5, an arginine finger generally forms H-bonds with the conserved glutamine (Q79) through its backbone carbonyl group and H-bonds with the γ-phosphate or β-γ bridge oxygen of GTP through the guanidinium group (see Figure 1.9). Mutation of this arginine to alanine would not disrupt the backbone interactions unless the position of the residue was shifted, which is possible. Conversely, the mutant p85-R274A still bound to Rab5-GDP. To further complicate matters, the BH-domain deletion mutant of p85 bound to Rab5-GTP but not Rab5-GDP (Chamberlain *et al.*, 2004) which suggests that other region(s) of p85 outside the BH domain help to bind Rab5. Interpretation of these findings is difficult, but it does suggest that the different conformations of Rab5 could be interacting with p85 in different ways, and possibly for different purposes.

5.1.4.1 p85 could be a GDF to Rab5

Generally, Rab5-GDP is cytosolic, bound to a GDI which makes contacts with both switch regions and the geranylgeranylated C-terminus (Figure 1.5 and 5.1 B). The mechanism of recruitment of Rab proteins to their target membranes remains controversial. Some research shows that nucleotide exchange is sufficient to release the tightly bound GDI from a Rab protein, as its affinity for the active conformation of Rab GTPases is very low (Wu *et al.,* 2010). Another study demonstrated that post-translational modification of the Rab, as well as direct competition by other Rab binding proteins, was effective in GDI displacement (Oesterlin *et al.*, 2012). However, for a GEF to stimulate guanine nucleotide exchange or for the Rab to be modified by enzymes (*i.e.* phosphocholination by AnkX), the GDI must be displaced, because GDI, GEF and AnkX interact with a similar epitope on the GTPase (Wu *et al.,* 2010; Oesterlin *et al.*, 2012). Thus, GDI displacement factors (GDFs) have been assumed to fill the role for GDI displacement at the target membrane.

One family of GDFs, the Ypt interacting proteins (Yip)s, has been discovered in yeast. Yip3 and its human homologue prenylated Rab acceptor-1 (PRA-1) were found to induce dissociation of Rab9 from Rab9-GDI complexes (Sivars *et al.,* 2003). PRA-1 may facilitate GDI release in a non-specific manner because it interacts with many prenylated Rab proteins in mammalian cells (Bucci et al., 1999; Martincic et al., 1997). The mode of action of GDI displacement by Yips is not fully understood, though it is hypothesized that the Rab C-terminal isoprenyl groups are transferred from the GDI to the GDF (Pfeffer and Aivazian, 2004).

It has been suggested in the literature that p85 could be involved in recruiting Rab5 to the plasma membrane, acting as a GDF on the inactive Rab5-GDP (Chamberlain *et al.*, 2010; Mellor *et al.,* 2012). From the binding data available, it is unclear whether p85 binds to Rab5-GDP in the cellular environment. Pull-down data in this thesis and previously reported (Chamberlain *et al.,* 2004) made use of purified Rab proteins loaded with the guanine nucleotide of choice, therefore the complication of GDI binding was not tested. If p85 did bind Rab5-GDP *in vivo*, it would need to displace the GDI or bind to a region of Rab5 which is not involved in binding GDI. Fluorescence resonance energy transfer (FRET) experiments using fluorophore-tagged Rab5 and p85 could be used to characterize their interaction *in vivo*.

Moreover, the use of dominant-negative (S34N) and GTP-locked (Q79L) mutants of Rab5 in the FRET analysis would clarify whether p85 binds to Rab5-GDP *in vivo*.

One region of Rab5 that was not investigated for p85 binding was the C-terminal hypervariable region (AA 186-215; Figure 5.1) because it was not included in the Rab5-GDP or Rab5-GNP crystal structures and it had been found previously to not be involved in effector binding (Zhu *et al.,* 2007). This region is predicted, by comparison with the solved structure of the Ypt1:GDI complex, to bind loosely to the GDI protein via conserved hydrophobic residues V199 and L201 and the two gernanylgeranyl groups attached to C212 and C213, which are bound in a separate hydrophobic compartment of GDI (Rak *et al.,* 2003; Pfeffer, 2005; Figure 5.1 A). The loose attachment of the hypervariable region to GDI may present AA 181-198 and 202-211 on the outside face of the Rab5-GDI complex (Figure 5.1 B), as seen in the Ypt1:GDI complex (Rak *et al.,* 2003). If that is the case, the residues would be available for binding with other proteins such as p85. If p85 binding to Rab5-GDP was confirmed *in vivo,* for example by a co-immunoprecipitation (and immunoblotting with both anti-Rab5 antibody and anti-active Rab5 antibody, which detects only Rab5-GTP, as a control) or by FRET, the hypervariable C terminus would be a good target for mutagenic binding studies to continue the search for the p85 binding site on Rab5.

There were other amino acids which were identified in the sequence alignment that were conserved in Rab5 and Rab4 but not Rab11, but were not investigated because they were not included in the crystal structure of Rab5 (1TU4 and 1R2Q). These amino acids were N10, T14, G190, G197, G199, and A214. Without knowledge of how these residues are positioned in the tertiary structure of Rab5 it cannot be known whether they are available for p85 interaction. Because the p85 binding site on Rab5 was not determined in this thesis, these amino acids are good candidates for mutation and testing based on the original hypothesis.

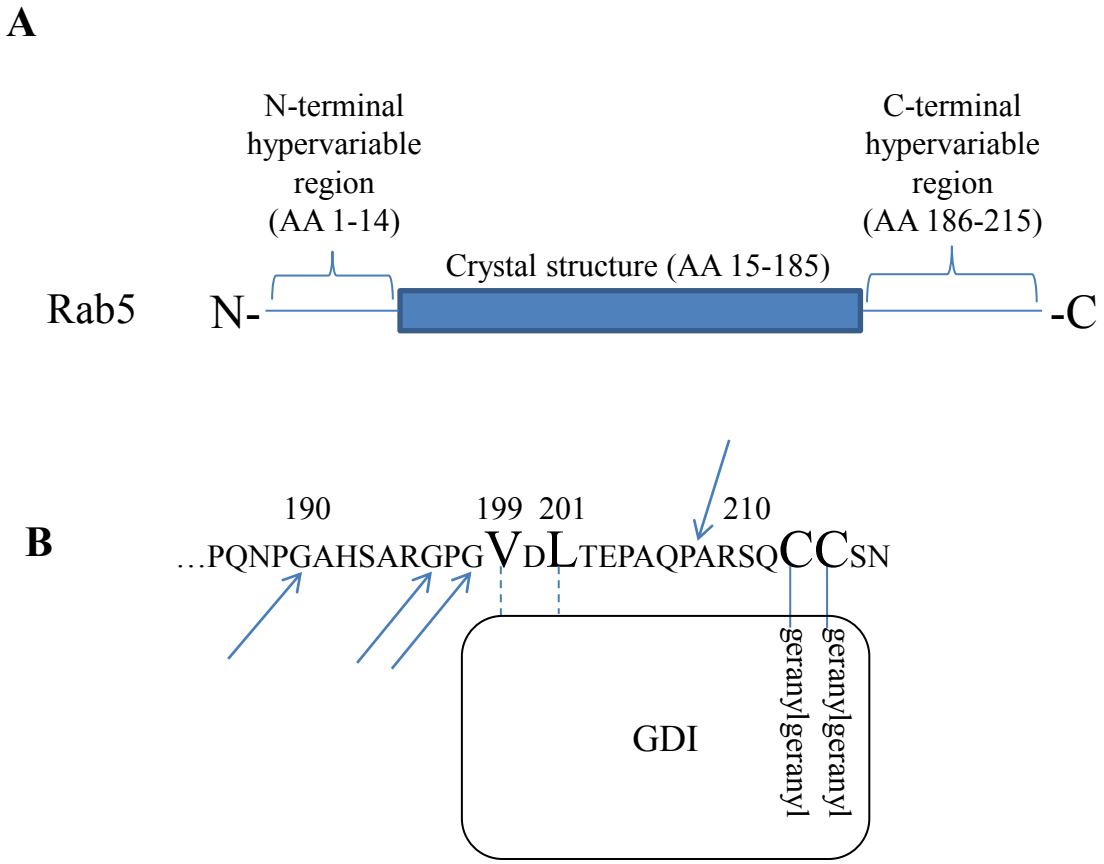

Figure 5.1 Sequence of Rab5 C-terminal hypervariable region. A. Representation of the amino acid sequence present in the crystal structure of Rab5 (PDB ID: 1R2Q, 1TU4) in relation to the N- and C-terminal hypervariable regions. **B.** Sequence of the C-terminal hypervariable region. Valine 199 and leucine 201 interact with a hydrophobic domain of GDI (*dashed lines*). Conserved cysteines 212 and 213 interact with GDI via post-translationally added geranylgeranyl groups. Arrows indicate residues which are conserved between Rab5 and Rab4 but not Rab11 amino acid sequence, and therefore may be involved in p85 binding.

5.1.4.2 p85 binding to Rab5 could be activation-state dependent

To determine how a small GTPase normally interacts with its GAP, a structural alignment of Rab5-GNP (1R2Q) with the small GTPase Cdc42 (1AM4), of the Rho subfamily, was performed (Figure 5.2 A). The crystals showed good structural similarity. Cdc42 has been co-crystallized with its GAP, p50rhoGAP ("rhoGAP"), and therefore the residues involved in polar interactions between them could be determined (Rittinger *et al.*, 1997a). The structural alignment identified Rab5 amino acids that corresponded to residues of Cdc42 which made polar contacts with rhoGAP, which could be tested for effect on p85 binding, including: S29, F57, R81, and Y82 (Figure 5.2 B). Of these residues, F57, R81, and Y82 were found to be involved in p110β binding of Rab5 (discussed in greater detail below) and thus would not be available for binding to p85. The orientation of serine 29 does not change between activation states.

As a comparison, another structural alignment was performed with Rab5-GNP (1R2Q) and Rho (1TX4), which was also co-crystallized with rhoGAP (Rittinger *et al.*, 1997b; Figure 5.2 C). Again, the same four residues in positions equivalent to Rab5 S29, F57, R81 and Y82 were found to be involved in polar contacts with the GAP (Figure 5.2 E). However, in this second alignment, there was a second set of polar contacts including Rab5 equivalent residues E106, R110, and N113 (Figure 5.2 D). Both E106 and N113 were mutated and investigated in the site A pull-down experiments (Figure 4.4) and their mutation did not affect p85 binding. Therefore, from the two structural alignments with Rho-family proteins, Cdc42 and Rho, the only new candidate amino acids for p85 binding to Rab5 that have not been pursued, or are not already involved in p110β binding, were S29 and R110. The side chain of arginine 110 points outwards in the Rab5-GDP crystal structure and folds inwards in the active Rab5-GNP crystal, so its involvement in p85 binding would make the interaction conformation dependent. Some Rab5 mutations, *i.e.* F145A, E172R, K179A and K180A, had different effects on p85 binding when in the GDP- vs. GTP-bound conformation, which also supports the activation-state dependence of p85 binding to Rab5.

The crystal structure of the p85 BH domain has also been determined (Musacchio *et al.*, 1996). Alignment of rhoGAP (1AM4) and p85BH (1PBW) has been described previously (Fidyk and Cerione, 2002). In their study, attention was paid to the lack of switch stabilizing

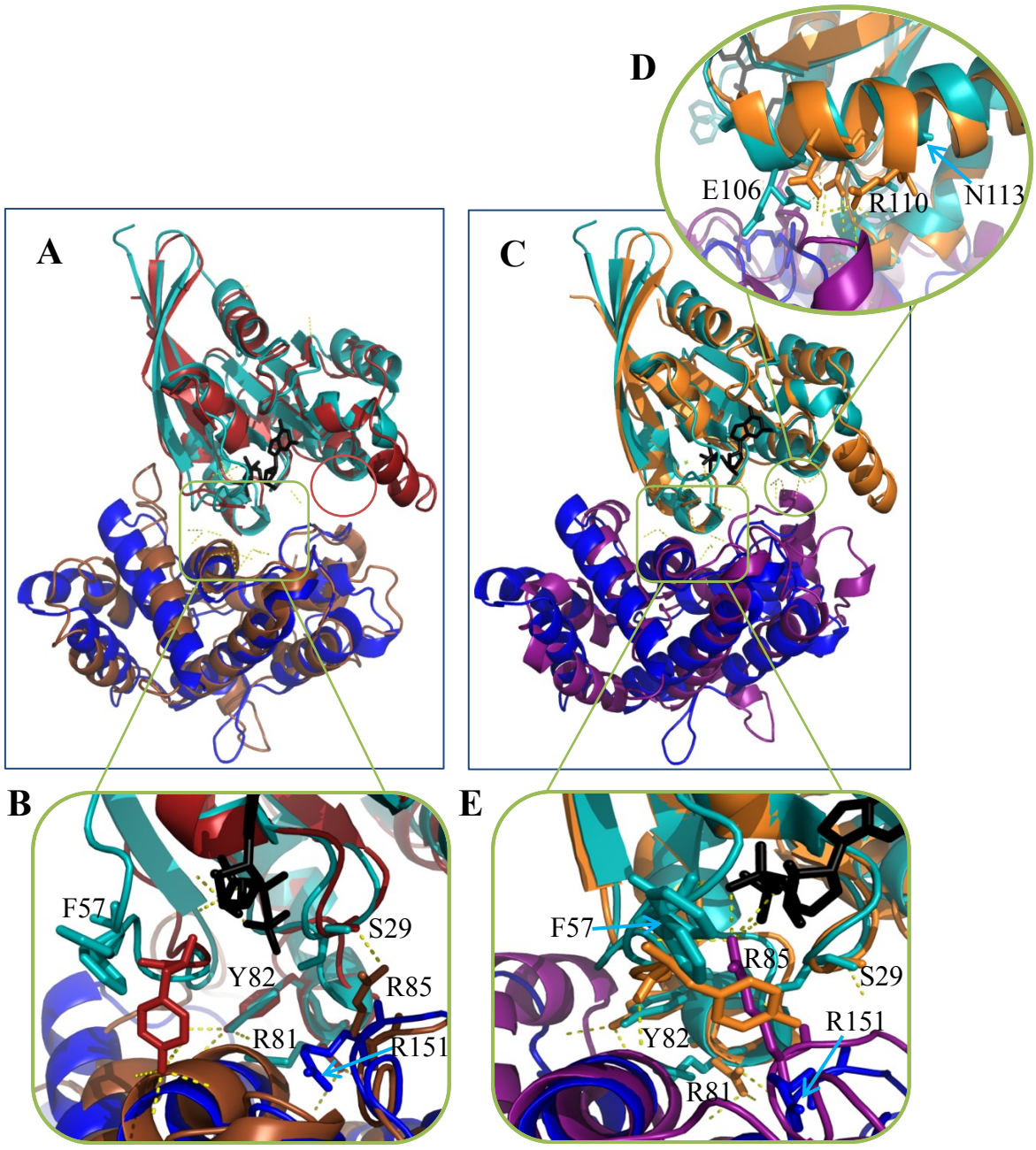

Figure 5.2 Structural alignment of Rho protein/GAP complexes with Rab5-GNP and p85 BH domain. **A.** Cdc42 (*red*) co-crystallized with p50rhoGAP (*brown*) (PBD ID: 1AM4) was aligned with Rab5-GNP (*teal*, 1R2Q) and the BH domain of p85 (*blue*, 1PBW) using PyMOL. GNP in black; yellow dashes indicate polar contacts between Cdc42 and p50rhoGAP**. B.** Close up view of the interaction interface. Rab5 amino acids (*teal*) in equivalent positions to those of Cdc42 involved in polar contacts with p50rhoGAP are numbered. p85-R151 in blue, p50rhoGAP-R85 in brown. **C.** Rho (*orange*) co-crystallized with p50rhoGAP (*purple*) (PDB ID: 1TX4) was aligned with Rab5-GNP (*teal*) and the BH domain of p85 (*blue*) as in A. **D.** Close up of polar contacts between Rho and p50rhoGAP that are not seen in Cdc42:p50rhoGAP interaction. Equivalent amino acids of Rab5 are indicated. **E.** Same as B, but for the Rho/Rab5, p50rhoGAP/p85BH alignment.

contacts available on the p85 structure. However, the catalytic arginine finger R274 was pointing inwards in the alignment with rhoGAP crystal 1AM4 (Figure 5.3 A) as well as when aligned with the structure of p120rasGAP, 1WQ1 (Figure 5.3 B). Another arginine of p85,R151, aligned well with the arginine finger of rhoGAP, R85 (Figure 5.3 C) and that of p120rasGAP, R789 (Figure 5.3 D). Since mutation of R151 scarcely affected p85 GAP activity while mutation of R274 greatly reduced GAP activity (Chamberlain *et al.*, 2004), it has already been established that the arginine finger of p85 is R274. Thus, if R274 is facing inwards in the alignment with rhoGAP and p120rasGAP, the alignment may not accurately portray the method of action of p85 GAP activity and its interaction with Rab5.

5.2 Experiments to determine the p110β binding site on Rab5

5.2.1 Myc_3-iSH2-p110 does not co-immunoprecipitate with p85

Phosphatidylinositol 3`kinase is an obligate heterodimer (Hirsch *et al.,* 2007). The class IA isoforms, which are the focus of this thesis, require interaction of p110 and p85/p55 subunits for stability (Klippel *et al.,* 1993). Thus, the generation of a p110β protein source which did not bind p85 *in vivo* was necessary to isolate the binding event between Rab5 and p110β. Using the template of LT Williams' lab (Hu *et al.,* 1995), a chimeric protein was generated which encoded the iSH2 domain of p85 attached N-terminally to the full-length p110 protein by a glycine linker (Figure 4.7 A). This protein was readily detected in transfected COS-1 cell lysates through its triple Myc tag using anti-Myc antibodies (Figure 4.8). As predicted, the iSH2 domain containing p110 proteins showed little or no binding to either FLAG-p85 or endogenous p85 in a co-immunoprecipitation assay (Figure 4.8 B and D). The iSH2 domain of the chimera would be able to bind to the ABD of p110, thus stabilizing the chimeric p110 protein as well as saturating a major contact point between p110 and p85, precluding the binding of full-length p85 to that site. While the iSH2 domain was able to stabilize p110, it would not be able to provide inhibitory contacts to the helical or kinase domain of p110 since these are provided by other regions of p85. Therefore, the Myc_3-iSH2-p110 protein would be expected to be constitutively active, as it was for LT Williams (Hu *et al.,* 1995). The lipid kinase activity of the chimera generated in this thesis was not tested. The isolation of p110 from p85 binding was the sole purpose of the chimera to be used in pull-down experiments with Rab5.

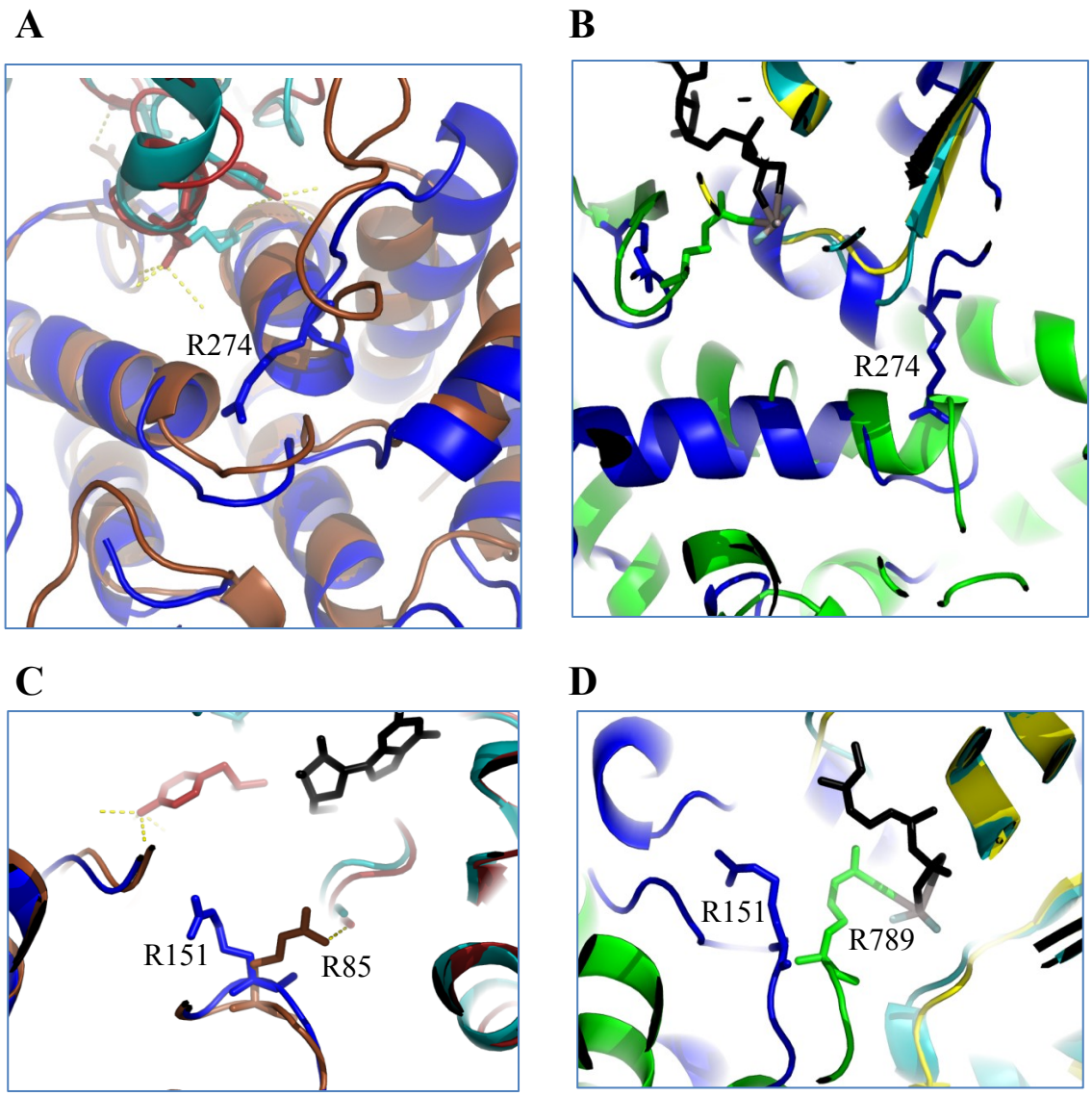

Figure 5.3 Arginine finger orientation from structural alignment of the p85 BH domain with p50rhoGAP and p120rasGAP. **A.** Structural alignment between p85 BH domain (PDB ID: 1PBW, *blue*) and p50rhoGAP (1AM4, *brown*). Close up of the arginine finger of p85, R274. **B**. Structural alignment between p85 BH domain (1PBW, *blue*) and p120rasGAP (1WQ1, *green*). Close up of p85-R274. **C.** Alignment as in A. Close up of p85-R151, which aligns with the arginine finger of p50RhoGAP, R85. **D.** Alignment as in B. Close up of p85-R151, which aligns with the arginine finger of p120rasGAP, R789.

5.2.2 Pull-down experiments with Myc_3-iSH2-p110β and Rab5 mutants in the switch regions

In 1999, Christoforidis and colleagues demonstrated that the p110β isoform only binds to active Rab5 by affinity chromatography (Christoforidis *et al.*, 1999). Therefore it was hypothesized that the residues of Rab5 involved in binding p110β were within the switch regions of the protein and that the interaction was conformation dependent. Therefore, the iSH2/p110 chimera was used in pull-down binding experiments to identify Rab5 mutants that reduced binding to p110, without the complication of p85 binding. The p110 binding to wild-type Rab5 correlated well with published results: Myc_3-iSH2-p110β only bound to Rab5wt-GTP (Figure 4.9). As expected, Myc_3-iSH2-p110α did not bind Rab5 in either activation state (Figure 4.9).

Mutations of amino acids in switch I and switch II regions of Rab5 were then tested for binding to Myc_3-iSH2-p110β. Some Rab5 mutants had variability in p110β binding which was not ideal. Most Rab5-GDP lanes have a trace amount of p110β binding, which could be attributed to the incomplete stripping/loading of Rab5 with the nucleotide of choice, as previously shown by Cody Bergman in his thesis (Bergman, 2012). Therefore there could be some residual Rab5-GTP on the glutathione-Sepharose beads after nucleotide exchange, and therefore a potential binding partner for small amounts of p110β.

Mutations of Rab5 that reduced p110β binding were I53A, F57A, W74A, Q79L, E80R, R81E, Y82A, H83E, L85A, M88A, Y89A and R91E which are depicted as a binding site on the Rab5 protein crystal structure in Figure 4.12. Interestingly, S84A did not affect binding despite its location in the center of the binding site. The hydroxyl group of S84 may not make polar contacts with p110β, but the backbone of the protein might still be involved in binding and would not have been affected by its mutation to alanine. Most of the residues mutated which reduced p110β binding reside in the switch II region of Rab5, whereas the only mutation in switch I that reduced binding was E47A, and it only had a small effect compared to the other mutations. Three residues from the "inter-switch" region (or the sequence between the switch I and switch II regions *i.e.* AA 53-77) were also involved in the binding interface: I53, F57, and W74. Looking at the crystal structures of Rab5 (Figure 4.3 A vs. B), switch I (*purple*) adopts a greater difference between activation states than does switch II (*red*), therefore its stabilization

should make the greater difference in activation energy required for the reaction. A possible reason for the greater representation of switch II in the p110β binding site is the structural variability in the switch II region due to non-conservative substitutions between Rab proteins, while the inter-switch and switch I regions derive specificity in binding by their conformation which is indirectly influenced by packing of secondary structure within the protein core (Mishra *et al.*, 2010).

5.2.3 The binding site of p110β on Rab5

It is possible that there are more Rab5 residues involved in binding p110β which were not identified in this thesis. Other Rab5 amino acids in the switch II region, *i.e.* A86 and Y90 were not tested but could make contacts with p110β, as well as amino acids proximal to I53: G54, A55, and A56, which were involved in binding other effectors, Rabenosyn-5 and EEA-1 (Mishra *et al*., 2010; Eathiraj *et al*., 2005). The data available for Rab5 effector binding sites, including EEA1, Rabenosyn-5, Rabaptin-5 and APPL1, was summarized in Table 5.1 and compared to the results of binding studies with p110β.

Co-crystal structures including Rab5 and effector were used to determine residues involved in binding to EEA1 (Mishra *et al.*, 2010) and Rabaptin-5 (Zhu *et al.*, 2004), whereas the binding site for APPL1 (Zhu *et al.*, 2007) and Rabenosyn-5 (Eathiraj *et al.*, 2005) were inferred from crystal structures not containing Rab5 and mutational binding assays, as was done with p110β in this thesis. Both EEA1 and Rabenosyn5 bound Rab5 via a FYVE zinc-finger motif. Rab5 bound to the PH domain of APPL1 in the context of APPL1 BAR-domain:PH-domain dimers. Similarly, Rab5 interacted with the coiled-coil C-terminal domains of Rabaptin-5 dimers. The RBD of p110β was demonstrated previously (Kurosu and Katada, 2001) to be the binding site for Rab5.

The binding site of p110β on Rab5 included a majority of residues also involved in binding Rab5 effectors (Table 5.1). The need for a unique binding epitope to ensure specificity of effector recruitment and binding became apparent when the extensive structural and sequence homology between other members of the Ras superfamily of small GTPases and Rab5 was considered. Positioning of functional groups is important for effector recognition of their Rab binding partner. Amino acids F57, W74 and Y89, for example, are called the invariant hydrophobic triad (Merithew *et al.*, 2001; Table 5.1, highlighted in orange), because they show

Table 5.1 Rab5 amino acids involved in binding effectors. Rab5 amino acids involved in binding with at least one of 5 effectors: Rabenosyn-5 (Eathiraj *et al*., 2005), EEA-1 (Mishra *et al*., 2010), Rabaptin-5 (Zhu *et al.,* 2004), APPL1 (Zhu *et al*., 2007) and p110β (this thesis) are indicated in the left column. If mutation of the amino acid (mut binding) affected binding to the effector or if the crystal structure revealed a contact point with that amino acid, a Y signifies "yes" or important for binding. If the mutation did not affect binding, or the crystal structure showed no interaction with that amino acid, a N depicts "no" or not important for binding. Y/N means both positive and negative results have been demonstrated. "-" means the amino acid has not been tested for binding. The invariant hydrophobic triad amino acids are highlighted in orange. Unique amino acids of Rab phylogenic group 5 are highlighted in green. Amino acids which were important for binding all effectors tested and are not included in the groups above are highlighted in light purple. Amino acids specific to binding p110β are highlighted in blue.

Amino acid involved in binding (Y/N)	**Rabenosyn-5** (Rab22 crystal structure & mut binding)	**EEA-1** (crystal structure)	**Rabaptin-5** (crystal structure & mut binding)	**APPL1** (mut binding)	**p110beta** (mut binding)
Q20	Y	N	N	-	-
K22	N	Y	N	-	-
L38	N	N	N	N	-
K42	Y	N	N	Y	-
Q44	N	N	N	Y	N
H46	N	N	N	Y	N
E47	N	N	N	-	Y/N
F48	N	N	N	Y	-
Q49	N	Y	N	N	-
E50	Y/N	Y	N	N	-
S51	Y	Y	N	-	-
T52	N	Y	N	-	-
I53	Y	Y	N	N	Y
G54	Y	Y	Y	-	-
A55	Y/N	Y	Y	-	-
A56	Y	Y	N	-	-
F57	Y	Y	Y	N	Y
L58	N	N	Y	-	-
T59	Y/N	N	Y	-	-
Q60	N	N	N	-	-
K70	Y	N	N	-	-
E72	Y/N	Y	N	-	-
W74	Y	Y	Y	Y	Y
Q79	N	N	N	Y	Y
E80	N	N	N	-	Y
R81	Y	N	Y	-	Y
Y82	Y	Y	Y	-	Y
H83	N	N	N	-	Y
S84	Y	Y	N	-	N
L85	Y	Y	Y	Y	Y
P87	N	N	N	-	-
M88	Y	Y	Y	Y	Y
Y89	Y	Y	Y	Y	Y
R91	Y	Y	N	-	Y

drastic conformation differences between Rab proteins while still being highly conserved in all Rab protein sequences. These three residues have been implicated in Rab5 binding with effectors EEA-1, Rabenosyn-5, Rabaptin-5, APPL1 and now p110β.

Rab5 is a member of phylogenic group 5 of Rab GTPases, which also includes Rab21 and Rab22 (Pereira-Leal and Seabra, 2001). Both A56 and M88 (Rab5 AA numbering) are unique residues to this phylogenic group and are substituted with non-conservative residues in other groups; *e.g.* A56 is substituted with aspartate in Rab4 (group 2), while M88 is substituted with serine in Rab1 (group 1), Rab2 and Rab4 (group 2) and Rab6 (group 6) and with alanine in Rab3 (group 3) (Zahraoui *et al.*, 1989). All effectors mentioned in Table 5.1 bound a similar Rab5 epitope including the hydrophobic triad, the unique residue M88 of phylogenic group 5 as well as L85. Alanine 56 was not mutated and tested for binding with either APPL1 or p110β, and therefore, it is unknown if this residue is as important to group 5 binding to effectors as M88.

Rab5 residues unique to binding p110β were E80 and H83. These residues were mutated to a residue of opposite charge, and therefore their effect on p110β binding was substantial. In the wild-type Rab5-GNP crystal structure (1R2Q) H83 forms a hydrogen bond with E117 on α-helix #3 of Rab5 (Figure 5.4 D), so it is possible that the H83E mutation could be destabilizing to the Rab5 switch II loop because of charge repulsion between it and E117, causing displacement of many residues. Therefore, it is unknown if H83 makes contacts with p110β that are disrupted in the H83E mutant or if the mutation caused a large conformational change in Rab5 which reduced binding of p110β. Similarly, though E80 does not make intrachain contacts with its functional group, substitution of this residue to arginine may cause some charge repulsion from Rab5 residue R110, which is also positioned on α-helix 3 and very near to E80 in the crystal structure (Figure 5.4 D). Therefore it is unclear whether these amino acids are involved directly in p110β binding, or if their mutation distorted Rab5 folding to negatively impact p110β binding.

APPL1 binding to Y82 was not tested (Zhu *et al.*, 2007), but all other effectors bound this residue (Eathiraj *et al.*, 2005; Zhu *et al.*, 2004; Mishra *et al.*, 2010; Figure 4.12). Another residue which was not tested in APPL1 or in p110β binding studies was G54 which bound to all

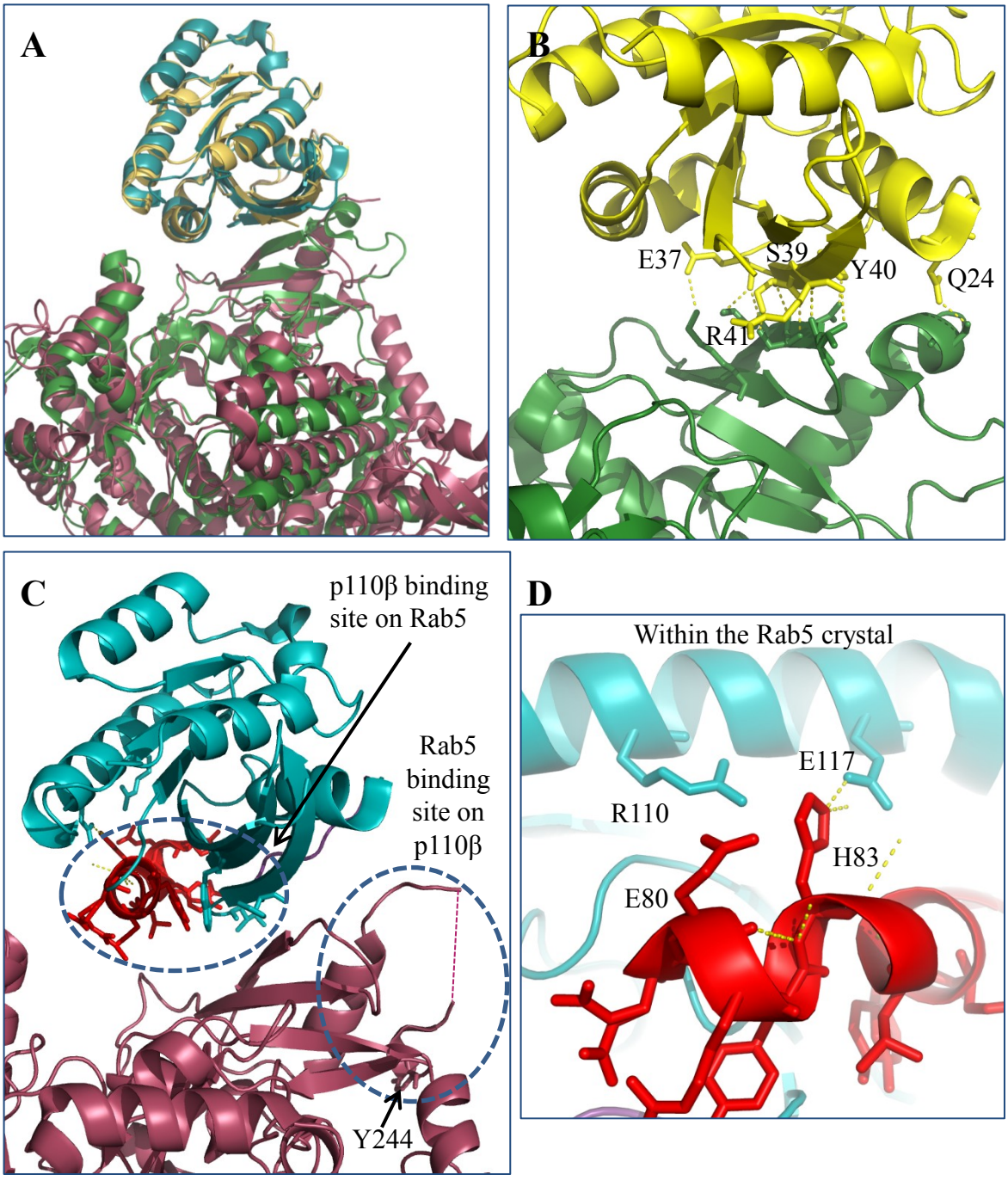

Figure 5.4 Structural alignment of Ras/Rab5 and p110γ/p110β illustrates differences in binding interfaces. **A.** Structural alignment overlay of the Ras:p110γ complex (1HE8) with Rab5 (1R2Q) and p110β (2Y3A) crystals. Ras in yellow; Rab5 in teal; p110γ in green; p110β in red/pink. **B.** Close up of Ras:p110γ interface with Ras residues involved in polar contacts represented. **C.** Close up of Rab5 and p110β interface. Residues involved in binding according to pull-down assay ($n \geq 3$) are shown as stick models and indicated by dashed circles. Switch I ribbon in purple; switch II ribbon in red. **D.** Close up of Rab5 intrachain hydrogen bonding between H83 and E116. Proximity of E80 and R110 should be noted as their side-chains may repel each other in the E80R mutant.

other effectors mentioned. Therefore, some residues which may also be involved in binding p110β are G54 and A56. Though the role of glycine in p110β binding would likely rely on backbone interactions or through facilitating tight turns in Rab5 secondary structure, mutation of these residues to an amino acid with a bulky or charged functional group may disrupt binding by steric hindrance or charge repulsion, respectively.

One consideration of all the Rab5 mutants that reduced binding to p110β is their ability to properly bind nucleotide, which was not tested in this thesis. Whenever a protein is mutated, its functionality is put to question. Because many of the amino acids were mutated in an important catalytic region of Rab5, it is important to test whether the protein can still function. Binding of GTP and its hydrolysis is critical for the function of GTPases, and can be tested by a few methods: one is an antibody which is specific for a Rab5 epitope only present on GTP-bound Rab5; another is the binding of radioactive [α-^{32}P]-labeled nucleotide which can be detected by autoradiography. Either of these assays should be performed with the Rab5 mutants that do not bind p110β before further study or evaluation of these proteins is explored.

5.3 Experiments to determine the Rab5 binding site on p110β

5.3.1 The binding site of Rab5 on p110β

A sequence alignment between p110α and p110β demonstrated the difference between the two isoforms in the RBD (Figure 4.14). When the two structures were aligned, it was noted that a loop at the "top" of the RBD as in Figure 4.14 was missing from the crystallized protein, because of disorder (Zhang *et al.*, 2011). This loop seemed a promising site for binding, as it varied greatly between p110α and p110β, and would be flexible to interact with the switch regions of Rab5. Therefore, residues within this loop, as well as some residues around it, were mutated in the context of the Myc_3-iSH2-p110β protein, and tested for binding with Rab5. It was found that some, but not all of the residues tested, were important for binding Rab5. Specifically, E238R and Y244A had the largest reduction of binding to Rab5-GppCp, whereas I234A reduced binding to Rab5-GppCp by about 70% (Figure 4.13 C and D). Residues that did not affect binding to Rab5 were D239R and L232A, despite their proximity to E238 and I234, respectively. There may be additional residues involved in the binding interface, but no other residues were mutated at this time.

A structural alignment of the Rab5-GNP (1R2Q) crystal with a co-crystal structure of Ras-p110γ (1HE8) suggested a different binding motif between the family members (Figure 5.4). Ras engaged residues including Q24, E37, S39, Y40 and R41 for the interaction with p110γ (Figure 5.4 B), while pull-down results demonstrated that Rab5 used residues in the switch II region (AA 77-95) to bind p110β (Figure 4.11 and Figure 5.4 C). In a p110β structural alignment with p110γ, the (p110β) Rab5-binding residue Y244 faces away from the Rab5 switch II region (Figure 5.4 C) while residues I234 and E238 of p110β were in the disordered region of the p110β crystal. Therefore, though p110β bound Rab5 via its RBD, the interaction mechanism is different from p110γ binding to Ras.

The p110β binding site on Rab5 shares many residues with effectors and GAP proteins alike. Therefore, it is important to determine whether p110β is in fact a regulator of Rab5 or an effector. Because of the GAP activity of p85, it was expected that p110β may be involved in Rab5 deactivation by virtue of being bound to p85. However, the catalytic activity of p110β provides PtdIns-3,4,5-P_3, an important precursor in the generation of the PtdIns-3-P on early endosomes, making it an effector of Rab5 (Shin *et al.*, 2005). It was proposed that p110β engages the switch regions of Rab5 in order to stabilize the transition state and drive the hydrolysis of GTP. The binding sites between Rab5 and p110β have been identified and involved mainly residues from switch II of Rab5. It is unknown if the p110β-RBD:Rab5-switch II contacts stabilize the transition state of Rab5. A GAP assay, whereby [α-^{32}P]-GTP hydrolysis is measured by thin layer chromatography and autoradiography, would need to be performed with p85 added to Rab5 alone, or in the presence of p110β, in order to establish the effect of p110β on p85 GAP activity towards Rab5. Since p110β is difficult to purify because of its instability without bound p85 and the iSH2-domain containing p110β construct does not express well in bacterial cells this assay has not been pursued. Another way to determine if p110β stabilizes the transition state of Rab5 would be to crystallize the complex of Rab5-GDP-AlF_4 (a transition state analogue), p85 and p110.

5.4 Future studies, overall effects of the non-binding mutants of both Rab5 and p110β

In this thesis, the p110β binding site on Rab5 was determined. The overlap of critical residues with those involved in binding other Rab5 effectors supports the theory of temporal regulation of Rab5. If both regulatory and effector proteins bind a similar epitope on the Rab5 structure, they would be in competition with each other for binding. In the working model, membrane bound Rab5-GDP is activated initially by a GEF, *e.g.* Rin-1, in response to growth factor signaling and becomes involved in internalization of activated receptors (Figure 5.5 B).

Interaction of active Rab5 with phosphatidylinositol 3′-kinases such as Vps34 and p110β, and phosphatases PtdIns-4-phosphatase and PtdIns-5-phosphatase should occur first to promote lipid identity and uncoating of the internalized vesicles (Figure 5.5 C). Tethering factors such as effectors EEA-1 and Rabenosyn-5 bind to both Rab5-GTP and PtdIns-3-P within the vesicle membranes and therefore would be recruited after the lipid kinases and phosphatases, when a sufficient level of PtdIns3P is achieved (Figure 5.5 D). Homotypic fusion of vesicles and heterotypic fusion of vesicles to the larger early/sorting endosome occur through the actions of tethering factors and their recruited SNARE proteins (not shown in the diagram).

During these steps of intracellular trafficking, Rab5-GTP has been bound to multiple effectors, sequestering its switch regions from regulatory proteins. But, once fusion is complete, Rab5 effectors are no longer needed and may be released from the early/sorting endosome. Rab5-GTP becomes available to GAPs and can be deactivated by GTP hydrolysis and removed from the membrane by GDI (Figure 5.5 E). It may be possible that GAPs are acting on Rab5 throughout the cycle, but GEFs (*e.g.* Rabex-5) reactivate Rab5 in a positive feedback loop designed to ensure Rab5 remains activated until vesicle fusion is completed (Figure 5.5 F). Therefore, by interacting with the same site on Rab5 (the switch I and II regions) effectors and regulators must compete for binding, resulting in a time-dependent sequential interaction pathway.

The importance of the Rab5:p110β interaction in cells can be tested by introducing non-binding mutants of either protein and evaluating the differences in endocytosis, intracellular receptor trafficking, as well as downstream RTK signaling compared to wild-type cells. However, evaluation of Rab5 mutants unable to bind p110β would be complicated by the consequences of other Rab5 effectors being unable to bind the Rab5 mutants, as many of their

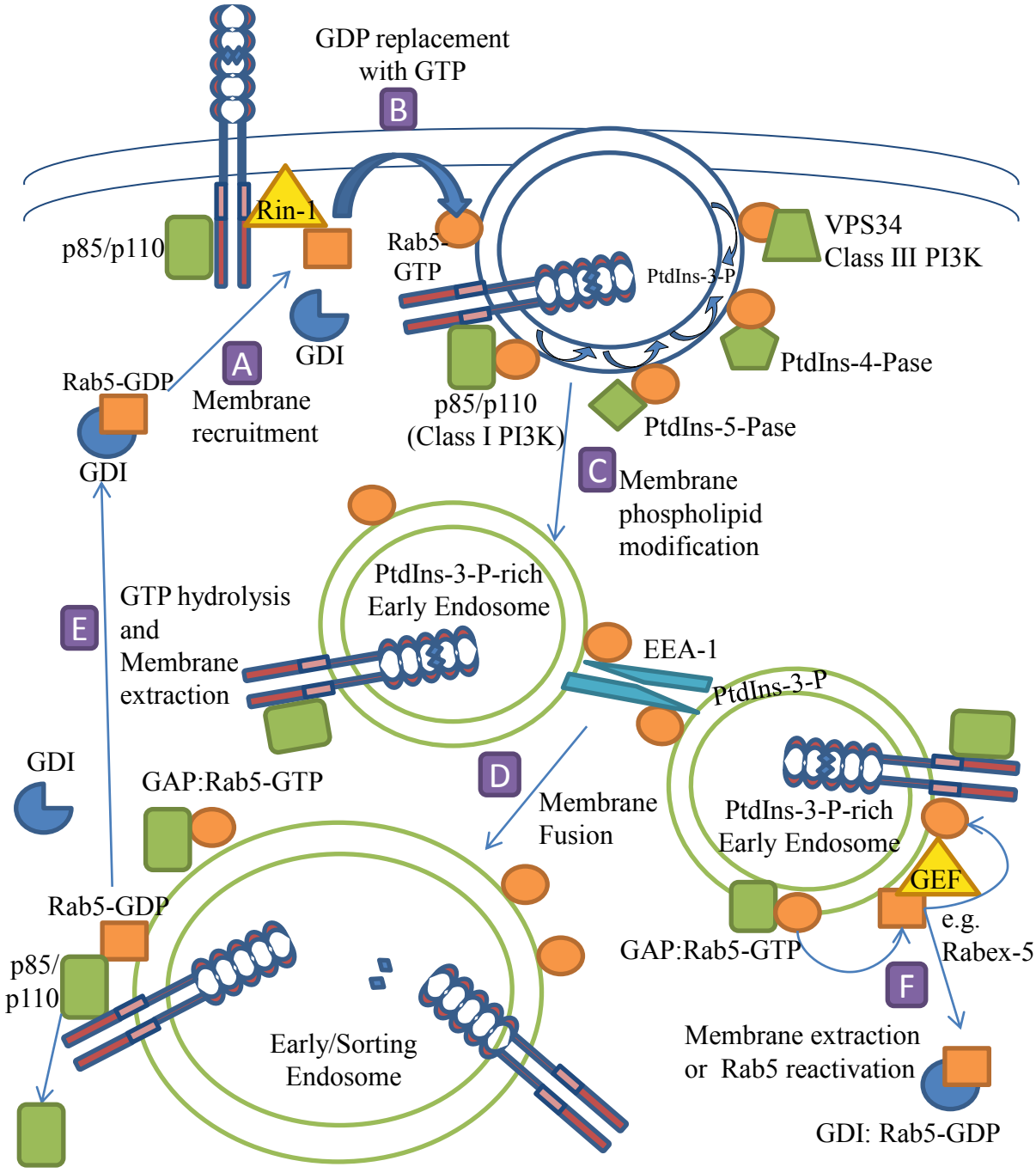

Figure 5.5 Temporal regulation of Rab5 endosomal trafficking. A. Inactive Rab5-GDP is bound to GDI in the cytosol. **B.** Rab5 is activated by a GEF at the plasma membrane. **C.** Active Rab5 interacts with phosphatidylinositol kinases and phosphatases. **D.** When the PtdIns3P concentration is optimal, tethering factors bind both Rab5 and PtdIns3P, and promote vesicle fusion. **E.** GAPs enhance GTP hydrolysis and return Rab5 to an inactive form, to which GDI binds and brings into the cytosol. **F.** GAPs acting on Rab5-GTP on endosomes which have not undergone fusion. The resulting Rab5-GDP is reactivated by a GEF in a positive feedback loop that promotes vesicle fusion.

binding sites on Rab5 overlap. It may be possible to selectively block p110β binding through the mutation of Rab5 residues specific for p110β binding, such as E80 and H83, but if their mutation affects the overall fold of the switch regions of Rab5, as predicted, there would be disruption of all Rab5 effector binding. Thus, it would be more effective and less confusing, if the p110β mutants unable to bind Rab5, E238R and Y244A, were introduced into cells instead. This may require knock-down of endogenous p110β by si-RNA followed by re-expression of an si-RNA insensitive p110β mutant in order to see the full effect of the mutations. When p110β was lost or limiting, transferrin receptor internalization (Jia *et al.*, 2008) and EGFR internalization (Ciarolo *et al.*, 2008) was impaired, but was restored by expression of a kinase-dead mutant of p110β. Theoretically, it was the lack of p110β:Rab5 interaction that caused this phenotype. Analysis of both transferrin receptor and EGFR internalization should be pursued in the p110β-E238R and -Y244A mutant expressing cells. Also, if p110β is stabilizing the switch regions of Rab5 during p85-mediated GTP hydrolysis, non-binding mutants E238R and Y244A may result in increased active Rab5 in cells, leading to enlarged early endosomes or a similar phenotype to p85-R274A expressing cells. Therefore, expression of Rab5-S34N should reverse the phenotype as it did in p85-R274A cells (Chamberlain *et al.*, 2008).

The mechanism of PI3K regulation of Rab5 is not yet fully understood. As a protein whose gene is often mutated in cancer, the function of wild-type p85α is of great interest (Samuels and Waldman, 2010; Cheung *et al.*, 2011; Sun *et al.*, 2010). The GAP function of p85 (Chamberlain *et al.*, 2004) theoretically limits the time and/or amount of homotypic early endosomal fusion by deactivation of Rab5 and therefore affects the proper trafficking of activated receptors (Chamberlain *et al.*, 2008). The ability of p85 to bind Rab5-GDP, and its significance, remains to be tested *in vivo*. The interaction between p110β and Rab5-GTP may be important for the generation of the lipid product PtdIns-3,4,5-P_3 on early endosomes, though p110β is recruited by the pY residues of RTKs through the p85 SH2 domain interactions and not by Rab-GTP. A non-catalytic function of p110β (Jia *et al.*, 2008; Ciarolo *et al.*, 2008) may be the p110β:Rab5-GTP switch region stabilization which is important for inactivation of Rab5 and early endosome development. This thesis has identified residues on both Rab5 and p110β which are involved in their interaction. The importance of the Rab5-GTP: p110β interaction may be elucidated through the characterization of these non-binding mutants in cells.

6.0 REFERENCES

Acconcia, F., Sigismund, S., and Polo, S. (2009). Ubiquitin in trafficking: the network at work. Exp Cell Res *315*, 1610-1618.

Ahearn, I.M., Haigis, K., Bar-Sagi, D., and Philips, M.R. (2012). Regulating the regulator: post-translational modification of RAS. Nat Rev Mol Cell Biol *13*, 39-51.

Ali, B.R., Wasmeier, C., Lamoreux, L., Strom, M., and Seabra, M.C. (2004). Multiple regions contribute to membrane targeting of Rab GTPases. J Cell Sci *117*, 6401-6412.

Andersson, E.R. (2012). The role of endocytosis in activating and regulating signal transduction. Cell Mol Life Sci *69*, 1755-1771.

Andreadi, C., Noble, C., Patel, B., Jin, H., Aguilar Hernandez, M.M., Balmanno, K., Cook, S.J., and Pritchard, C. (2012). Regulation of MEK/ERK pathway output by subcellular localization of B-Raf. Biochem Soc Trans *40*, 67-72.

Barbieri, M.A., Kong, C., Chen, P.I., Horazdovsky, B.F., and Stahl, P.D. (2003). The SRC homology 2 domain of Rin1 mediates its binding to the epidermal growth factor receptor and regulates receptor endocytosis. J Biol Chem *278*, 32027-32036.

Barbieri, M.A., Roberts, R.L., Gumusboga, A., Highfield, H., Alvarez-Dominguez, C., Wells, A., and Stahl, P.D. (2000). Epidermal growth factor and membrane trafficking. EGF receptor activation of endocytosis requires Rab5a. J Cell Biol *151*, 539-550.

Barbosa, M.D., Johnson, S.A., Achey, K., Gutierrez, M.J., Wakeland, E.K., Zerial, M., and Kingsmore, S.F. (1995). The Rab protein family: genetic mapping of six Rab genes in the mouse. Genomics *30*, 439-444.

Bartholomeusz, C., and Gonzalez-Angulo, A.M. (2012). Targeting the PI3K signaling pathway in cancer therapy. Expert Opin Ther Targets *16*, 121-130.

Brognard, J., Sierecki, E., Gao, T., and Newton, A.C. (2007). PHLPP and a second isoform, PHLPP2, differentially attenuate the amplitude of Akt signaling by regulating distinct Akt isoforms. Mol Cell *25*, 917-931.

Bucci, C., Chiariello, M., Lattero, D., Maiorano, M., and Bruni, C.B. (1999). Interaction cloning and characterization of the cDNA encoding the human prenylated rab acceptor (PRA1). Biochem Biophys Res Commun *258*, 657-662.

Bucci, C., Lutcke, A., Steele-Mortimer, O., Olkkonen, V.M., Dupree, P., Chiariello, M., Bruni, C.B., Simons, K., and Zerial, M. (1995). Co-operative regulation of endocytosis by three Rab5 isoforms. FEBS Lett *366*, 65-71.

Cain, C.C., Sipe, D.M., and Murphy, R.F. (1989). Regulation of endocytic pH by the Na+,K+-ATPase in living cells. Proc Natl Acad Sci U S A *86*, 544-548.

Chamberlain, M.D., Berry, T.R., Pastor, M.C., and Anderson, D.H. (2004). The p85alpha subunit of phosphatidylinositol 3'-kinase binds to and stimulates the GTPase activity of Rab proteins. J Biol Chem *279*, 48607-48614.

Chamberlain, M.D., Chan, T., Oberg, J.C., Hawrysh, A.D., James, K.M., Saxena, A., Xiang, J., and Anderson, D.H. (2008). Disrupted RabGAP function of the p85 subunit of phosphatidylinositol 3-kinase results in cell transformation. J Biol Chem *283*, 15861-15868.

Chamberlain, M.D., Oberg, J.C., Furber, L.A., Poland, S.F., Hawrysh, A.D., Knafelc, S.M., McBride, H.M., and Anderson, D.H. (2010). Deregulation of Rab5 and Rab4 proteins in p85R274A-expressing cells alters PDGFR trafficking. Cell Signal *22*, 1562-1575.

Chaussade, C., Rewcastle, G.W., Kendall, J.D., Denny, W.A., Cho, K., Gronning, L.M., Chong, M.L., Anagnostou, S.H., Jackson, S.P., Daniele, N., *et al.* (2007). Evidence for functional redundancy of class IA PI3K isoforms in insulin signalling. Biochem J *404*, 449-458.

Chen, P.I., Kong, C., Su, X., and Stahl, P.D. (2009). Rab5 isoforms differentially regulate the trafficking and degradation of epidermal growth factor receptors. J Biol Chem *284*, 30328-30338.

Chen, X., and Wang, Z. (2001a). Regulation of epidermal growth factor receptor endocytosis by wortmannin through activation of Rab5 rather than inhibition of phosphatidylinositol 3-kinase. EMBO Rep *2*, 842-849.

Chen, X., and Wang, Z. (2001b). Regulation of intracellular trafficking of the EGF receptor by Rab5 in the absence of phosphatidylinositol 3-kinase activity. EMBO Rep *2*, 68-74.

Cheung, L.W., Hennessy, B.T., Li, J., Yu, S., Myers, A.P., Djordjevic, B., Lu, Y., Stemke-Hale, K., Dyer, M.D., Zhang, F., *et al.* (2011). High frequency of PIK3R1 and PIK3R2 mutations in endometrial cancer elucidates a novel mechanism for regulation of PTEN protein stability. Cancer Discov *1*, 170-185.

Chiariello, M., Bruni, C.B., and Bucci, C. (1999). The small GTPases Rab5a, Rab5b and Rab5c are differentially phosphorylated in vitro. FEBS Lett *453*, 20-24.

Christoforidis, S., Miaczynska, M., Ashman, K., Wilm, M., Zhao, L., Yip, S.-C., Waterfield, M.D., Backer, J.M., and Zerial, M. (1999). Phosphatidylinositol-3-OH kinases are Rab5 effectors. Nat Cell Biol *1*, 249-252.

Ciraolo, E., Iezzi, M., Marone, R., Marengo, S., Curcio, C., Costa, C., Azzolino, O., Gonella, C., Rubinetto, C., Wu, H., *et al.* (2008). Phosphoinositide 3-kinase p110beta activity: key role in metabolism and mammary gland cancer but not development. Sci Signal *1*, ra3.

Dai, Y., Walker, S.A., de Vet, E., Cook, S., Welch, H.C., and Lockyer, P.J. (2011). Ca2+-dependent monomer and dimer formation switches CAPRI Protein between Ras GTPase-activating protein (GAP) and RapGAP activities. J Biol Chem *286*, 19905-19916.

Datta, S.R., Dudek, H., Tao, X., Masters, S., Fu, H., Gotoh, Y., and Greenberg, M.E. (1997). Akt phosphorylation of BAD couples survival signals to the cell-intrinsic death machinery. Cell *91*, 231-241.

Datta, S.R., Katsov, A., Hu, L., Petros, A., Fesik, S.W., Yaffe, M.B., and Greenberg, M.E. (2000). 14-3-3 proteins and survival kinases cooperate to inactivate BAD by BH3 domain phosphorylation. Mol Cell *6*, 41-51.

Dbouk, H.A., Pang, H., Fiser, A., and Backer, J.M. (2010). A biochemical mechanism for the oncogenic potential of the p110beta catalytic subunit of phosphoinositide 3-kinase. Proc Natl Acad Sci U S A *107*, 19897-19902.

De Luca, A., Maiello, M.R., D'Alessio, A., Pergameno, M., and Normanno, N. (2012). The RAS/RAF/MEK/ERK and the PI3K/AKT signalling pathways: role in cancer pathogenesis and implications for therapeutic approaches. Expert Opin Ther Targets *16 Suppl 2*, S17-27.

Di Guglielmo, G.M., Le Roy, C., Goodfellow, A.F., and Wrana, J.L. (2003). Distinct endocytic pathways regulate TGF-beta receptor signalling and turnover. Nat Cell Biol *5*, 410-421.

Diehl, J.A., Cheng, M., Roussel, M.F., and Sherr, C.J. (1998). Glycogen synthase kinase-3beta regulates cyclin D1 proteolysis and subcellular localization. Genes Dev *12*, 3499- 3511.

Doherty, G.J., and McMahon, H.T. (2009). Mechanisms of endocytosis. Annu Rev Biochem *78*, 857-902.

Eathiraj, S., Pan, X., Ritacco, C., and Lambright, D.G. (2005). Structural basis of family-wide Rab GTPase recognition by rabenosyn-5. Nature *436*, 415-419.

Egan, S.E., Giddings, B.W., Brooks, M.W., Buday, L., Sizeland, A.M., and Weinberg, R.A. (1993). Association of Sos Ras exchange protein with Grb2 is implicated in tyrosine kinase signal transduction and transformation. Nature *363*, 45-51.

Felder, S., Zhou, M., Hu, P., Urena, J., Ullrich, A., Chaudhuri, M., White, M., Shoelson, S.E., and Schlessinger, J. (1993). SH2 domains exhibit high-affinity binding to tyrosine-phosphorylated peptides yet also exhibit rapid dissociation and exchange. Mol Cell Biol *13*, 1449-1455.

Fernandez-Medarde, A., and Santos, E. (2011). Ras in cancer and developmental diseases. Genes Cancer *2*, 344-358.

Fidyk, N.J., and Cerione, R.A. (2002). Understanding the catalytic mechanism of GTPase-activating proteins: demonstration of the importance of switch domain stabilization in the stimulation of GTP hydrolysis. Biochemistry *41*, 15644-15653.

Fleming, T.P., Matsui, T., and Aaronson, S.A. (1992). Platelet-derived growth factor (PDGF) receptor activation in cell transformation and human malignancy. Exp Gerontol *27*, 523-532.

Foukas, L.C., Claret, M., Pearce, W., Okkenhaug, K., Meek, S., Peskett, E., Sancho, S., Smith, A.J., Withers, D.J., and Vanhaesebroeck, B. (2006). Critical role for the p110alpha phosphoinositide-3-OH kinase in growth and metabolic regulation. Nature *441*, 366-370.

Frasa, M.A., Koessmeier, K.T., Ahmadian, M.R., and Braga, V.M. (2012). Illuminating the functional and structural repertoire of human TBC/RABGAPs. Nat Rev Mol Cell Biol *13*, 67-73.

Gabelli, S.B., Mandelker, D., Schmidt-Kittler, O., Vogelstein, B., and Amzel, L.M. (2010). Somatic mutations in PI3Kalpha: structural basis for enzyme activation and drug design. Biochim Biophys Acta *1804*, 533-540.

Geering, B., Cutillas, P.R., Nock, G., Gharbi, S.I., and Vanhaesebroeck, B. (2007). Class IA phosphoinositide 3-kinases are obligate p85-p110 heterodimers. Proc Natl Acad Sci U S A *104*, 7809-7814.

Gietz, R.D., and Schiestl, R.H. (2007). High-efficiency yeast transformation using the LiAc/SS carrier DNA/PEG method. Nat Protoc *2*, 31-34.

Haas, A.K., Fuchs, E., Kopajtich, R., and Barr, F.A. (2005). A GTPase-activating protein controls Rab5 function in endocytic trafficking. Nat Cell Biol *7*, 887-893.

Hanahan, D., Jessee, J., and Bloom, F.R. (1991). Plasmid transformation of Escherichia coli and other bacteria. Methods Enzymol *204*, 63-113.

Hansen, C.G., and Nichols, B.J. (2009). Molecular mechanisms of clathrin-independent endocytosis. J Cell Sci *122*, 1713-1721.

Hart, M.J., Eva, A., Zangrilli, D., Aaronson, S.A., Evans, T., Cerione, R.A., and Zheng, Y. (1994). Cellular transformation and guanine nucleotide exchange activity are catalyzed by a common domain on the dbl oncogene product. J Biol Chem *269*, 62-65.

Heldin, C.-H., and Westermark, B. (1999). Mechanism of Action and In Vivo Role of Platelet-Derived Growth Factor. Physiological Reviews *79*, 1283-1316.

Hirsch, E., Costa, C., and Ciraolo, E. (2007). Phosphoinositide 3-kinases as a common platform for multi-hormone signaling. J Endocrinol *194*, 243-256.

Horiuchi, H., Lippe, R., McBride, H.M., Rubino, M., Woodman, P., Stenmark, H., Rybin, V., Wilm, M., Ashman, K., Mann, M., *et al.* (1997). A novel Rab5 GDP/GTP exchange factor complexed to Rabaptin-5 links nucleotide exchange to effector recruitment and function. Cell *90*, 1149-1159.

Houle, S., and Marceau, F. (2003). Wortmannin alters the intracellular trafficking of the bradykinin B2 receptor: role of phosphoinositide 3-kinase and Rab5. Biochem J *375*, 151-158.

Howes, M.T., Mayor, S., and Parton, R.G. (2010). Molecules, mechanisms, and cellular roles of clathrin-independent endocytosis. Curr Opin Cell Biol *22*, 519-527.

Hu, P., Margolis, B., Skolnik, E.Y., Lammers, R., Ullrich, A., and Schlessinger, J. (1992). Interaction of phosphatidylinositol 3-kinase-associated p85 with epidermal growth factor an platelet-derived growth factor receptors. Mol Cell Biol *12*, 981-990.

Hu, Q., Klippel, A., Muslin, A.J., Fantl, W.J., and Williams, L.T. (1995). Ras-dependent induction of cellular responses by constitutively active phosphatidylinositol-3 kinase. Science *268*, 100-102.

Hunyady, L., Baukal, A.J., Gaborik, Z., Olivares-Reyes, J.A., Bor, M., Szaszak, M., Lodge, R., Catt, K.J., and Balla, T. (2002). Differential PI 3-kinase dependence of early and late phases of recycling of the internalized AT1 angiotensin receptor. J Cell Biol *157*, 1211-1222.

Hurvitz, S.A., Hu, Y., O'Brien, N., and Finn, R.S. (2012). Current approaches and future directions in the treatment of HER2-positive breast cancer. Cancer Treat Rev.

Ignatiuk, A., Quickfall, J.P., Hawrysh, A.D., Chamberlain, M.D., and Anderson, D.H. (2006). The smaller isoforms of ankyrin 3 bind to the p85 subunit of phosphatidylinositol 3'-kinase and enhance platelet-derived growth factor receptor down-regulation. J Biol Chem *281*, 5956-5964.

Ilic, N., and Roberts, T.M. (2010). Comparing the roles of the p110alpha and p110beta isoforms of PI3K in signaling and cancer. Curr Top Microbiol Immunol *347*, 55-77.

Jaiswal, B.S., Janakiraman, V., Kljavin, N.M., Chaudhuri, S., Stern, H.M., Wang, W., Kan, Z., Dbouk, H.A., Peters, B.A., Waring, P., *et al.* (2009). Somatic mutations in p85alpha promote tumorigenesis through class IA PI3K activation. Cancer Cell *16*, 463-474.

Jechlinger, M., Sommer, A., Moriggl, R., Seither, P., Kraut, N., Capodiecci, P., Donovan, M., Cordon-Cardo, C., Beug, H., and Grunert, S. (2006). Autocrine PDGFR signaling promotes mammary cancer metastasis. J Clin Invest *116*, 1561-1570.

Jia, S., Liu, Z., Zhang, S., Liu, P., Zhang, L., Lee, S.H., Zhang, J., Signoretti, S., Loda, M., Roberts, T.M., *et al.* (2008). Essential roles of PI(3)K-p110beta in cell growth, metabolism and tumorigenesis. Nature *454*, 776-779.

Jozic, I., Saliba, S.C., and Barbieri, M.A. (2012). Effect of EGF-receptor tyrosine kinase inhibitor on Rab5 function during endocytosis. Arch Biochem Biophys *525*, 16-24.

Kang, S., Bader, A.G., Zhao, L., and Vogt, P.K. (2005). Mutated PI 3-kinases: cancer targets on a silver platter. Cell Cycle *4*, 578-581.

Klippel, A., Escobedo, J.A., Hu, Q., and Williams, L.T. (1993). A region of the 85-kilodalton (kDa) subunit of phosphatidylinositol 3-kinase binds the 110-kDa catalytic subunit in vivo. Mol Cell Biol *13*, 5560-5566.

Kotting, C., Kallenbach, A., Suveyzdis, Y., Eichholz, C., and Gerwert, K. (2007). Surface change of Ras enabling effector binding monitored in real time at atomic resolution. Chembiochem *8*, 781-787.

Kurosu, H., and Katada, T. (2001). Association of phosphatidylinositol 3-kinase composed of p110beta-catalytic and p85-regulatory subunits with the small GTPase Rab5. J Biochem *130*, 73-78.

Laemmli, U.K. (1970). Cleavage of structural proteins during the assembly of the head of bacteriophage T4. Nature *227*, 680-685.

Larkin, J.M., Donzell, W.C., and Anderson, R.G. (1986). Potassium-dependent assembly of coated pits: new coated pits form as planar clathrin lattices. J Cell Biol *103*, 2619-2627.

Lemmon, M.A., and Schlessinger, J. (2010). Cell Signaling by Receptor Tyrosine Kinases. Cell *141*, 1117-1134.

Leonard, D., Hayakawa, A., Lawe, D., Lambright, D., Bellve, K.D., Standley, C., Lifshitz, L.M., Fogarty, K.E., and Corvera, S. (2008). Sorting of EGF and transferrin at the plasma membrane and by cargo-specific signaling to EEA1-enriched endosomes. J Cell Sci *121*, 3445-3458.

Leonard, D.A., Lin, R., Cerione, R.A., and Manor, D. (1998). Biochemical studies of the mechanism of action of the Cdc42-GTPase-activating protein. J Biol Chem *273*, 16210-16215.

Leung, K.F., Baron, R., and Seabra, M.C. (2006). Thematic review series: lipid posttranslational modifications. geranylgeranylation of Rab GTPases. J Lipid Res *47*, 467-475.

Li, Y., Roy, B.D., Wang, W., Zhang, L., Sampson, S.B., Yang, Y., and Lin, D.T. (2012). Identification of two functionally distinct endosomal recycling pathways for dopamine D(2) receptor. J Neurosci *32*, 7178-7190.

Liu, C., and Tsao, M.S. (1993). In vitro and in vivo expressions of transforming growth factor-alpha and tyrosine kinase receptors in human non-small-cell lung carcinomas. Am J Pathol *142*, 1155-1162.

Manning, B.D., and Cantley, L.C. (2007). AKT/PKB signaling: navigating downstream. Cell *129*, 1261-1274.

Martincic, I., Peralta, M.E., and Ngsee, J.K. (1997). Isolation and characterization of a dual prenylated Rab and VAMP2 receptor. J Biol Chem *272*, 26991-26998.

Martys, J.L., Wjasow, C., Gangi, D.M., Kielian, M.C., McGraw, T.E., and Backer, J.M. (1996). Wortmannin-sensitive trafficking pathways in Chinese hamster ovary cells. Differential effects on endocytosis and lysosomal sorting. J Biol Chem *271*, 10953-10962.

McMahon, H.T., and Boucrot, E. (2011). Molecular mechanism and physiological functions of clathrin-mediated endocytosis. Nat Rev Mol Cell Biol *12*, 517-533.

Mellor, P., Furber, L.A., Nyarko, J.N., and Anderson, D.H. (2012). Multiple roles for the p85alpha isoform in the regulation and function of PI3K signalling and receptor trafficking. Biochem J *441*, 23-37.

Merithew, E., Hatherly, S., Dumas, J.J., Lawe, D.C., Heller-Harrison, R., and Lambright, D.G. (2001). Structural plasticity of an invariant hydrophobic triad in the switch regions of Rab GTPases is a determinant of effector recognition. J Biol Chem *276*, 13982-13988.

Milburn, M.V., Tong, L., deVos, A.M., Brunger, A., Yamaizumi, Z., Nishimura, S., and Kim, S.H. (1990). Molecular switch for signal transduction: structural differences between active and inactive forms of protooncogenic ras proteins. Science *247*, 939-945.

Mills, I.G., Jones, A.T., and Clague, M.J. (1999). Regulation of endosome fusion. Mol Membr Biol *16*, 73-79.

Mishra, A., Eathiraj, S., Corvera, S., and Lambright, D.G. (2010). Structural basis for Rab GTPase recognition and endosome tethering by the C2H2 zinc finger of Early Endosomal Autoantigen 1 (EEA1). Proc Natl Acad Sci U S A *107*, 10866-10871.

Moreland, J.L., Gramada, A., Buzko, O.V., Zhang, Q., and Bourne, P.E. (2005). The Molecular Biology Toolkit (MBT): a modular platform for developing molecular visualization applications. BMC Bioinformatics *6*, 21.

Musacchio, A., Cantley, L.C., and Harrison, S.C. (1996). Crystal structure of the breakpoint cluster region-homology domain from phosphoinositide 3-kinase p85 alpha subunit. Proc Natl Acad Sci U S A *93*, 14373-14378.

Nardella, C., Lunardi, A., Fedele, G., Clohessy, J.G., Alimonti, A., Kozma, S.C., Thomas, G., Loda, M., and Pandolfi, P.P. (2011). Differential expression of S6K2 dictates tissue-specific requirement for S6K1 in mediating aberrant mTORC1 signaling and tumorigenesis. Cancer Res *71*, 3669-3675.

Nassar, N., Hoffman, G.R., Manor, D., Clardy, J.C., and Cerione, R.A. (1998). Structures of Cdc42 bound to the active and catalytically compromised forms of Cdc42GAP. Nat Struct Biol *5*, 1047-1052.

Nassar, N., Horn, G., Herrmann, C., Scherer, A., McCormick, F., and Wittinghofer, A. (1995). The 2.2 A crystal structure of the Ras-binding domain of the serine/threonine kinase c-Raf1 in complex with Rap1A and a GTP analogue. Nature *375*, 554-560.

Oesterlin, L.K., Goody, R.S., and Itzen, A. (2012). Posttranslational modifications of Rab proteins cause effective displacement of GDP dissociation inhibitor. Proc Natl Acad Sci U S A *109*, 5621-5626.

Pacold, M.E., Suire, S., Perisic, O., Lara-Gonzalez, S., Davis, C.T., Walker, E.H., Hawkins, P.T., Stephens, L., Eccleston, J.F., and Williams, R.L. (2000). Crystal structure and functional analysis of Ras binding to its effector phosphoinositide 3-kinase gamma. Cell *103*, 931-943.

Paduch, M., Jelen, F., and Otlewski, J. (2001). Structure of small G proteins and their regulators. Acta Biochim Pol *48*, 829-850.

Pan, X., Eathiraj, S., Munson, M., and Lambright, D.G. (2006). TBC-domain GAPs for Rab GTPases accelerate GTP hydrolysis by a dual-finger mechanism. Nature *442*, 303-306.

Patton, D.T., Garcon, F., and Okkenhaug, K. (2007). The PI3K p110delta controls T-cell development, differentiation and regulation. Biochem Soc Trans *35*, 167-171.

Pei, L., Peng, Y., Yang, Y., Ling, X.B., Van Eyndhoven, W.G., Nguyen, K.C., Rubin, M., Hoey, T., Powers, S., and Li, J. (2002). PRC17, a novel oncogene encoding a Rab GTPase-activating protein, is amplified in prostate cancer. Cancer Res *62*, 5420-5424.

Pereira-Leal, J.B., and Seabra, M.C. (2001). Evolution of the Rab family of small GTP-binding proteins. J Mol Biol *313*, 889-901.

Pfeffer, S., and Aivazian, D. (2004). Targeting Rab GTPases to distinct membrane compartments. Nat Rev Mol Cell Biol *5*, 886-896.

Pfeffer, S.R. (2005). Structural clues to Rab GTPase functional diversity. J Biol Chem *280*, 15485-15488.

Poteryaev, D., Datta, S., Ackema, K., Zerial, M., and Spang, A. (2010). Identification of the switch in early-to-late endosome transition. Cell *141*, 497-508.

Praefcke, G.J., and McMahon, H.T. (2004). The dynamin superfamily: universal membrane tubulation and fission molecules? Nat Rev Mol Cell Biol *5*, 133-147.

Rak, A., Pylypenko, O., Durek, T., Watzke, A., Kushnir, S., Brunsveld, L., Waldmann, H., Goody, R.S., and Alexandrov, K. (2003). Structure of Rab GDP-dissociation inhibitor in complex with prenylated YPT1 GTPase. Science *302*, 646-650.

Raponi, M., Winkler, H., and Dracopoli, N.C. (2008). KRAS mutations predict response to EGFR inhibitors. Curr Opin Pharmacol *8*, 413-418.

Reebye, V., Frilling, A., Hajitou, A., Nicholls, J.P., Habib, N.A., and Mintz, P.J. (2012). A perspective on non-catalytic Src homology (SH) adaptor signalling proteins. Cell Signal *24*, 388-392.

Rittinger, K., Walker, P.A., Eccleston, J.F., Nurmahomed, K., Owen, D., Laue, E., Gamblin, S.J., and Smerdon, S.J. (1997a). Crystal structure of a small G protein in complex with the GTPase-activating protein rhoGAP. Nature *388*, 693-697.

Rittinger, K., Walker, P.A., Eccleston, J.F., Smerdon, S.J., and Gamblin, S.J. (1997b). Structure at 1.65 A of RhoA and its GTPase-activating protein in complex with a transition-state analogue. Nature *389*, 758-762.

Roach, W.G., Chavez, J.A., Miinea, C.P., and Lienhard, G.E. (2007). Substrate specificity and effect on GLUT4 translocation of the Rab GTPase-activating protein Tbc1d1. Biochem J *403*, 353-358.

Roskoski, R., Jr. (2010). RAF protein-serine/threonine kinases: structure and regulation. Biochem Biophys Res Commun *399*, 313-317.

Samuels, Y., and Velculescu, V.E. (2004). Oncogenic mutations of PIK3CA in human cancers. Cell Cycle *3*, 1221-1224.

Samuels, Y., and Waldman, T. (2010). Oncogenic mutations of PIK3CA in human cancers. Curr Top Microbiol Immunol *347*, 21-41.

Sarbassov, D.D., Guertin, D.A., Ali, S.M., and Sabatini, D.M. (2005). Phosphorylation and regulation of Akt/PKB by the rictor-mTOR complex. Science *307*, 1098-1101.

Schaefer, A., Miertzschke, M., Berken, A., and Wittinghofer, A. (2011). Dimeric plant RhoGAPs are regulated by its CRIB effector motif to stimulate a sequential GTP hydrolysis. J Mol Biol *411*, 808-822.

Schnatwinkel, C., Christoforidis, S., Lindsay, M.R., Uttenweiler-Joseph, S., Wilm, M., Parton, R.G., and Zerial, M. (2004). The Rab5 effector Rabankyrin-5 regulates and coordinates different endocytic mechanisms. PLoS Biol *2*, E261.

Seachrist, J.L., and Ferguson, S.S. (2003). Regulation of G protein-coupled receptor endocytosis and trafficking by Rab GTPases. Life Sci *74*, 225-235.

Sebolt-Leopold, J.S., and Herrera, R. (2004). Targeting the mitogen-activated protein kinase cascade to treat cancer. Nat Rev Cancer *4*, 937-947.

Shevchuk, A.I., Novak, P., Taylor, M., Diakonov, I.A., Ziyadeh-Isleem, A., Bitoun, M., Guicheney, P., Lab, M.J., Gorelik, J., Merrifield, C.J., *et al.* (2012). An alternative mechanism of clathrin-coated pit closure revealed by ion conductance microscopy. J Cell Biol *197*, 499-508.

Shima, F., Ijiri, Y., Muraoka, S., Liao, J., Ye, M., Araki, M., Matsumoto, K., Yamamoto, N., Sugimoto, T., Yoshikawa, Y., *et al.* (2010). Structural basis for conformational dynamics of GTP-bound Ras protein. J Biol Chem *285*, 22696-22705.

Shin, H.W., Hayashi, M., Christoforidis, S., Lacas-Gervais, S., Hoepfner, S., Wenk, M.R., Modregger, J., Uttenweiler-Joseph, S., Wilm, M., Nystuen, A., *et al.* (2005). An enzymatic cascade of Rab5 effectors regulates phosphoinositide turnover in the endocytic pathway. J Cell Biol *170*, 607-618.

Sigismund, S., Argenzio, E., Tosoni, D., Cavallaro, E., Polo, S., and Di Fiore, P.P. (2008). Clathrin-mediated internalization is essential for sustained EGFR signaling but dispensable for degradation. Dev Cell *15*, 209-219.

Sigismund, S., Woelk, T., Puri, C., Maspero, E., Tacchetti, C., Transidico, P., Di Fiore, P.P., and Polo, S. (2005). Clathrin-independent endocytosis of ubiquitinated cargos. Proc Natl Acad Sci U S A *102*, 2760-2765.

Sivars, U., Aivazian, D., and Pfeffer, S.R. (2003). Yip3 catalyses the dissociation of endosomal Rab-GDI complexes. Nature *425*, 856-859.

Snow, B.E., Krumins, A.M., Brothers, G.M., Lee, S.F., Wall, M.A., Chung, S., Mangion, J., Arya, S., Gilman, A.G., and Siderovski, D.P. (1998). A G protein gamma subunit-like domain shared between RGS11 and other RGS proteins specifies binding to Gbeta5 subunits. Proc Natl Acad Sci U S A *95*, 13307-13312.

Somsel Rodman, J., and Wandinger-Ness, A. (2000). Rab GTPases coordinate endocytosis. J Cell Sci *113 Pt 2*, 183-192.

Sorkin, A., and von Zastrow, M. (2009). Endocytosis and signalling: intertwining molecular networks. Nat Rev Mol Cell Biol *10*, 609-622.

Spang, A. (2009). On the fate of early endosomes. Biol Chem *390*, 753-759.

Stenmark, H. (2009). Rab GTPases as coordinators of vesicle traffic. Nat Rev Mol Cell Biol *10*, 513-525.

Stokoe, D., Stephens, L.R., Copeland, T., Gaffney, P.R., Reese, C.B., Painter, G.F., Holmes, A.B., McCormick, F., and Hawkins, P.T. (1997). Dual role of phosphatidylinositol-3,4,5-trisphosphate in the activation of protein kinase B. Science *277*, 567-570.

Su, X., Kong, C., and Stahl, P.D. (2007). GAPex-5 mediates ubiquitination, trafficking, and degradation of epidermal growth factor receptor. J Biol Chem *282*, 21278-21284.

Sun, M., Hillmann, P., Hofmann, B.T., Hart, J.R., and Vogt, P.K. (2010). Cancer-derived mutations in the regulatory subunit p85alpha of phosphoinositide 3-kinase function through the catalytic subunit p110alpha. Proc Natl Acad Sci U S A *107*, 15547-15552.

Takahashi, S., Kubo, K., Waguri, S., Yabashi, A., Shin, H.-W., Katoh, Y., and Nakayama, K. (2012). Rab11 regulates exocytosis of recycling vesicles at the plasma membrane. Journal of Cell Science.

Takeuchi, K., and Ito, F. (2011). Receptor tyrosine kinases and targeted cancer therapeutics. Biol Pharm Bull *34*, 1774-1780.

Terzyan, S., Zhu, G., Li, G., and Zhang, X.C. (2004). Refinement of the structure of human Rab5a GTPase domain at 1.05 A resolution. Acta Crystallogr D Biol Crystallogr *60*, 54-60.

Topp, J.D., Gray, N.W., Gerard, R.D., and Horazdovsky, B.F. (2004). Alsin is a Rab5 and Rac1 guanine nucleotide exchange factor. J Biol Chem *279*, 24612-24623.

Ueki, K., Fruman, D.A., Yballe, C.M., Fasshauer, M., Klein, J., Asano, T., Cantley, L.C., and Kahn, C.R. (2003). Positive and negative roles of p85 alpha and p85 beta regulatory subunits of phosphoinositide 3-kinase in insulin signaling. J Biol Chem *278*, 48453-48466.

Vanhaesebroeck, B., and Waterfield, M.D. (1999). Signaling by distinct classes of phosphoinositide 3-kinases. Exp Cell Res *253*, 239-254.

Vasudevan, K.M., and Garraway, L.A. (2010). AKT signaling in physiology and disease. Curr Top Microbiol Immunol *347*, 105-133.

Vercauteren, D., Vandenbroucke, R.E., Jones, A.T., Rejman, J., Demeester, J., De Smedt, S.C., Sanders, N.N., and Braeckmans, K. (2010). The use of inhibitors to study endocytic pathways of gene carriers: optimization and pitfalls. Mol Ther *18*, 561-569.

Vetter, I.R., and Wittinghofer, A. (2001). The guanine nucleotide-binding switch in three dimensions. Science *294*, 1299-1304.

Vieira, A.V., Lamaze, C., and Schmid, S.L. (1996). Control of EGF receptor signaling by clathrin-mediated endocytosis. Science *274*, 2086-2089.

Vivanco, I., and Sawyers, C.L. (2002). The phosphatidylinositol 3-Kinase AKT pathway in human cancer. Nat Rev Cancer *2*, 489-501.

Vogt, P.K. (2011). PI3K p110beta: more tightly controlled or constitutively active? Mol Cell *41*, 499-501.

Vogt, P.K., Hart, J.R., Gymnopoulos, M., Jiang, H., Kang, S., Bader, A.G., Zhao, L., and Denley, A. (2010). Phosphatidylinositol 3-kinase: the oncoprotein. Curr Top Microbiol Immunol *347*, 79-104.

Wang, J., and Pantopoulos, K. (2011). Regulation of cellular iron metabolism. Biochem J *434*, 365-381.

Welcker, M., Singer, J., Loeb, K.R., Grim, J., Bloecher, A., Gurien-West, M., Clurman, B.E., and Roberts, J.M. (2003). Multisite phosphorylation by Cdk2 and GSK3 controls cyclin E degradation. Mol Cell *12*, 381-392.

Wiley, H.S., and Burke, P.M. (2001). Regulation of receptor tyrosine kinase signaling by endocytic trafficking. Traffic *2*, 12-18.

Wilson, D.B., and Wilson, M.P. (1992). Identification and subcellular localization of human rab5b, a new member of the ras-related superfamily of GTPases. J Clin Invest *89*, 996-1005.

Woodman, P.G. (2000). Biogenesis of the sorting endosome: the role of Rab5. Traffic *1*, 695-701.

Wu, Y.W., Oesterlin, L.K., Tan, K.T., Waldmann, H., Alexandrov, K., and Goody, R.S. (2010). Membrane targeting mechanism of Rab GTPases elucidated by semisynthetic protein probes. Nat Chem Biol *6*, 534-540.

Xiao, G.H., Shoarinejad, F., Jin, F., Golemis, E.A., and Yeung, R.S. (1997). The tuberous sclerosis 2 gene product, tuberin, functions as a Rab5 GTPase activating protein (GAP) in modulating endocytosis. J Biol Chem *272*, 6097-6100.

Yamamoto, K., Altschuler, D., Wood, E., Horlick, K., Jacobs, S., and Lapetina, E.G. (1992). Association of phosphorylated insulin-like growth factor-I receptor with the SH2 domains of phosphatidylinositol 3-kinase p85. J Biol Chem *267*, 11337-11343.

Yu, J., Wjasow, C., and Backer, J.M. (1998). Regulation of the p85/p110alpha phosphatidylinositol 3'-kinase. Distinct roles for the n-terminal and c-terminal SH2 domains. J Biol Chem *273*, 30199-30203.

Yuan, T.L., and Cantley, L.C. (2008). PI3K pathway alterations in cancer: variations on a theme. Oncogene *27*, 5497-5510.

Zahraoui, A., Touchot, N., Chardin, P., and Tavitian, A. (1989). The human Rab genes encode a family of GTP-binding proteins related to yeast YPT1 and SEC4 products involved in secretion. J Biol Chem *264*, 12394-12401.

Zerial, M., and McBride, H. (2001). Rab proteins as membrane organizers. Nat Rev Mol Cell Biol *2*, 107-117.

Zhang, X., Vadas, O., Perisic, O., Anderson, K.E., Clark, J., Hawkins, P.T., Stephens, L.R., and Williams, R.L. (2011). Structure of lipid kinase p110beta/p85beta elucidates an unusual SH2-domain-mediated inhibitory mechanism. Mol Cell *41*, 567-578.

Zhou, B.P., Liao, Y., Xia, W., Zou, Y., Spohn, B., and Hung, M.C. (2001). HER-2/neu induces p53 ubiquitination via Akt-mediated MDM2 phosphorylation. Nat Cell Biol *3*, 973-982.

Zhu, G., Chen, J., Liu, J., Brunzelle, J.S., Huang, B., Wakeham, N., Terzyan, S., Li, X., Rao, Z., Li, G., *et al.* (2007). Structure of the APPL1 BAR-PH domain and characterization of its interaction with Rab5. EMBO J *26*, 3484-3493.

Zhu, G., Liu, J., Terzyan, S., Zhai, P., Li, G., and Zhang, X.C. (2003). High resolution crystal structures of human Rab5a and five mutants with substitutions in the catalytically important phosphate-binding loop. J Biol Chem *278*, 2452-2460.

Zhu, G., Zhai, P., Liu, J., Terzyan, S., Li, G., and Zhang, X.C. (2004). Structural basis of Rab5-Rabaptin5 interaction in endocytosis. Nat Struct Mol Biol *11*, 975-983.